Influence of new network architectures and usages on RF human exposure in cellular networks

Amirreza Chobineh

INSTITUT POLYTECHNIQUE DE PARIS

TELECOM Paris

IP PARIS

INFLUENCE OF NEW NETWORK ARCHITECTURES AND USAGES ON RF HUMAN EXPOSURE IN CELLULAR NETWORKS

Thèse de doctorat de l'Institut Polytechnique de Paris
Préparée à Télécom Paris

École doctorale n°626 Institut Polytechnique de Paris (ED IP Paris)
Spécialité de doctorat : Réseaux, Informations, Communications

Thèse présentée et soutenue à Palaiseau, le 02 Juillet 2020, par

Amirreza Chobineh

Composition du Jury :

Hélène Roussel
Sorbonne Université   Présidente

Philippe De Doncker
Université Libre de Bruxelles   Rapporteur

Christian Person
IMT Atlantique   Rapporteur

Shermila Mostarshedi
Université Gustave Eiffel   Examinatrice

David Lautru
Université Paris Nanterre   Examinateur

Philippe Martins
Ecole Télécom Paris   Examinateur

Emmanuelle Conil
Agence National des Fréquences   Co-Directrice de thèse

Joe Wiart
Ecole Télécom Paris   Directeur de thèse

Thèse de doctorat

ACKNOWLEDGEMENTS

ABSTRACT

In coming years, there will be a sharp growth in wireless data traffic due to the increasing usage of mobile phones and implementation of IoT technology. Therefore, mobile network operators aim to increase the capacity of their networks, to provide higher data traffic with lower latency, and to support thousands of connections. One of the primary efforts toward these goals is to densify today's cellular Macrocell networks using Small cells to bring more coverage and higher network capacity. Small cell antennas emit lower power than Macrocells and are often deployed at lower heights. As a consequence, they are closer to the user and can be implemented massively. The latter can result in an important raise in public concerns.

Mobile phones are used on the one hand, for a large variety of data usages that require different amounts of data and throughput and on the other hand for making phone calls. Voice over IP applications such as Skype has become very popular since they provide cheap international voice communication and can be used on mobile devices. Since LTE systems only support packet services, the voice service uses Voice over LTE technology instead of classical circuit-switched voice technology as in GSM and UMTS.

The main objective of this thesis is to characterize and analyze the influence of new network architectures and usages on the actual human exposure induced by cellular networks. In this respect, several measurement campaigns were carried out in various cities and environments.

Regarding the EMF exposure in heterogeneous networks, results suggest that by implementing Small cells, the global exposure (i.e. exposure induced by mobile phone and base station antenna) reduces due to the fact that by bringing the antenna closer to the user the emitted power by mobile phone and the usage duration reduce owing to power control schemes implemented in cellular network technologies. However, the magnitude of exposure reduction depends on the location of the Small cell with respect to Macrocells. Moreover, to assess the EMF exposure of indoor users induced by Small cells, two statistical models are proposed for the uplink and downlink exposures in an LTE heterogeneous environment based on measurements.

The last part of the thesis is devoted to the assessment of the exposure for new types of usages through measurements. Results suggest that the amount of uplink emitted power and the emission time duration by a mobile phone is highly dependent on the usage and

network technology. Voice call communications require a continuous and generally low throughput in order to maintain the communication during the call. On the contrary, in data usage, the mobile phone requires higher data and throughput to perform the task as fast as possible. Therefore, during a voice call even if the user is using the mobile phone for a relatively long time, the exposure time duration should be lower since the usage does not require high amounts of data. The temporal occupation rate for several types of voice calls for different technologies is assessed through measurements.

RÉSUMÉ

Dans les années à venir, le trafic de données dans les réseaux cellulaires connaîtra une forte croissance en raison de l'augmentation d'utilisation des téléphones mobiles et de la mise en œuvre de la technologie des objets connectés. Par conséquent, les opérateurs de réseaux mobiles visent à augmenter la capacité de leurs réseaux avec une latence plus faible et à supporter des milliers de connexions simultanément. L'un des principaux efforts est de densifier les réseaux Macrocells actuels par les Small cells afin d'offrir plus de couverture et de débit aux utilisateurs. Les antennes Small cells émettent de faibles puissances et sont souvent déployées à de faibles hauteurs. En conséquence, ils sont plus proches des utilisateurs, peuvent être déployés massivement mais génèrent également des inquiétudes chez les riverains.

Les téléphones portables sont utilisés pour une grande variété d'utilisations qui nécessitent différentes quantités de données et de débit. Les applications de voix sur IP telles que Skype sont devenues très populaires car elles fournissent une communication vocale internationale peu onéreuse et peuvent être utilisées sur les appareils mobiles. Étant donné que les systèmes LTE ne prennent en charge que les services par paquets, le service vocal utilise la technologie voix sur LTE au lieu de la technologie « circuits » classique comme avec le GSM et UMTS.

L'objectif principal de cette thèse est d'évaluer l'influence des nouvelles architectures des réseaux et usages sur l'exposition actuel du publique induite par les réseaux cellulaires. À cet égard, plusieurs campagnes de mesures ont été menées dans différentes villes et environnements.

En ce qui concerne l'exposition aux champs électromagnétiques dans les réseaux hétérogènes, les résultats suggèrent qu'en déployant les Small cells, la puissance émise par le téléphone mobile, en raison de la proximité de l'antenne et par conséquent l'exposition global diminue.

De plus, pour évaluer l'exposition EMF des utilisateurs indoor induite par les Small cells, deux modèles statistiques sont proposés pour les expositions montante et descendante induite dans un réseau hétérogène LTE.

La dernière partie de cette thèse est consacrée à l'évaluation de l'exposition aux nouveaux types d'usages. Les résultats suggèrent que la puissance émise et la durée d'émission par un téléphone mobile dépendent fortement de l'usage et de la technologie du réseau. Les communications voix nécessitent un débit continu et généralement faible afin de maintenir la communication pendant l'appel. Au contraire, dans le cas de l'usage données, le téléphone mobile nécessite des débits plus élevés pour effectuer la tâche le plus rapidement. Par conséquent, pendant un appel voix, même si l'utilisateur utilise le téléphone portable pendant une durée relativement longue, la durée de l'exposition est moins longue car l'utilisation ne nécessite pas une grande quantité de données. Ainsi, le taux d'occupation temporelle de plusieurs types d'appels voix pour différentes technologies est évalué par les mesures.

.

Contents

LIST OF TABLES

LIST OF FIGURES

xiv

LIST OF ABBREVIATIONS AND ACRONYMS

ANFR   Agence National des Fréquences

BS   Base Station

EI   Exposure Index

EMF   Electromagnetic Field

FDTD   Finite-Difference Time-Domain

GEV   Generalized Extreme Value

GSM   Global System for Mobile Communication

ICES   International Committee on Electromagnetic Safety

ICNIRP   International Commission on Non-Ionizing Radiation Protection

IEEE   Institute of Electrical and Electronics Engineers

LEXNET   Low Electromagnetic Fields Exposure Network.

LTE   Long Term Evolution

MC   Macro Cell

PLE   Path Loss Exponent

QoS   Quality of Service

RF   Radio Frequency

SAM   Specific Anthropomorphic Mannequin

SAR   Specific Absorption Rate

SC   Small Cell

UE   User Equipment

UMTS   Universal Mobile Telecommunication System

PRB   Physical Resource Block

1. GENERAL INTRODUCTION

Since the 1990s, wireless communication systems, particularly cellular networks, have experienced an exceptional development. This has resulted in the emergence of new technologies, such as smartphones and tablets. Global System for Mobile Communication (GSM), Universal Mobile Telecommunication Systems (UMTS), and Long-Term Evolution (LTE) network technologies are largely deployed all over the world to provide users with voice and data communication. This phenomenal progress in technologies, applications, and wireless devices has led to strong growth in data traffic over the last decade [1]. To respond to such demand, cellular network operators continuously try to improve the efficiency of their networks.

To face 5G ambitious aims which are to provide higher data traffic, lower latency, and support thousands of connections, operators came up with new solutions. One of the main steps toward these goals is to offload traffic from Macrocells (MC) by densifying current networks with Small cells (SC) which results in more coverage, capacity, and better performance. SC antennas are emitted low power and are often deployed at low heights, consequently, they are closer to the user and can be implemented massively. The latter can result in an important raise in public concerns.

Concerns about possible health effects of RF-EMF have arisen to the same extent as the growth of wireless telecommunication technologies. Thus far, the main health effects of EMF exposure in radiofrequency (RF) domain are recognized as thermal overheating of human tissues due to the penetration and absorption of EMF into the body. Concerning the non-thermal sanitary effects of EMF, research projects are taking place continuously to characterize these effects but they remain non-conclusive [2]. To guarantee protection for public and workers against EMF exposure, international organizations such as the International Commission for Protection against Non-Ionizing Radiation (ICNIRP) [3] have recommended a series of limits. While compliance testing and safety standards are based on the worst-case exposure assessment, epidemiological studies focus on the real case exposure evaluation.

Multiple metrics are introduced to assess the exposure depending on characteristics of the source such as output power, frequency, exposure duration, etc. Incident field metrics are used for electric and magnetic fields in terms of power density. Specific absorption rate (SAR) is used to assess the proportion of the absorbed energy in the human body. Dose metrics present a comparative quantity by combining the intensity of exposure (field strength or SAR) and the exposure duration.

Concerning cellular networks, people are mainly exposed by two types of sources: on the one hand from sources implemented by network operators such as base stations (BS) or picocell boxes (i.e. downlink exposure) and on the other hand from the user equipment (UE) (i.e. uplink exposure) such as mobile phones. Studies [4] have demonstrated that there is a strong correlation between the power received from a BS and the emitted power by the UE due to the downlink (DL) and uplink (UL) power control algorithms implements in cellular technologies which enable the UE to adapt its output power to the variations of the communication channel. In other words, when the UE experiences a good channel quality, it reduces the emitted power and vice versa. As a consequence, the DL and UL exposure are strongly related and should be assessed simultaneously. In this respect, Global exposure (i.e. exposure induced by mobile phone and base station antenna) [5], [6] has been introduced as a metric that combines the UL and DL doses which provide meaningful information about the actual exposure of a person (see 2.6.2). To assess the actual EMF exposure for a population, many exposure configurations should be taken into account due to the diversity of network technologies, sources, usages, environments, people's lifestyles, etc. In this context, the Exposure Index (EI) metric is introduced which takes into consideration the Global exposure and a large number of parameters to assess the exposure of a given population in a geographical area by providing a comprehensible output (see Section 2.6.2) [6].

This thesis is composed of three main chapters. Chapter 2 introduces the state of art on RF-EMF exposure problematic as well as a brief explanation on existing protection limits (see Section 2.2) and frequently used methods and protocols to assess the normative and actual exposures induced by near field and far-field sources through numerical simulations and in situ measurements (Section 2.3). Variabilities related to SAR assessments and influencing parameters are discussed in Section 2.4.1.2. Global exposure and Exposure Index assessments are presented in Section 2.6. Finally, Section 2.7 and Section 2.8 focus on the influence of new network architectures and new usages on global exposure.

Chapter 3 presents the work carried out to characterize the exposure in a homogenous and multiple heterogeneous LTE networks through several measurement campaigns. Measurement results are analyzed in terms of UL emitted power and DL received power by UE, DL electric field, and throughput (see Section 3.3 and Section 3.4). To assess the Exposure Index for indoor population, the UL and DL exposures are modeled based on measurement results using

statistical modelling methods (see Section 3.5). Finally, using these models the Exposure Index is computed for a scenario including indoor and outdoor users in Section 3.6.

Chapter 4 is devoted to the characterization of the exposure for different types of usages in GSM, UMTS, and LTE technologies through several measurement campaigns. Results including the UL power emitted and DL received power density from BS for different technologies, usages, and environments are presented in Section 4.3. Section 4.4 focuses on the temporal variation of the UL emitted power by UE during voice communication in circuit-switched and packet-switched technologies.

2. HUMAN EXPOSURE INDUCED BY ELECTROMAGNETIC FIELDS

2.1. Human exposure to EMF

2.1.1 Electromagnetic Field

The EMF generated by RF sources is composed of correlated electric E and magnetic H fields having magnitude, phase, and direction. The relations and variations of these electric and magnetic fields, as well as, charges and currents associated with these EMFs are governed by the well-known Maxwell equations (**1**) and (**2**). Consider a media having respectively permittivity, permeability and conductivity equal to ε, μ, and σ, the Maxwell equations applied to the EMF induced by electric and magnetic currents J_i and M_i in frequency domain can be written as:

$$\nabla \times \boldsymbol{E} = -\boldsymbol{M_i} - j\omega\mu\boldsymbol{H} \tag{1}$$

$$\nabla \times \boldsymbol{H} = \boldsymbol{J_i} + \sigma\boldsymbol{E} + j\omega\varepsilon\boldsymbol{E} \tag{2}$$

Where E (V/m) and H (A/m) are a complex spatial form of respectively electric and magnetic fields. J_i (A/m^2) and M_i (V/m^2) are the electric and magnetic currents supplied to the sources. The equation (**3**) representing the conservation of power law is obtained via equations (**1**) and (**2**):

$$-\nabla \cdot \left(\frac{1}{2}\boldsymbol{E} \times \boldsymbol{H}^*\right) = \frac{1}{2}\boldsymbol{H}^* \cdot \boldsymbol{M_i} + \frac{1}{2}\boldsymbol{E} \cdot \boldsymbol{J_i^*} + \frac{1}{2}\sigma|\boldsymbol{E}|^2 + j2\omega\left(\frac{1}{4}\mu|\boldsymbol{H}|^2 - \frac{1}{4}\varepsilon|\boldsymbol{E}|^2\right) \tag{3}$$

Stating that within the volume V bounded by surface S, the supplied power P_s (4), is equal to the power P_e existing in S plus the power P_{abs} absorbed within that volume plus the electric (W_e) and magnetic (W_s) energies stored within that same volume.

$$P_s = P_e + P_{abs} + j2\omega(\overline{W}_m - \overline{W}_e) \tag{4}$$

Where :

$$P_s = -\frac{1}{2}\iiint_V (\boldsymbol{H}^* \cdot \boldsymbol{M_i} + \boldsymbol{E} \cdot \boldsymbol{J_i^*})dv = supplied\ complex\ power\ (W) \tag{5}$$

$$P_e = \oiint_S \left(\frac{1}{2} \boldsymbol{E} \times \boldsymbol{H}^* \right) \cdot ds = exiting\ complex\ power\ (W) \tag{6}$$

$$P_{abs} = \frac{1}{2} \iiint_V \sigma |\boldsymbol{E}|^2 dv = dissipated\ real\ power\ (W) \tag{7}$$

$$\overline{W}_m = \iiint_V \frac{1}{4} \mu |\boldsymbol{H}|^2 dv = time - average\ magnetic\ energy\ (J) \tag{8}$$

$$\overline{W}_e = \iiint_V \frac{1}{4} \varepsilon |\boldsymbol{E}|^2 dv = time - average\ electric\ energy\ (J) \tag{9}$$

The integrand part of P_e represents the time average Poynting vector (averaged power density).

$$\mathcal{P} = \frac{1}{2} Re[\boldsymbol{E} \times \boldsymbol{H}^*] \tag{10}$$

2.1.2 Exposure metrics: Specific Absorption Rate (SAR)

In the radiofrequency domain, between 100 kHz and 6 GHz, the human exposure to an EMF is quantified through the specific absorption rate (SAR) (11) which is the ratio of the absorbed electromagnetic power by the considered tissue and the mass of the tissue.

$$SAR = \frac{Absorbed\ power\ in\ volume\ V}{mass\ of\ the\ volume\ V} \tag{11}$$

The average SAR in volume V is the absorbed power P_{abs} (**7**), dividing by the mass M_{mass} in that volume and can be expressed as in equation (**12**):

$$SAR = \frac{P_{abs}}{M_{mass}} = \frac{\frac{1}{2} \iiint_V \sigma |\boldsymbol{E}|^2 dv}{\iiint_V \rho dv} \tag{12}$$

For one tissue considering ρ and σ constant in volume V, the local SAR can be defined by equation (**13**):

$$SAR = \frac{P_{abs}}{M_{mass}} = \frac{\frac{1}{2}\iiint_V \sigma|\boldsymbol{E}|^2 dv}{\iiint_V \rho dv} = \frac{1}{V}\iiint_V \frac{\sigma|\boldsymbol{E}|^2}{2\rho}dv = \frac{1}{V}\iiint_V SAR\, dv = \frac{\sigma|\boldsymbol{E}|^2}{2\rho} \qquad (13)$$

According to (**13**), the SAR value is directly linked to the electric field strength induced in the tissue.

The scientific community uses two basic types of quantifications to monitor and control exposure to electromagnetic radiation: the whole-body SAR, which measures the average of the power absorbed by the whole body defined as the total absorbed power by the body divided by the mass of the body and the local SAR which is used when the exposure is being assessed in a more local area of the body, for example, an organ. In this case, the local SAR is the total absorbed power by that organ divided by the mass of the organ. Local SAR can be also assessed by quantifying the absorbed power by a cube of 1g (SAR1g) or 10g (SAR10g) and dividing by masses of 1 or 10 grams respectively. The whole-body SAR is usually used to evaluate far-field induced exposure (e.g induced by base stations) and local SAR to evaluate near-field induced exposure (as induced by mobile phone).

2.2. Protection limits

To protect humans from health hazards linked to EMFs, international organizations such as International Commission on Non-Ionizing Radiation Protection (ICNIRP) [3] and International Committee on Electromagnetic Safety (ICES) [7] have set a series of exposure limits. At the European level, the council recommendation 1999/519/EC [8] on the limitation of exposure of the general public to electromagnetic fields is based on ICNIRP limits which are composed of a series of fundamental limits (the basic restrictions, BRs) and derived limits (the reference levels, RLs). These basic restriction values are presented in Table 1 for the occupational and general public for whole-body and local exposure.

SAR is directly linked to the electric field induced in the tissues and cannot be measured in situ. Thus quantities that are more easily evaluated, called 'reference levels' RLs have been derived from the BRs to provide a more practical means of compliance verification with the guidelines [9].

Table 1, Basic restrictions for time-varying electric, magnetic and electromagnetic fields from ICNIRP 1998 guidelines [9].

Exposure Scenario	Frequency Range	Whole-body average SAR (W/kg)	Local head/torso SAR (W/kg)	Local Limb SAR (W/kg)
Occupational	100 kHz – 6 GHz	0.4	10	20
General Public	100 kHz – 6 GHz	0.08	2	4

Averaging time of 6 minutes for local SAR.
Local SAR is averaged over the mass of 10g.

RLs are expressed in electric field strength (V/m) or magnetic field strength (A/m) or power density (W/m^2) and they are defined to be conservative. The latter are derived such that under worst-case exposure conditions they will result in similar exposures to those specified by BRs. The compliance to RLs implies necessarily to respect BRs. However contrary to BRs, the RLs are frequency dependent. As further presented in Section 2.3.1.2, RL values for different frequencies are deduced from numerical simulations by taking into account the SAR variabilities in terms of different factors such as frequency bands, human morphology, age, etc. E-field, H-field, and incident plane wave power density far-field restriction levels are presented for the occupational and general public for whole-body exposure in Table 2. It should be noted that a new version of ICNIRP guidelines has been published in March 2020 [10].

Table 2, reference levels for whole-body exposure to time-varying far-field electric, magnetic and electromagnetic fields, from 1 MHz to 300 GHz from ICNIRP 1998 guidelines [9]

Exposure Scenario	Frequency Range	E-field strength (V/m)	H-field strength (A/m)	Incident plane wave power density (S_{inc}) (W/m^2)
Occupational	1 – 10 MHz	610/f	1.6/f	---
	>10-400 MHz	61	0.16	10
	>400-2000 MHz	$3f^{0.5}$	$0.0081f^{0.5}$	f/40
	>2-300 GHz	137	0.36	50
General Public	1 – 10 MHz	$87/f^{0.5}$	0.73/f	---
	>10-400 MHz	28	0.073	2
	>400-2000 MHz	$1.375f^{0.5}$	$0.0037f^{0.5}$	f/200
	>2-300 GHz	61	0.16	10

1. f is frequency in MHz
2. For frequencies between 100 kHz and 10GHz, S_{inc}, E^2 and H^2 are to be averaged over 6 minutes.
3. "---" indicates that this cell is not relevant to reference levels
4. For frequencies exceeding 10GHz, S_{inc}, E^2 and H^2 are averaged over any $68/f^{1.05}$-min period (f in GHz)

To evaluate the exposure induced by a device or an antenna, different protocols and methods have been established based on measurement or numerical computation. Through measurements it is possible to assess the field and the induced SAR, avoiding numerical modeling uncertainties. Numerical SAR assessment is useful when performing measurement is not possible or it is very difficult, for instance, to assess the exposure in a living body.

A series of methods and protocols have been developed to perform compliance tests and actual exposure evaluation. There are two main exposure evaluation categories:

1) Exposure induced by BS antennas
2) Exposure induced by UE

The next section is dedicated to different methods for exposure assessment through experimentation and measurement.

2.3. Exposure assessment for base stations antennas

2.3.1 Numerical assessment

2.3.1.1. SAR assessment

Numerical SAR assessment requests first to model sources and the human body and after that to perform numerical assessments using methods such as the finite difference in time-domain (FDTD)[11] or multilayer approaches which are largely used over the past decade to assess the EMF absorbed by the biological tissues [12]–[15]. These computational methods are based on realistic heterogeneous body and source models. Existing body models have been developed using Magnetic Resonance Imaging (MRI), computed tomography or anatomical images. These models are represented by voxel images of thin slices of the body. Each voxel corresponds to a type of body tissue with specific dielectric properties. In this regard, a series of human body models have been developed such as Virtual Family [16], ANR (Agence National de Recherche) project Kidpocket [17] and ANR project Fetus [17]. Examples of these human models are presented in Figure 1. Dielectric properties such as permittivity and conductivity of different tissues for each frequency band are measured [18] and used to assess the absorbed EMF by these tissues.

Numerical simulations such as FDTD method could also be used to assess the exposure in the far-field zone of an antenna. However, because of the limits of computational methods, it is quite impossible (due to the lack of memory and time-consuming computations) to compute the human exposure located far from the antenna. To overcome such limits, the equivalence principle [19] [20] and the relative Huygens box can be used. In the far-field zone of the antenna, the source of exposure can be approximated as a plane wave or a sum of multiple plane waves. The numerical simulation adapted to FDTD is done by inserting a human model into a virtual box ("Huygens box") whose dimension is slightly larger than the model's body.
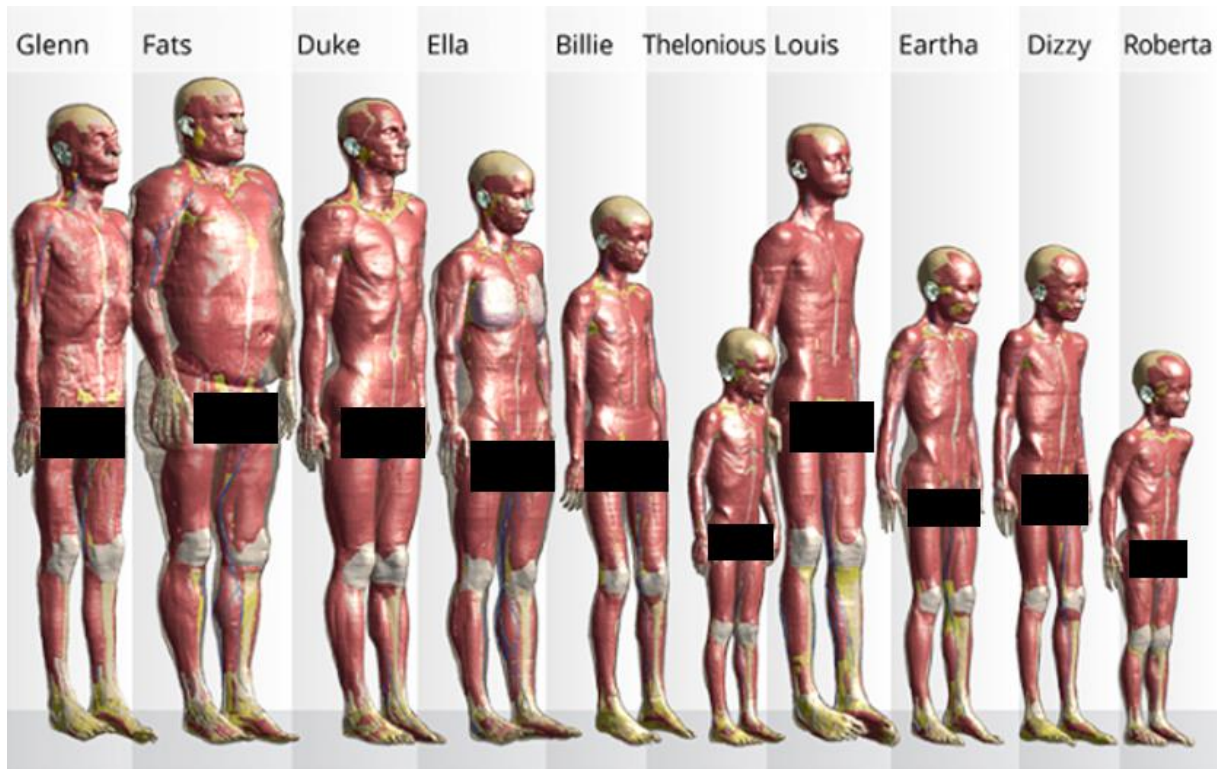
Figure 1, Virtual Family human models [21]

The equivalent current corresponding to the plane wave around the virtual box can be computed through the equivalence principle. By exciting these equivalent currents, it is possible to evaluate the field in the entire Huygens box. Then the exposure (SAR) value to this field can be computed by FDTD method [22].

2.3.1.2. SAR transfer function

Since SAR assessment is a complex and time-consuming matter, studies were conducted to define transfer functions, assessing the absorbed power by the human body from the incident field. A series of advanced numerical methods and phantoms were used to characterize these transfer functions in terms of variabilities of SAR [22]–[24].

Considering the human body as an antenna, the equivalent surface of the body evolves with wavelength hence the rate of the absorbed power by the human body varies in terms of frequency. Figure 2 shows the whole-body SAR values in terms of frequency for different types of human bodies for standing position. As we can see, absorbed power by the human body in 60 MHz to 100MHz frequency band is higher since the average human body size (1.5 to 1.8 m) is close to the size of a dipole having its resonance in this frequency. Consequently, the human body shows a good efficiency for absorbing EMF energy at this frequency band [22]. This

dependency of the absorbed power to frequency has been taken into account while defining reference levels (see Table 2).
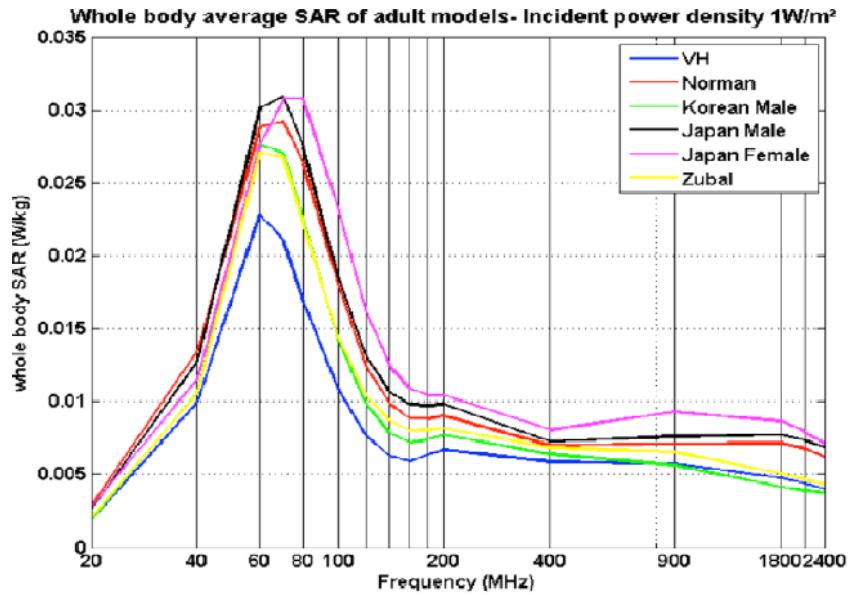
Figure 2, Whole-body SAR variation in terms of frequency for different human models for standing position [22]

In order to assess the influence of children's morphology on RF exposure, several children models at different ages have been studied [22]. As it is shown in Figure 3, the absorbed power in small-sized people can be higher than in larger people. Furthermore, the absorbed power in children is higher than adults due to their body size. This is due to the fact that the absorption cross-section and body surface area are strongly correlated [25].
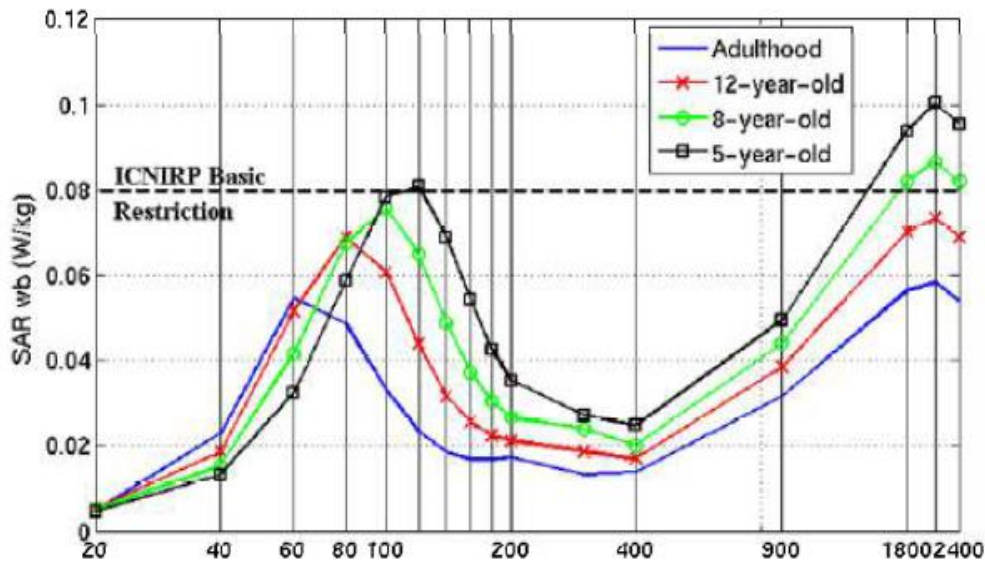
Figure 3, SAR values in terms of frequency for different ages [22]

Another parameter that highly influences the absorbed power by a human body is the polarization and angle of arrival of the incident field. Figure 4 shows the amount of received power by a human body model assessed through FDTD and Huygens box methods at 2.1 GHz frequency in the standing position for different angles of arrival [26], [27]. The highest whole-body SAR values are induced by plane wave incident to the front and back of the model, while the lowest whole-body SAR values are induced by plane-wave incident to the sides of the model. According to [26] The whole-body SAR values induced by horizontal polarization are up to 30% higher than the case with vertical polarization.

Another factor that affects the amount of absorbed power is body posture. It is shown that a change in body posture can significantly affect the way that power is absorbed [28]. Figure 5 represents the variation of SAR in terms of frequency for different posture and wave polarizations.
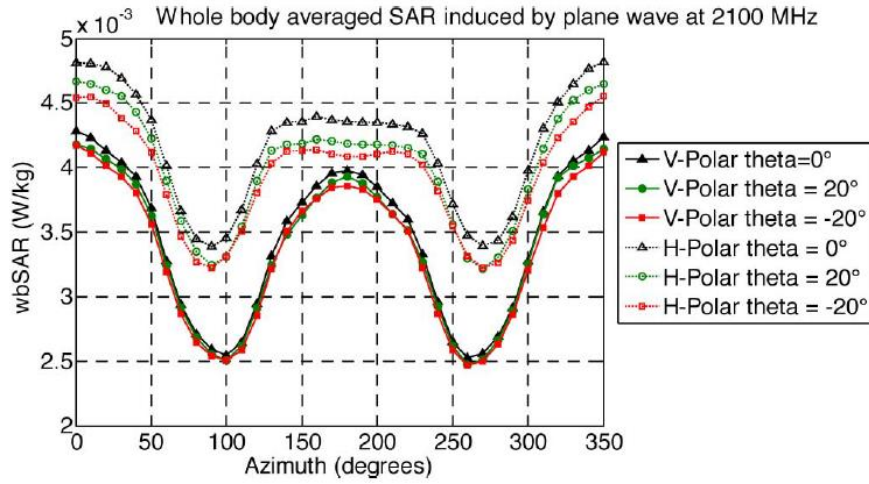
Figure 4, Whole-body averaged SAR for polar-wave exposure from three elevations in both V and H-polarizations and from azimuth from 0° to 360° at 2100 MHz. The incident power is 1W/m²[26]
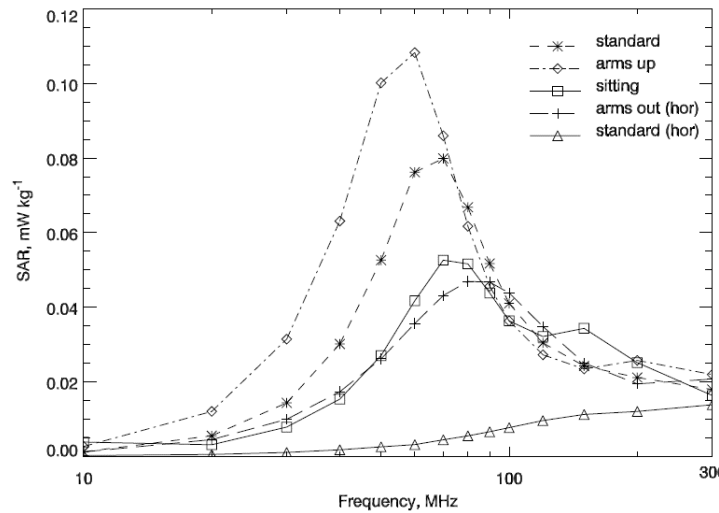
Figure 5, Whole-body averaged SAR for different body postures and wave polarizations (hor: horizontal polarization)[28]

2.3.1.3.Source modeling for boundary compliance

Considering base station antennas, it is important to specify methods and protocols to check the compliance to the BRs or the RLs and if needed to specify the compliance boundaries (a.k.a. safety perimeter) that guarantee a human exposure below the limits outside these areas. One of the main difficulties is that compliance boundaries are not often in the far-field zone of the antenna therefore the far-field gain approximation formula is involving errors. Hence, in order

to assess the exposure in these compliance boundaries, several studies have been performed to define efficient models of base station antennas in the near-field zone. The method called synthetic modeling [29] is based on modeling the radiated near field of one unit cell of the antenna array computed in the volume of interest. The near field of the full antenna is derived by superposing horizontally shifted field contributions of the unit cell. The shift corresponds to the distances between cell units. This model is particularly precise when the coupling between cell units is minimized. In this case, the model approximates accurately the radiated nearfield at about two wavelengths away from the antenna as presented in Figure 6.
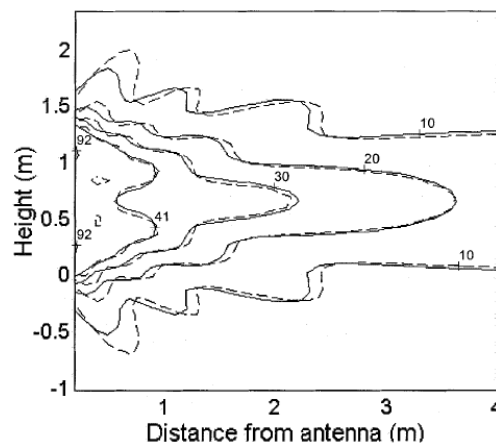
Figure 6, Electric field (V/m) in the E plane, computed by the synthetic model (solid line) and the gain based model (dashed line) [29]

Other methods can be used, for instance, in [30] the field is assessed in the vicinity of a collinear array antenna in terms of waves.

2.3.2 Experimental assessment

2.3.2.1.Extrapolation and averaging methods used to assess the far-field exposure

Experimental exposure assessment in the far-field zone of an antenna is based on E-field measurement and comparison to reference levels because as explained before in-situ SAR assessment is not possible. Generally, the field measured at one point in a complex environment is affected by shadowing and fast fading because of environment reflections, obstructions and diffractions [31], [32].

Shadowing is mainly linked to the environmental obstructions which affect wave propagation such as a building or a hill that obstructs the main wave path [33]. In complex environments, reflections and refractions can also affect the energy of waves due to constructive and destructive interferences. The fast fading effect is mainly due to reflection and refraction caused by objects in a complex environment which causes strong local fluctuations. Due to fast fading, a narrowband measurement performed at one point can vary from a measurement performed a few centimeters away. Thus in order to reduce uncertainties due to fading, standardization bodies have proposed different averaging methods in time and space as in CENELEC EN 50492 [34] or IEC-62232 [35] describing a protocol to estimate the incident field over a human body cross-section. On the one hand, a spatial averaging method is performed based on [36] which consists of averaging the electric field measured in a series of points placed on a grid with a specific distance between them, to reduce the measurement uncertainty. An example of a measurement grid is presented in Figure 7. It is noted that at least three points should be measured and by increasing the number of points the measurement uncertainty reduces. On the other hand, the ICNIRP defines 6 minutes time-averaging period for measuring the RMS field.
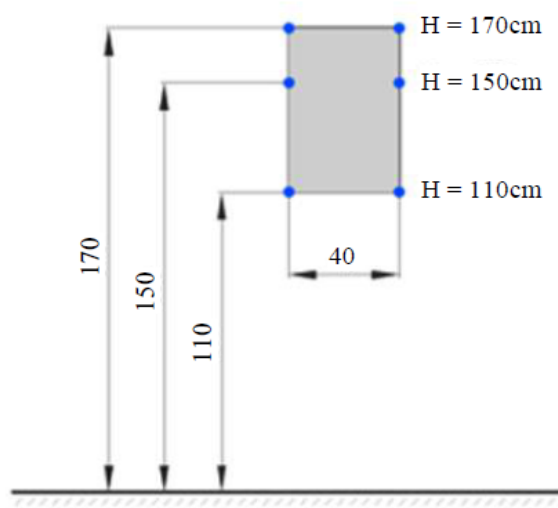
Figure 7, Example of measurement points location for spatial averaging [36]

In the case of cellular network antennas, another parameter that can affect the BS emitted power is the traffic supported by that BS as it is shown in Figure 8. It is important to note that the time of field measurement plays an important role in the E-field assessment of a cellular antenna. To check the compliance with regulatory limits, the maximum exposure conditions have to be

taken into account and the measurement result might have to be extrapolated to the worst-case scenario.

The extrapolation process is based on the measurement of time-dependent channels. For instance, GSM for 2G technology is based on time division multiple access (TDMA) and the downlink signal emitted by the BS is composed of a constant power signal called BCCH (Broadcast Common Channel) and a series of channels (TRX) dedicated to transporting users data. Thus for GSM, the extrapolated process consists of the BCCH signal and multiplying by the number of transmitters TRX.
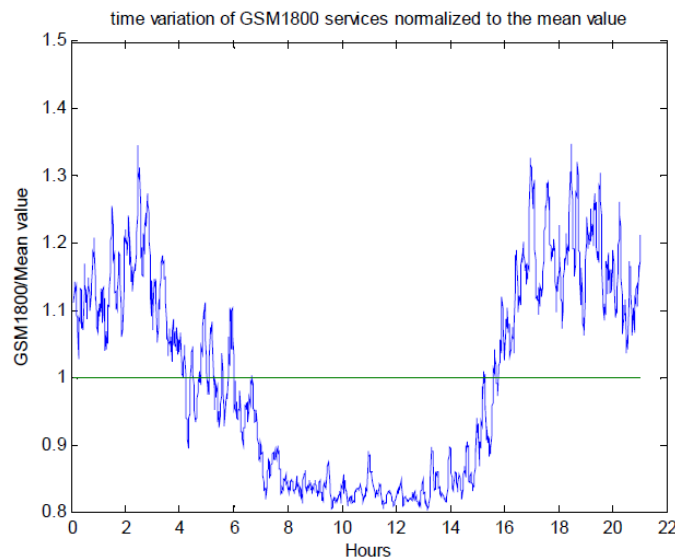
Figure 8, the variation of the emitted field by a GSM antenna during 24-hour, normalized to its mean value at 1800 MHz

UMTS for 3G is based on the wideband code division multiple access code (WCDMA). All the users connected to the same BS are served at the same time and the BS communicates with UEs through a common channel called CPICH (Common Pilot Channel). In WCDMA the number of TRX is the proportion of common channel power to the maximum power delivered by the antenna.

LTE for 4G is using orthogonal frequency division multiple access (OFDMA). In LTE technology, reference signals are transmitted periodically with a constant power. Specific LTE measurement systems enable to decode LTE signals and to measure the level of reception of these reference levels. To avoid the use of LTE decoder, an alternative solution has also been

developed based on the measurement of the broadcast channel PBCH (Physical Broadcast Channel).

In the case of 5G, the NR (New Radio) is also using orthogonal frequency division multiple access and works are ongoing in standardization bodies to elaborate an extrapolation process. The use of beam steering antennas with high variability in time and space makes it very difficult to define an extrapolation process. The signalization data can be emitted with a different radiation pattern than the traffic data.

In France, Agence National des Fréquences (ANFR) is maintaining an up-to-date protocol to ensure compliance with the regulatory limits indicated in a French decree based on the 1999 EU recommendation. A national surveillance process allows requesting for free in situ exposure assessment in the residential area and any place accessible to the public. More than 3000 measurements are perfumed every year and the measurement results are accessible online [37].

The type of environment has an important effect on exposure. Regarding outdoors, exposure is mainly affected by the number of surrounding buildings and antennas. In indoors, exposure depends on outdoor sources as well as indoor sources such as wifi and Femtocells. Because of path loss due to walls or windows glasses the received power level from outdoor BSs in an indoor area is less than outdoor areas depending on the architecture of the indoor space, materials used in walls, number of windows and doors and also in buildings the exposure can vary from floor to floor. In the case of indoor sources, their number and their positions, the structure of rooms and furniture can affect the exposure. One of the main problems in assessing exposure in indoor areas is the lack of information about the position of sources or furniture and space architecture especially in private environments [38]. These mentioned aspects provide uncertainties on the assessment of exposure, however, since people spend about 70% of their time in indoor areas the assessment of exposure in indoor areas is crucial [39].

2.3.2.2.Measurement systems

The exposure to the incident field is mainly assessed by measurements via personal dosimeters, spectrum analyzers or field meters using wideband or frequency-selective filters and antennas (see Figure 9). Regarding the exposure assessment, two types of measurement exist in terms of frequency: Broadband measurements measure a wide range of frequencies (typically from 100 kHz to 6 GHz) via a field meter and a broadband antenna and a single value is obtained for the whole frequency band. Narrowband (frequency-selective) measurements consist of a very narrow frequency band dedicated to a service or technology, using an antenna and a spectrum

analyzer. In the end, for each frequency band, one E-field value is obtained. These measurements determine the influence of each technology or service on the total exposure value.

In order to verify compliance of exposure to RLs through measurement, international standards such as EN 62232 [35] set minimum requirements for measurement systems and complex and quite long protocols to assess the exposure. Alternatively, in epidemiological studies [40], a series of devices called Personal ExposiMeters (PEM)[41] are used to assess the narrowband measurements on different frequency bands at the same time. Due to its lightweight and its simple user interface, PEMs can be worn by a person to assess personal exposure to RF-EMF. PEMs have a limited dynamic range (typically between 0.05 to 5 V/m) thus very high and very low values cannot be measured by these devices. Moreover, since PMEs are worn by a person, the vicinity of the ExposiMeters to the body affects the measured values by the PME.

Figure 9, E-field measurement equipment, left: wideband field meter (Narda NBM 550), middle: Selective spectrum analyzer (Narda SRM-3006), right: Exposimeter (MVG Spy)

Until now the exposure induced by sources placed far from a person has been discussed. Regarding the recent types of network antennas such as small cells and Femtocells, where the distance between the antenna and the human body is in order of a few meters, we should take into consideration the proximity of the antenna and human body. In these cases, the human body is not placed very close to the antenna so modeling the source and human body together is quite impossible. Besides, the human body is not placed in the far-field zone of the antenna where we could consider plane wave approximation. Thus the source in the intermediate distance is modeled by the spherical wave expansion (SWE) method [20], [42], [43]. Since the distance between the human body and source is far enough to neglect the coupling, we can use

the equivalence principle to assess the exposure of the human body placed at an intermediate distance of the antenna through numerical methods such as FDTD.

Figure 10, Spherical wave coefficients can be measured by MVG "Starlab" near-field measurement system [44].

2.4. Exposure assessment for user device

2.4.1 Numerical assessment

2.4.1.1.Source modeling

When the EM source is located close to the body, the human body's biological tissues are in the near-field zone of the source. Consequently, there is a strong coupling between the source and biological tissues. In order to model a near-field EM source such as mobile phones or tablets, voxel digital models of the device are used to take into account the characteristics of the real device such as the size, battery, screen, and the antenna. On this matter, in IEC 62704 [45] a series of protocols have been developed to properly model a wireless communication system taking into account the necessary complexities. An example of a modeled mobile device is presented in Figure 11 [46]. This mobile phone of dimensions 5.4 * 1.6 * 1.5 cm is modeled with a 2 mm resolution with a dipole antenna at the bottom of the model operating at 1940 MHz band.
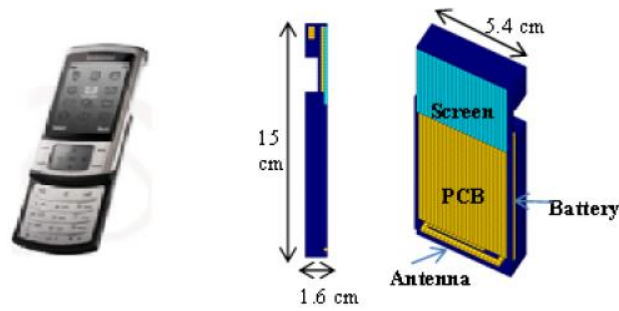
Figure 11, a 3D mobile phone model [46]

The SAR value in numerical human body models can be assessed using these near-field sources under different exposure conditions. The model of the handset does not have to be entirely identical to the real models and it can be simplified depending on the objective. Generally, the handset model should be identic the real one in terms of antenna shape, the position of RF energy input, and the characteristics of the antenna such as the return loss S11.

2.4.1.2.SAR variability

Despite the existence of BRs and compliance testing procedures, several studies have been carried out to assess the exposure for different conditions. The international epidemiological studies such as Cephalo, Interphone, Cosmos, Mobi-Kids, and Geronimo [47], [48] focus on brain exposure induced as a result of vicinity of the mobile phone during a voice call to the head tissues. In these studies, human brain exposure assessment has been carried out in different situations such as cheek and tilt positions [49], [50]. In order to assess the influence of phone antenna location, several studies have been carried out [24], [51] using Virtual Family head models and several types of phone models [46] with different antenna location. The exposure induced by these mobile phones has been computed by the FDTD method and the SAR value for different areas of head and brain has been concluded. These studies conclude that the position of the antenna in mobile phones and the number of antennas highly affect the induced exposure.

In addition to the source model and the location of the antenna, the emitted power by mobile phone influences the absorbed power. Concerning compliance testing, the mobile phone is forced to emit at its maximum power but the usual power emitted by mobile phones in real situations depends on network technology, environment, the quality of channel between mobile phone and BS, and also the body loss. Since the human body is placed in the near-field zone of

the mobile antenna, important coupling occurs between the body and the antenna which results in a strongly modified antenna pattern [52] (see Figure 12). This means that in different directions, the head-antenna radiation pattern is different hence the emitted power by mobile phone varies depending on the rotation of the user's head in relation to the base station.
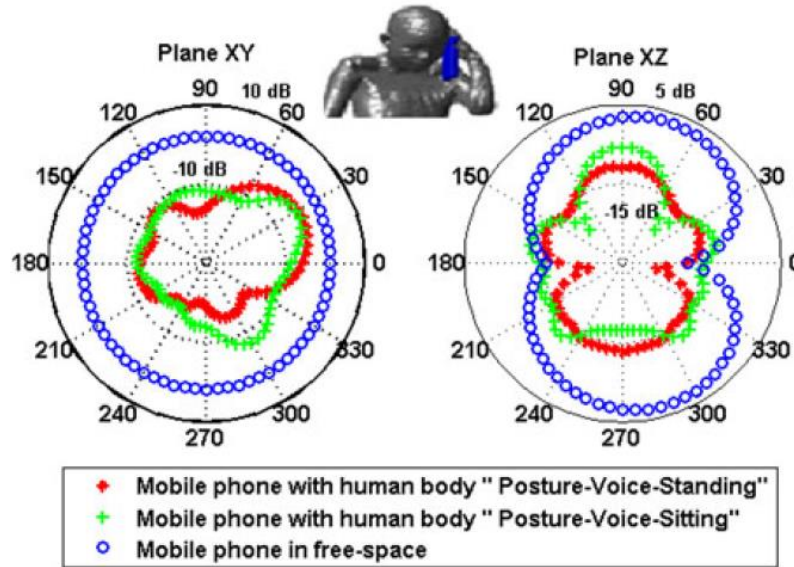
Figure 12, Radiation patterns of mobile phone in free space (blue) and with human body (red and green) to characterize the effect of coupling with head [52]

2.4.2 Experimental measurement for compliance testing in laboratory

The power emitted by the device can vary highly depending on network technology, handover procedures, adopted power control algorithms, etc [4], [53], [54]. In a compliance test point of view, these variabilities should be taken into account before putting the device to the market. In this regard, several methods and protocols are established to certify the level of exposure of the user device.

SAR measurement is performed by the E-field measurement inside the head phantom (SAM) or a phantom body filled with equivalent liquid. This setup consists of a robotically positioned probe and a SAR phantom filled with a tissue-equivalent simulating liquid. The robot is controlled by a computer to move the probe into the phantom's head while measuring the E-field (see Figure 13).

The main advantage of performing measurements is the possibility to assess the SAR value without dealing with uncertainties related to the body and source modeling. However, SAR

measurement becomes impossible when dealing with heterogeneous tissues because of the modification in the tissues in the vicinity of the measurement probe. To overcome this limit, in case of compliance testing, using a phantom head with an equivalent head liquid designed to overestimate the exposure and forcing the device to emit at its maximum power during the measurement can be used to apply the worst-case scenario. In this context, national research projects such as Comobio, Merodas, Adonis and Multipass granted by ANR (Agence National de la Recherche) have investigated the required measurement equipment and measurement protocols to assess the human exposure for SAR assessment.

A large number of studies carried out investigating the measurement probes, the E-field scanning systems [55], [56] and dielectric properties of human tissues [18], [57], [58]. Several studies are also dedicated to analyzing, test positions, and SAM phantom shape to guaranty that the measured SAR on phantom is always higher than the real SAR induced in head. The equivalent liquid has also been designed to guaranty a conservative assessment of SAR [59].
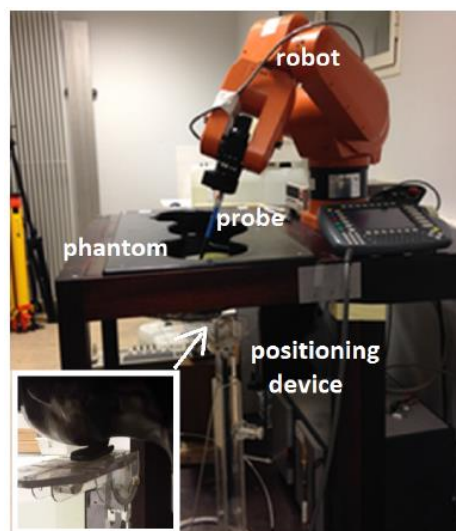
Figure 13, SAR measurement setup

This SAR measurement method is very time consuming and the number of configurations to be tested is increasing with the last mobile phone generation. To reduce the measurement time and facilitate the measurement procedure an improved vector-based measurement approach has been developed [60], [61]. This method uses arrays of probes instead of one single probe to assess the field in phantoms head. In this method, arrays of fixed probes are placed in a head phantom and the device under measurement which is controlled by a robot is placed near the head to perform the measurement (see Figure 14). By using this method, a full field

measurement can be performed instantaneously. Therefore it is possible to perform a large number of measurements to assess the SAR values for different configurations in a short period of time. Standardization of vector-based measurements is recently published in IEC 62209-3:2019 [62].
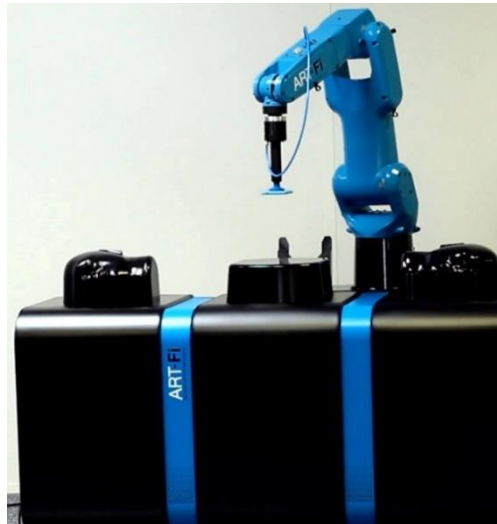
Figure 14, Vector-based SAR measurement setup [60]

2.5. Actual exposure assessment

As mentioned before, worst-case scenarios are used to check the compliance of the level of exposure. In this case, the exposure assessment is conservative and can lead to an overestimation of the exposure. However, the levels of exposure assessed for the purpose of compliance are not representative of the actual exposure occurred daily. Actual exposure assessment is a very useful concept because, on the one hand, the general public can understand how they are exposed in day to day life and on the other hand it is useful for epidemiological studies to verify that no health effects are caused below the exposure levels.

Considering cellular networks, the downlink exposure is linked to the amount of power density received by the human body and the uplink exposure is linked to the amount of power emitted by users' devices. In cellular networks the downlink exposure is continuous since the BSs emits all the time however the uplink exposure is induced only when the device is being used. For both cases, the exposure depends on the posture of the person. Two main postures are considered in the assessment of uplink and downlink exposures: standing and sitting. Generally, standing posture is used to assess the exposure of a person outdoor and the sitting posture for indoor environments.

Several projects and studies have been conducted to characterize the actual exposure induced by different wireless communication networks such as LEXNET and AMPERE projects. In [63] a series of sensors are implemented over an urban environment and performed temporal downlink E-field measurement over one year on GSM and UMTS technologies frequency bands. As presented in Figure 15, it can be observed that the measured total downlink E-field during one day varies highly depending on the time of the day. During the night the exposure is very low however during the day the exposure is higher because of the traffic variation. The total measured E-field for one week also shows the variability of the level of exposure during different days of a week for the same reason.

BS antennas are high powered transceivers which transmit continuously. However, the value of absorbed peak density power highly depends on the distance between the person and the BS antenna. Studies have demonstrated that more than 60% of measured total downlink EMF exposure values were below 0.003 W/m^2 and less than 1% above 0.095W/m^2 and all the values were below recommended exposure limits [64].

Considering the uplink exposure, for the compliance testing the user equipment is forced to emit at its maximum power during measurement. However, in real networks, the emitted power by the device depends on the power control algorithms that optimize the link between BS and the device.
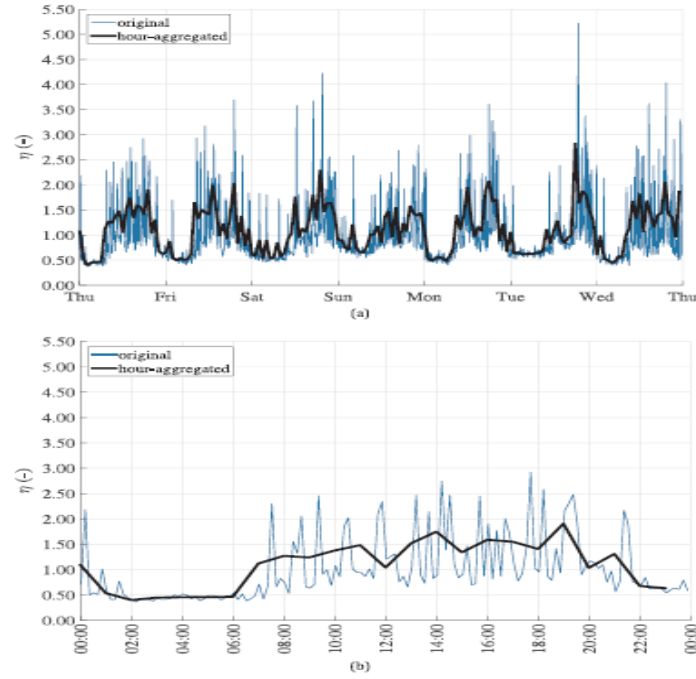
Figure 15, Relative total electric-field strength measured during one week (a) and one day (b)[63]

Part of studies [65], [66] have shown that in GSM networks, handover procedure (the process of transferring an ongoing call or data session from one BS to another) has a great influence on the measured mean emitted power using Test Mobile Phones (TEMS) or software-modified phones (SMP). Once the handover procedure is finished, the network starts to adapt UE's power to the minimum necessary. Statistical analysis of uplink emitted power in a GSM network shows that the UE emits about 20-50% of its maximum transmission power (2W theoretically). In the case of UMTS, the handover procedure does not affect the emitted power by UE. Studies have shown that the mean power emitted by UMTS in voice call usage was close to 1% the maximum power (0.25W theoretically) [54]. However, in both cases, the emitted power by UE depends on the path loss between UE and BS.

The emitted power by UE depends also on usage. For instance, the exposure of a person using UE in voice circuit mode is linked to the mean power emitted by UE during the call duration, however, in data usage mode, the emitted power and the duration of power emission depends on throughput. As a result, it depends on available uplink resources and interferences. In LTE the emitted power by UE depends also on the number allocated uplink resources block to the UE.
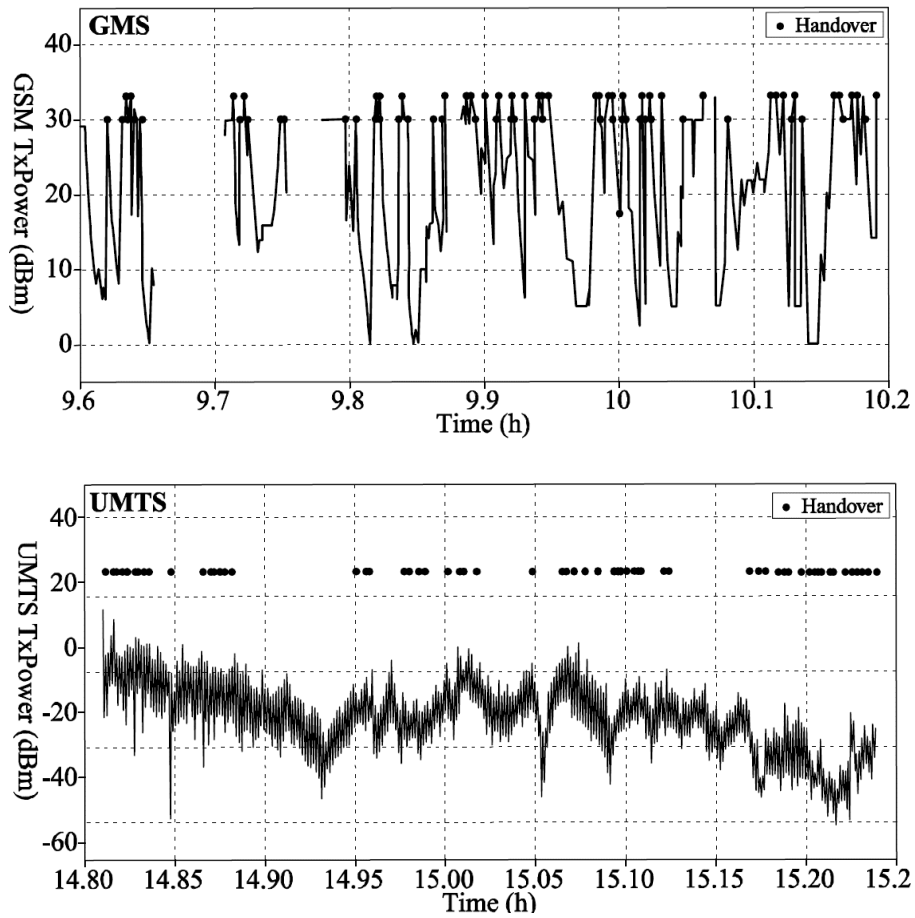
Figure 16, The influence of handover on transmitted power for GSM (up) and WCDMA (down) In voice call mode. Instantaneous power (filled curve) and handover (dots)

2.6. Global Exposure

2.6.1 Relation between RX and TX

Studies have shown that when the received signal from the base station is higher, the emitted power by UE is lower and vice versa [54]. In 3G, due to its fast and efficient power adaptation algorithms, the emitted power depends highly on the received power from the BS and it varies from -60dBm to 23 dBm. In 2G, the same effect has been observed, however, because of the maximum emission during handover, less efficient power adaptation procedure and the limited power emission dynamic range in GSM [4] the negative correlation between the revived power density and the emitted power by UE is less obvious (see Figure 17).
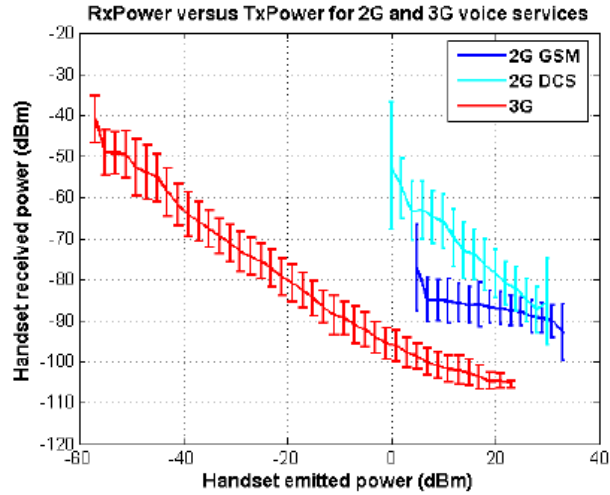
Figure 17, the measured received power by UE in terms of uplink emitted power in GSM (blue curve), DCS (light blue) and UMTS (red), vertical lines represent the standard deviation and the horizontal line the average RX [4]

LTE uses a very efficient power control algorithm (see Section 3.5). This power control algorithm depends on a series of parameters including the path loss between UE and BS measured by UE. Briefly, if the path loss between BS and UE is higher which means that the received power density by UE is lower, the emitted power by UE will be higher to compensate for the path loss. The correlation between TX and RX can be observed in Figure 18.

This strong correlation between the emitted power and the received power density by UE drives us to conclude that in case of actual exposure, the uplink and downlink exposure should not be assessed separately. Furthermore, the global exposure of a person induced by cellular networks is a combination of exposure induced by user's devices and the exposure induced by the BSs.
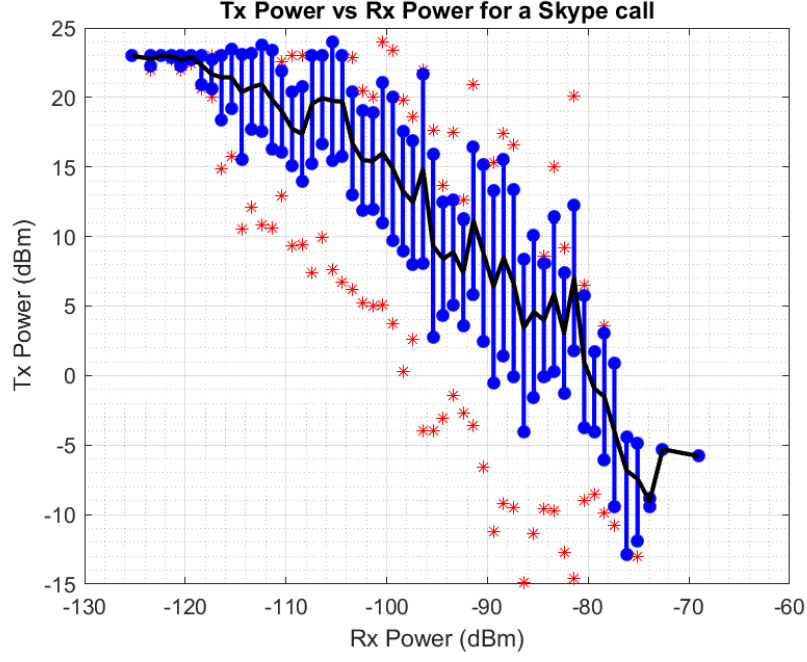
Figure 18, RX and TX measured in LTE technology, black line represents the mean value, blue line the standard variation, and red points the minimum and maximum measured values of TX.

Global exposure is a notion, in which the uplink and downlink exposure of a user is taken into account simultaneously. This notion provides more information about user exposure and sources of exposure. For instance, if a user is located far from a BS thus users downlink exposure is very low, it does not mean that the user's global exposure is low since the UE emits at its maximum power [43].

$$Global\ Exposure = Exposure_{user\ device} + Exposure_{base\ station} \qquad (14)$$

As it is mentioned earlier, the downlink exposure is permanent since the network antenna emits at all times, however, the uplink exposure is induced only when the mobile phone is used hence it is variable in time. Therefore, it is of interest to compare these exposures averaged over time. To assess the average global exposure over time T, the equation (14) can be extended to:

$$Global\ Exposure\ = \frac{T_1}{T} WBSAR(posture(t),t)_{user\ device} + WBSAR(posture(t),t)_{base\ station} \qquad (15)$$

Where T_1 is the time that the device is in power emission state and T is the time that the exposure is averaged over. It is worth mentioning that instead of whole-body SAR values, local SAR (averaged SAR over an organ, part of body, head etc.) can be used.

In order to easily assess the SAR value induced by cellular networks in downlink and uplink directions, a series of Reference SAR data are computed in the context of LEXNET project [67] using numerical simulation platforms based on FDTD method. These values are computed for uplink and downlink exposures for Virtual Family anatomical body models for standing and sitting postures. Three different usages are considered: a mobile phone voice communication (phone near the head), mobile phone and tablet data usage (device in users hands in front of body), and also laptop usage (laptop placed on knees). These reference SAR values for different frequencies are presented in Table 3 in uplink and downlink directions. The uplink SAR values induced by users device are normalized to a reference transmitted power of 1W and the downlink SAR values induced by an incident frontal plane wave are normalized to a reference received power density of 1W/m2.

Table 3, Whole-body SAR values W/kg for child and adult models for different usage and frequency bands

WBSAR	Usage	Downlink/ Uplink	Frequency band		
			900 MHz (GSM)	1940 MHz (UMTS)	2600 MHz (LTE)
Child sitting	Voice	Downlink	0.0089	0.0071	0.0066
		Uplink	0.029	0.011	0.014
Adult sitting	Voice	Downlink	0.0056	0.0043	0.0039
		Uplink	0.012	0.0052	0.0047
Child standing	Voice	Downlink	0.0084	0.0077	0.0071
		Uplink	0.029	0.01	0.015
Adult standing	Voice	Downlink	0.0052	0.0046	0.0042
		Uplink	0.012	0.0052	0.0053
Child sitting	Data	Downlink	0.0088	0.0071	0.0065
		Uplink	0.011	0.0135	0.0094
Adult sitting	Data	Downlink	0.0046	0.0043	0.0038
		Uplink	0.0056	0.0081	0.0037
Child standing	Data	Downlink	0.0090	0.0077	0.0072
		Uplink	0.01	0.0109	0.0083
Adult standing	Data	Downlink	0.0052	0.0047	0.0042
		Uplink	0.0049	0.0039	0.0029

As it is mentioned earlier, these values allow us to assess the downlink exposure by measuring or computing the received power by the human body from the base station and the uplink exposure can be assessed by measuring or computing the emitted power by UEs antenna.

2.6.2 Global exposure and Exposure Index (EI)

As previously stated, the methods used to verify compliance of exposure do not take into account the uplink and downlink exposure simultaneously. For this reason, a new metric called Exposure Index (EI) has been introduced in the framework of FP7 LEXNET project. EI enables the quantification of population exposure. It quantifies the whole or partial body global exposure (induced by UE and infrastructures), averaged over time and over a population in a given geographical area taking into account space, time, population, usage, and technology. EI metric aggregates the exposure induced by both near-field and far-field sources for a given geographical area and can be described as the following [6]:

$$EI^{SAR} = \frac{1}{T} \sum_t^{N_T} \sum_p^{N_P} \sum_e^{N_E} \sum_r^{N_R} \sum_c^{N_C} \sum_l^{N_L} \sum_{pos}^{N_{pos}} f_{t,p,e,r,l,e,pos} \left(\sum_u^{N_U} (d^{UL} \bar{P}_{Tx}) + d^{DL} \bar{S}_{RXinc} \right)$$

(16)

EI^{SAR} is the Exposure Index value, the average exposure of the population of the considered geographical area over the considered time frame T. SAR refers to whole-body SAR, organ-specific SAR or localized SAR.

- N_T is the number of considered Time periods of time frame T
- N_P is the number of considered Population categories
- N_E is the number of considered Environments
- N_R is the number of considered Radio Access Technologies (RAT)
- N_C is the number of considered Cell types
- N_L is the number of considered Load profiles
- N_{Pos} is the number of considered Postures
- N_U is the number of considered Usages with devices

EI takes into consideration different exposure sources and exposure situations. The formulation of EI contains a set of different parameters such as different time periods (t), different

population categories (p), different environments (e), network technologies (r), cell types (c), different load profiles (l), body postures (pos) and usages (u).

Ptx is the mean TX power transmitted by UE during the uplink usage period. $S_{Rx,inc}$ represents the mean incident power density on the human body during period t. The coefficient d^{UL} is the uplink normalized exposure induced by UE. It is expressed as an absorbed dose normalized to a transmitted power of 1 W:

$$d^{UL}_{s/kg} = \frac{TD^{UL}_{t,p,l,e,r,c,u,pos[s]} SAR^{UL}_{p,r,u,pos[\frac{W}{kg}]}}{P^{ref}_{TX[W]}} \tag{17}$$

Where:

TD^{UL} is the time duration of usage u, for user profile l, when connected to the RAT r, operating in cell type c, in environment e, for the population category p, in the posture pos, during the time period t.

SAR can be the whole body or an organ-specific or tissue-specific SAR value for the usage u and the posture pos, in the frequency band of RAT r, and the population category p, calculated for an incident emitted power of P^{ref} and normalized to this power.

The coefficient d^{DL} is associated with the exposure induced by the downlink. It is expressed as an absorbed dose normalized to an incident power density of 1W/m2.

$$d^{DL}_{[\frac{s}{kg}]} = \frac{TD^{DL}_{t,p,e,r,c,pos[s]} SAR^{DL}_{p,r,pos[\frac{W}{kg}]}}{S^{ref}_{inc}} \left[\frac{W_s}{kg} / \frac{W}{m^2}\right] \tag{18}$$

Where:

TD^{DL} is the time duration of posture pos, when connected to the RAT r, operating in cell type c, in the environment e, for the population p, during the time period of t.

SAR^{DL} can be the whole body or an organ-specific or tissue-specific SAR value induced by the base station or access points of RAT r, in the population p, for the posture pos, normalized to the power density S^{ref}.

Finally, the coefficient f is the fraction of the population p, with user profile l, in posture pos connected to RAT r for cell type c in environment e during time t.

2.6.3 Exposure index assessment in classic cellular networks

As mentioned earlier, EI is a transfer function that takes into account a highly complex set of data such as geographical areas, the period of the day, age, networks, usages, etc. EI has been assessed for a scenario involving an urban Macrocell LTE network in [6]. Life segmentation data are collected through the surveys in different countries to understand how different categories of population segment their daily lives. ICT usage data are collected by measuring network Key Performance Indicators (KPIs) to find out the uplink and downlink traffic, user's usages, the number of voice calls, duration of voice calls and Power densities and transmitted powers were calculated using network planner simulation tools. Results show that the EI value for whole-body SAR of the over 15 years old population of the seventh district of Paris, considering a Macrocell network is $3.19 \times 10^{-7} \, W/_{kg}$.

The average global exposure for the population induced by macro 3G networks in different geographical areas in France and Serbia is compared in [68]. By using survey data on age distribution over the population and measured ICT data, the EI induced by 3G Macrocell networks has been computed as $5.6 \times 10^{-7} \, W/_{kg}$ and $6.2 \times 10^{-7} \, W/_{kg}$ respectively in French urban and suburban area while in case of Serbia it is estimated to be respectively $2.9 \times 10^{-7} \, W/_{kg}$ and $2.7 \times 10^{-7} \, W/_{kg}$. The results show that the average EMF exposure can significantly differ from one geographical area to another due to the impact of network architecture and ICT usage differences. It is also shown that the contribution of uplink exposure is much higher (95%) than the downlink exposure (5%) in global exposure. Also, indoor exposure has a much greater impact on global exposure comparing to outdoor exposure. This is due to the higher emitted uplink power by UEs in indoor areas. Indeed these values can differ for other countries, for different technologies and periods thus should not be generalized.

2.7. Exposure in heterogeneous networks

As explained in Chapter 1, today operators are adopting new network architectures such as heterogeneous networks (HetNets) where small cell (SC) base stations will be densely deployed within Macrocells (MCs), providing also a smooth migration path towards the fifth-generation (5G). In contrast to MCs, SCs are low-powered, low-height base stations with coverage ranging from 10 meters up to a few hundred meters [69]. Deploying SCs results in offloading traffic from Macrocells, hence, network performance, coverage, and capacity is increased. Dense

deployment of SCs, in indoor as well as in outdoor environments, would provide better propagation conditions for the connected user equipment and therefore, high-speed connectivity.

According to 3GPP several classes of relay antennas have been standardized:

- **Long range antennas**: (emission power more than 6.3 W): This class of antennas (also called Macrocells) are used for the usual network of operators and they cover fairly large cells (several hundred meters in urban areas several kilometers in rural areas).

- **Medium range antennas**: (emission powers between 0.25 W and 6.3 W): This Antenna class refers to transmitters intended for use outdoors, on street furniture for example. These antennas (also called "Small cells"), coverage area varies from a few tens to a few hundred meters.

- **Local coverage antennas**: (emission powers between 0.1 W and 0.25 W) this class of antennas (also called "Micro cells") is used to improve the coverage inside buildings, for example in shopping malls, offices, or parking.

- **Residential coverage antennas**: (emission powers less than 0.1 W) this class corresponds devices used in private homes (also called "Femtocells"), with coverage comparable to that of WiFi routers.

Depending on the initial coverage of the macro network and the network loads, the deployment of small antennas makes it possible to reduce the transmission power of the mobile (comparing to macro networks), and/or increase the throughput due to vicinity to the small cell antenna.

A series of studies have been carried out to assess the impact of heterogeneous network architecture on exposure. Studies on indoor UMTS Femtocell deployments show that the emitted power by UE thus the uplink exposure can be drastically reduced thanks to the vicinity of UE to the base station [70]. The magnitude of the uplink exposure reduction depends on the UE usage time [71]. If a person is a heavy mobile user the reduction in uplink exposure results in significantly lower global exposure. However, if the UE is not used, the global exposure is increased because in this case the uplink exposure contribution is not significant and the downlink exposure is the sum of the exposure induced by existing Macrocells, Femto and Small cells.

In case of Femtocell deployment in a train environment, it is shown that the exposure induced due to handover procedure is eliminated thus the uplink exposure especially in the case of GSM technology is reduced. In any case, the global exposure depends on a series of parameters such

as the output power of the Femtocell, the number of Femtocells, the number of users in the train, and also how long users use their UEs [72]. Implementing a Femtocell in a train instead of relying on Macrocell reduces EI for the considered scenario[6] due to the reduction of UL exposure contribution to EI.

The exposure induced in a densified SC LTE network has been characterized through simulations [73] for a scenario in which a series of SCs are uniformly distributed in an LTE network with constant inter-site-distance. It is demonstrated that in a denser network the downlink and uplink throughput are higher compared to an only Macrocell scenario. Furthermore, the received power density is lower due to the traffic offloaded by SCs thus interference reduction, and the emitted power by UE is also lower due to the vicinity of UE and SC [74], [75]. Despite these results, there is a lack of information about the induced exposure in a real heterogeneous LTE network. As it is mentioned earlier in this chapter, indoor exposure assessment is a crucial task since the population spends most of their time in indoor areas. In this regard, modelling the exposure induced by outdoor SCs can provide the possibility to estimate the exposure of indoor population and also to assess the EI for the whole population. Chapter 3 is dedicated to answer to these needs by assessing the uplink and downlink exposure induced by outdoor Small cells in real LTE networks and compare them to the ones induced in Macrocell networks.

2.8. The influence of Technology and Usage on human exposure

Since the introduction of smartphones, mobile phones are used for a variety of tasks including making calls. Users use their mobile phones to make Voice over IP calls which provide a better voice/sound quality with lower costs, especially for international calls. LTE technology provides a native VoIP service called Voice over LTE (VoLTE) which is largely used internationally by cellular network operators to offer voice calls through LTE.

Regarding voice calls, the exposure depends on various parameters such as the design of the mobile phone, the position of the mobile phone and its antenna according to the head and the emitted power of the device during a voice call. The influence of the design of the mobile phone, as well as the effect of the position relative to the user on RF exposure, has been carried out in previous studies [52]. The emitted power by the UE, however, is a highly variable parameter which depends on the technology and algorithms through which voice communication is performed such as power control algorithms, voice activity detection (VAD), compression and

encapsulation algorithms, conversation rate, distance from the base station, etc [53]. Regarding mobile phone VoIP applications, each application uses its specific compression, encapsulation and VAD algorithms. Native VoIP applications such as VoLTE seems to have a better performance in terms of quality service and bandwidth utilization thanks to their optimized use of physical layer resources. Hence, the variation of the emitted power of mobile phone using these applications should be investigated for deferent technologies.

A series of studies have been conducted to evaluate the emitted power by mobile phone in real conditions for different usages regarding human exposure assessment. The variation of the emitted power by UE in a GSM network has been investigated through statistical approaches [53]. It is demonstrated that the emitted power by UE is principally determined by the power control mechanism. Regarding the uplink emitted power by UE connected to UMTS network studies have demonstrated that on average the UE emits less than 1% of the time at its maximum power [54]. It is also demonstrated that the emitted uplink power highly depends on the downlink received field from the base station. This study [76] illustrates that the radiated power by UE during switched circuit call and VoIP call in UMTS network show that the mean emitted power by UE during a UMTS VoIP call can be up to three times higher than the emitted power during a UMTS switched circuit call, however, the emitted power level even in case of a VoIP call is very low [77].

The amount of emitted power in terms of application is measured for data uploading, VoIP voice call, streaming, Facebook browsing, and circuit-switched voice call usage in both UMTS and LTE technologies [78] in only one location. Therefore, the effect of channel condition on the emitted power is not taken into account which makes it impossible to compare the emitted powers in different technologies, however, the highest power levels occur during data uploading applications.

In Chapter 4 the assessment of the actual UL emitted power for different usages and technologies in multiple indoor and outdoor locations is investigated. Moreover, contrary to data usage, voice call communication requires a constant, continuous, and relatively low throughput. This implies the fact that the amount of power emitted by UE as well as the exposure duration during a call should be different from the data usage. In addition, new types of voice communication use different technologies to transmit data whose effects on exposure should be investigated. The last section of Chapter 4 is dedicated to assess the exposure duration for different voice technologies and compare them to each other.

2.9. Conclusion

This chapter was dedicated to providing the current state of the art on human exposure assessment. The variability of SAR in terms of influencing parameters such as body morphology, frequency, and age is presented. Two main types of exposure assessments exist. Normative exposure assessment for worst-case exposure evaluation and actual exposure assessment to evaluate the actual day to day RF-EMF exposure of a person or a population. EI metric enables the assessment of actual population exposure by using a large number of parameters such as technology, usage, cell type, user's posture, and exposure time for both the downlink and uplink exposures.

Densifying Macrocell networks by small cells will have an important impact on human exposure, especially in UL direction. The vicinity of the UE to the BS antenna will provide a better channel quality thus due to UL power control algorithms the UE TX power will be reduced. The impact of SC implementation is investigated in the next chapter.

UL exposure is linked to the usage because the UE TX power, throughput, and emission duration vary for different usages. Besides, each technology uses a specific power control method which affects the UE TX power and emission duration. The effect of these new usages on actual exposure is investigated in Chapter 4 for GSM, UMTS, and LTE technologies.

3. INFLUENCE OF NETWORK DENSIFICATION ON HUMAN EXPOSURE

3.1. Introduction

Current cellular networks mainly consist of Macrocells (MC) which are high power emitted cell sites typically located at on a tower or on buildings to cover a large area (up to several kilometers) with an output power of typically tens of watts (see Section 2.5.4). Since MCs cover a large area, the number of connected users to one MC and data traffic can be high enough to saturate the cell capacity in crowded environments and during internet rush hours. Also, MCs cell-edge users may suffer from poor channel quality due to their distance to MC antennas. To overcome these limitations and to respond to the expected extreme increase in data traffic in the future, cellular network operators are densifying their networks by adding Small cells (SC) to their existing networks to locally increase cell capacity and coverage. SCs are low power cells with output power less than 6.3 watts placed at lower heights (comparing to MCs). Figure 19 illustrates an example of implemented SC on street furniture.

Figure 19, Implemented SC on top of a bus station in Amsterdam [79].

The extensive implementation of such SCs will significantly improve network performances in terms of coverage and network capacity. However, this may influence human exposure to RF-EMFs. As mentioned in Chapter 1, the UL and DL exposure are different in a heterogeneous network (compared to homogeneous one) since the SC antenna is closer to the user, the emitted power by SCs is lower and SCs will be deployed massively comparing to classical MCs. This chapter is dedicated to characterizing the UL and DL exposure in an LTE classical MC network and in heterogeneous networks in different configurations through measurements performed in three different cities with different network architectures.

Previous studies [6], [72], [80] are mainly based on results from simulations, thus exposure induced in heterogeneous networks should be investigated in actual scenarios through

experimentation. Moreover, due to the difficulties regarding performing measurements in indoor areas, there is a lack of information about real exposure in indoor environments, nevertheless, the latter is a crucial task since the population spends most of their time in indoor areas [4][5]. In this regard, modelling the exposure induced by SCs can provide the possibility to estimate the exposure of indoor and outdoor populations and also to assess the EI for the population.

Toward this, three measurement campaigns have been carried out in three different cities: The first one has been carried out at Basel, Switzerland, in a homogenous MC network, The second and third campaigns have been carried out in LTE heterogeneous networks including MCs and SCs in two French urban cities Annecy (4 SC sites) and Montreuil (5 SC sites).

In the following sections, measurement configuration and materials are presented. Experimental assessments are discussed for each measurement campaign as well as models built to assess the global exposure and Exposure Index (EI) (see Section 2.6.2) for a population. Finally, with the help of this model, the exposure of users located in outdoor as well as indoor environments are assessed and the EI is computed for a simplified scenario.

3.2. Measurement description

Narrowband E-field measurements have been performed to characterize the variation of E-field generated by cellular networks at specific frequency bands used by different operators by using a spectrum analyzer (Narda SRM-3006) connected to an isotropic three-axis E-field antenna with a frequency range of 30 MHz-3 GHz. The dynamic range of the spectrum analyzer and the antenna is 0.2 mV/m-200 V/m [83]. For campaigns where the spectrum analyzer is used, the E-field is recorded in frequency bands corresponding to downlink LTE bands of network operator.

In LTE technology, RSRP (Reference Signal Received Power) and RSSI (Received Strength Signal Indicator) are used by the user equipment (UE) to assess the signal level and channel quality, as it is specified by 3GPP 36.213 [69]. The RSRP is the average narrowband received power of the resource elements that carry cell-specific reference signals from the primary BS. RSSI is the wideband received power including interferences from other cells, computed only over the UE allocated band. As a result, the total received power over the whole bandwidth from one BS is not proportional to reported RSSI but to RSRP. Hence RSRP can be considered as a measure of DL exposure induced by the BS that UE is connected to, even though it does not take into account environment noise and interferences.

The UL exposure is linked to the emitted power by UE but also to the user's posture (see Chapter 2). Considering only data usage for which the mobile phone is held by hands in front of the user, the UE TX power can be measured to perform comparison and analysis in terms of EMF exposure. According to 3GPP, the UE TX power is determined through a series of uplink power control algorithms [69]. In case of LTE, on PUSCH (Physical Uplink Shared Channel) channel, a complex and efficient algorithm is implemented to control the emitted power on the data channel. This algorithm is explained in Section 3.5 and takes into account a series of parameters such as the number of uplink allocated resource blocks and the measured path loss between UE and BS.

As mentioned in Chapter 2, the exposure's dose or the averaged exposure over a given time are linked to the power emitted from BSs and UE as well as the exposure duration. In case of DL exposure, since the BS antennas are emitting permanently the DL exposure is permanent and the amount of received power density by the human body depends on the path loss between UE and BS, on BS data traffic and on the number of users connected to the BS. Regarding UL exposure, the duration (for data usage) may be inversely proportional to the data throughput. In other words, for a constant data volume, the transmission time is lower with higher throughput. Consequently, to assess and characterize the UL exposure, both UE TX power and throughput have to be taken into account. In this regard, the best-suited method to assess UE TX power, RX power, and throughput is to use handheld drive test solutions (a.k.a. trace mobile phones). These special mobile phones are capable of performing measurements as an end-user allowing to measure and record the RSRP, UE TX power, throughput, uplink power control algorithm parameters, etc. Hence, we have used three different trace mobile phones during measurements:

- Viavi JDSU [84] solution installed on Samsung Galaxy S4
- AZENQOS [85], developed by Freewill FX Company Limited and installed on LG Nexus 5X.
- Nemo Handy Handheld Measurement Solution [86] installed on a Sony Xperia XZ Premium.

There are some differences between these trace mobile phones. While the sampling period of JDSU is not constant, that of AZQ and Nemo is constant where each sample is the average value over the sampling period. To be able to compare the measurement results of these trace mobile phones the data is post-processed by computing average values per second. Moreover, JDSU and Nemo provide TX power over the PUSCH channel however AZQ provides the total emitted power including PUCCH (Physical Uplink Control Channel), SRS (Sounding

Reference Signal) and PRACH (Physical Random Access Channel) channels. Nemo handy, JDSU and AZQ trace mobiles are used in Annecy and Montreuil measurement campaigns while only Nemo Handy is used in Basel campaign.

3.3. Basel measurement campaign (Macrocell measurements)

A measurement campaign has been carried out in June 2019 at Basel, Switzerland on 14 sites. Sites have been chosen to cover urban and sub-urban environments including 12 indoor and 2 outdoor locations. Network architecture consists of only MCs and measurements have been performed on 3 operators.

Table 4, list of measurement locations

Nr	Floor(s)	Location type	Environment	Micro-environments: more specifically
1	1	Public building	Urban	Swiss TPH offices on the 3rd floor.
2	1	Public building	Urban	Department store, restaurant
3	1	Public building	Urban	Library
4	0	Public building	Industrial	Department store, Entrance
5	0	Public building	Industrial	Shopping center
6	0	Public building	Suburban	Library
7	0	Public building	Suburban	Library
8	2	Public building	Rural	Library, Cafe
9	0	Transport (train station)	Urban	Waiting area
10	0	Transport (train station)	Suburban	Waiting area
11	0	Public building	Suburban	Cafe
13	0	Public building	Suburban	Cafe
13	0	Outside 2	Suburban	Playground
14	0	Outside 3	Rural	Playground

At each location, measurements are performed on one stationary point. Nemo Handy trace mobile phone is used to measure the UE emitted and received power, throughput and power

control algorithm parameters. The mobile phone was forced to connect only to LTE network. To mimic an uplink data usage, trace mobiles were programmed to upload a 100 MB file to a server through FTP protocol. The choice of 100 MB file is to record enough data to capture the variation of throughput. In order to simplify the measurement protocol and enable the repeatability of the experiment, the trace mobile phone was programmed to repeatedly upload the file for 5 minutes.

Since measurements are performed at a static point for each location, the level of RX and TX powers can differ from one location to another depending on the distance to the base station, the number of doors, windows, walls, furniture and interior architecture of the location. **Erreur ! Source du renvoi introuvable.** and Figure 21 illustrate the TX and RX powers for two different locations and it can be seen that at each location the TX and RX powers levels are different. Since measurements are performed on various sites in indoor and outdoor environments, the aggregation of all 14 sites covers nearly all the possible values for TX and RX powers.
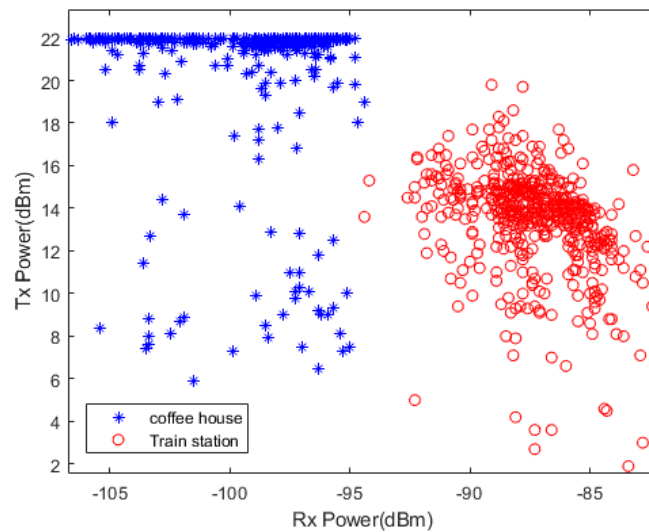
Figure 20, TX and RX power variations for two different locations for LTE data usage measured in Basel.
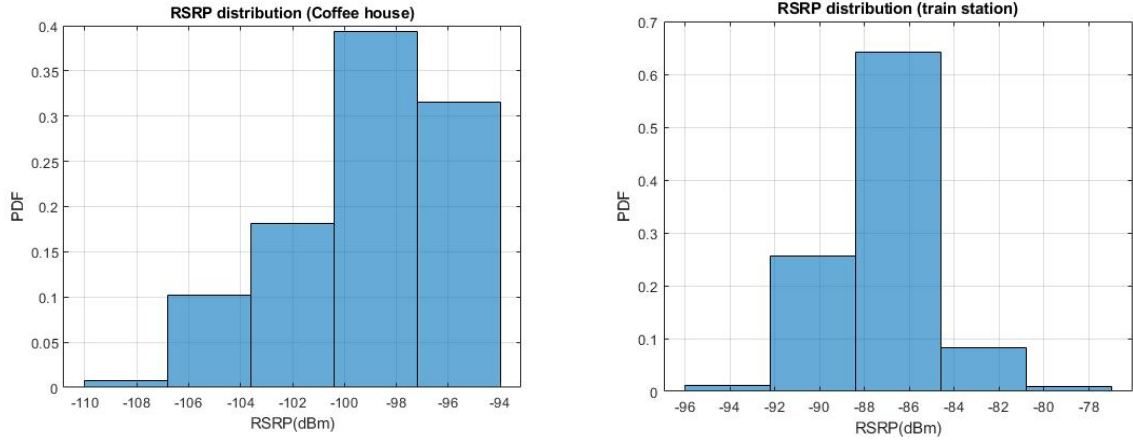
Figure 21, The distribution of RX values for two different locations for LTE data usage measured in Basel.

Results for indoor and outdoor locations have been investigated. Measured data consist of the recorded values for three operators in these environments. As explained in Section 2.6.1, the uplink emitted power is determined in a way to adapt to the channel condition especially path loss. Path loss is inversely proportional to the RSRP. The distribution of RSRP for Basel measurements is presented in Figure 22.

Accordingly, measured RSRP for indoor locations is on average 20 dB lower than the measured RSRP for outdoor cases (see Table 5), illustrating that the path loss in indoor locations is higher comparing to outdoor locations due to the loss in walls and furniture. As shown in Figure 23, the emitted power by UE is higher in indoor locations due to the lower measured RSRP values.
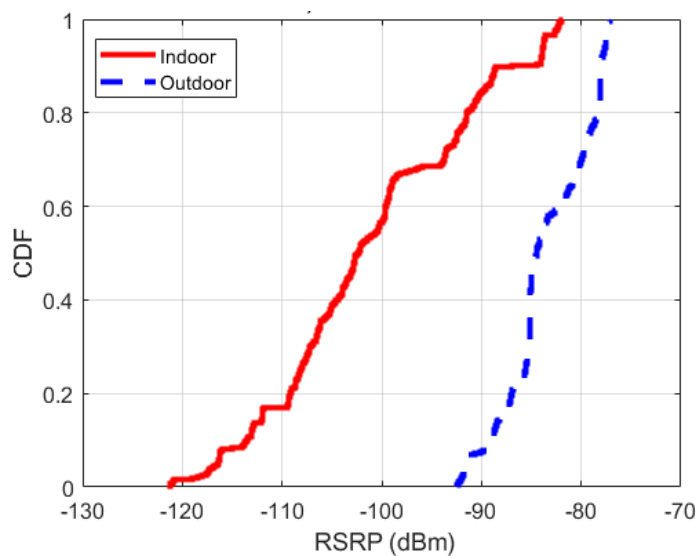
Figure 22, CDF of measured RSRP for indoor and outdoor locations in Basel campaign
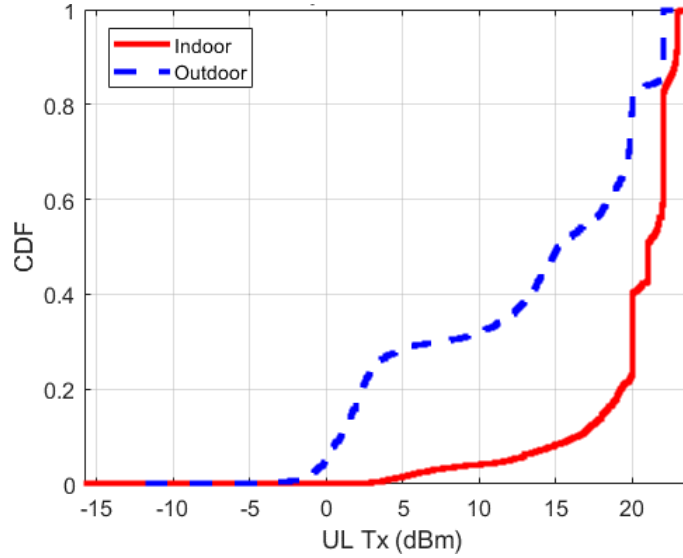
Figure 23, CDF of measured LTE uplink emitted power by UE for indoor and outdoor locations in Basel trial

It is worth mentioning that the UE TX power is roughly inversely proportional to the RSRP value, however, it is also linked to other parameters such as available physical resource blocks (PRBs). Besides, the UE TX power is limited by its maximum authorized value which in this case is 24 dBm. This correlation between received and emitted power is observed in GSM and UMTS technologies as well [4], [54]. These results show that for indoor users, the received power by UE is on average 20 dBm lower, comparing to the outdoor users, however, the average emitted power by UE in indoor areas is 7dBm higher due to the lower measured RSRP in indoor areas (see Table 5).

The contribution of all 14 sites in measured RSRP and UE TX power is represented in Figure 24. It can be observed that the UE emits higher than 0 dBm most of the time. This is due to the fact that the number of allocated PRBs to the user is relatively high since it is transferring data continuously. Also, the majority of measurements are performed in indoor areas where path loss is high and UE emits at its maximum allowed power (24 dBm). For higher RX values, the emitted power is reduced down to -10 dBm. Figure 25 represents the PDF of the UE TX power for all the measurements.

Table 5, Measured RSRP and UE TX powers for indoor and outdoor locations in Basel campaign

Parameter	Scenario	Mean (dBm)	Median (dBm)	Quantile 95% (dBm)
RX (RSRP)	Indoor	-101.6	-102.4	-83.7
	Outdoor	-83.4	-84.5	-77.6
	Aggregated	-97,6	-98.9	-81,2
UE TX power	Indoor	20	21	23
	Outdoor	13.7	15.20	22
	Aggregated	18.7	20.8	23
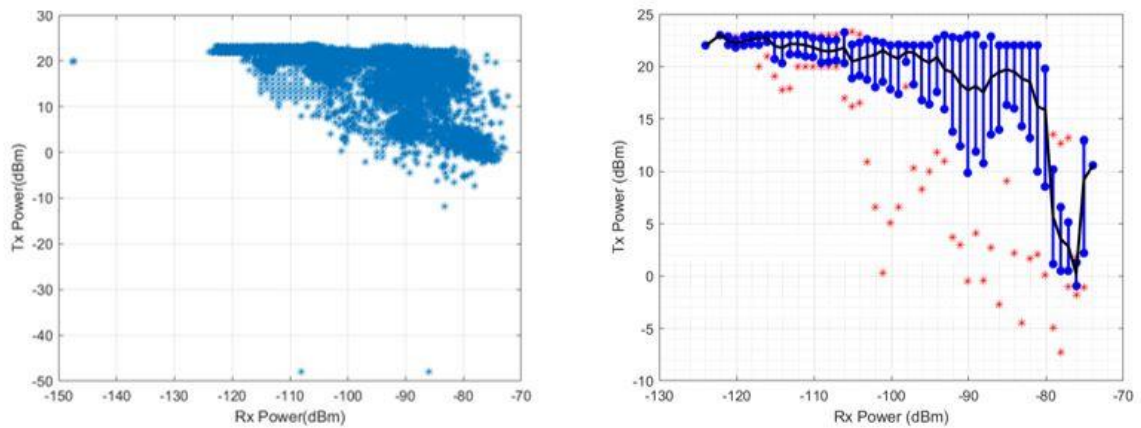
Figure 24, UE TX vs RSRP for LTE technology in Basel campaign, on the left scatter plot and on the right red dots represent the minimum and maximum values, blue lines represent the standard deviation and black lines represent the average value
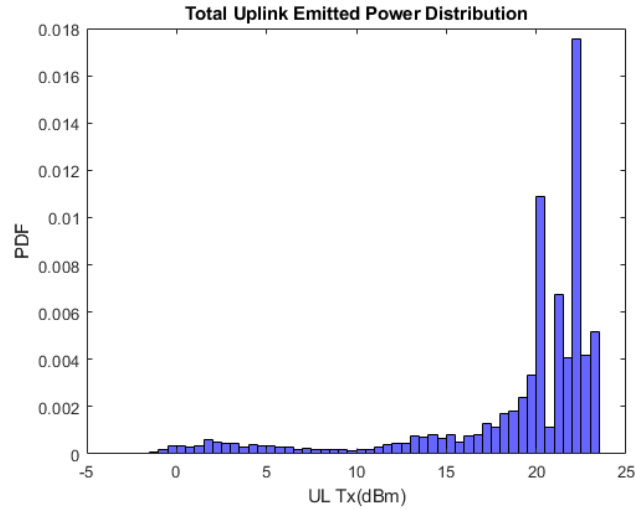
Figure 25, PDF of measured UL emitted power for all measurements

3.4. Annecy and Montreuil measurement campaigns (Small cell measurement trials)

3.4.1 Measurement description

In France, between 2016 and 2017, trials have been conducted by different mobile operators on the deployment of clusters of LTE SCs completing the LTE MC existing networks [87]. During two of these trials, we had the opportunity to perform a series of measurements on the SC sites installed on top of advertisement panels and bus stops (see Figure 26).
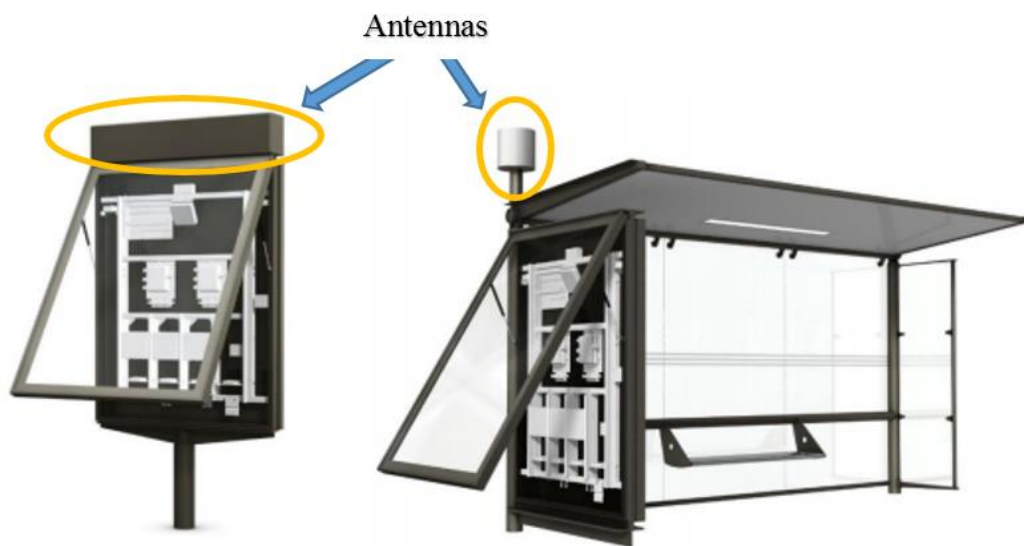
Figure 26, SCs installed on top of bus stops and advertisement panels

Our first set of experiments on heterogeneous networks is performed in Annecy, France in 2017. Annecy trial consists of four SC sites, two of which were placed near to an MC antenna and the other two on the MC cell edge. SCs provide coverage for LTE technology at 2600 MHz with a frequency band of 20 MHz. SCs were equipped with directional antennas at a height of 3m. Annecy is a tourist city with a population density of 1900 people/km². Since measurements were placed during the low season (January-February), the number of users connected to the SC simultaneously tends to be low.

The second experiment on heterogeneous networks was executed in Montreuil during July 2017. Montreuil trial consists of five SC sites. Two LTE frequency bands were activated on SCs: 1800 MHz with 20 MHz of bandwidth and 2600 MHz with 15 MHz of bandwidth. Contrary to the Annecy trial, in Montreuil, Carrier Aggregation (CA) was activated in the downlink direction. CA is a technique used in LTE networks to increase the throughput by assigning multiple frequency bands to a user simultaneously. Thus, UE and BS have a higher channel capacity and a higher maximum throughput. In case of Montreuil, an MC can assign up to 3 frequency bands (800MHz, 1800MHz and 2600MHz) and SC can assign up to 2 frequency bands (1800MHz and 2600MHz) to a UE.

Comparing to Annecy, Montreuil has a higher population density as 12 000 people/km². Lots of offices and stores are placed in the center of Montreuil where measurements are performed. Table 6, summarizes the characteristics of both trials.

Table 6, SC measurement campaigns characteristics

City	Annecy	Montreuil
Population density	1 900 person/km²	12 000 person/km²
Number of sites	4	5
LTE frequency bands	2600 MHz	1800 MHz 2600 MHz
Antenna type	Directive	Directive
Height of antennas	3 m	3 m or 5 m
Experimentation date	January-February 2017	July-August 2017
DL carrier aggregation	OFF	ON

Three types of measurements have been performed on these sites:

1. **Stationary measurements**: A fixed position has been chosen to perform measurements for each SC where people stay much time such as under the bus station (see Figure 27).

   a) E-field measurements with Narda SRM-3006 for one hour. The measurement antenna was placed on a tripod at 1.5m above the ground. The measured E-field is an average value of over 30s. These assessments allow us to assess the uncertainties regarding, fast fading and the traffic variations. 100 samples have been collected during one hour of measurement through SRM-3006 for each SC and the result consists of the total E-field measured on three frequency bands 800MHz, 1800MHz and 2600MHz.

   b) TX/RX UE measurements: Measurement for 15 minutes in Annecy and 30 minutes in Montreuil with Nemo handy during which the trace mobile phones upload and download FTP files.

2. **Spatial measurements**: Measurements have been performed while walking around each SC to a distance of nearly 100m that is assumed to be about the coverage area of the SC. Almost the same path has been followed two times, each time with a single trace mobile phone (see Figure 28). Following two times the same path, allows us to reduce uncertainties regarding body shadowing and cell traffic. We tried to reduce the body shadowing effect by crossing the same streets in two different directions. Each path takes about 40 minutes of walking measurement.

   a. E-field measurements: Narda SRM-3006 has been used to measure E-field variations on different DL frequency bands. The recorded E-field values are averaged over 10s on three frequency bands 800MHz, 1800MHz and 2600MHz.

   b. TX/RX measurements: for each path a single trace mobile phone is used. Trace mobiles were locked to LTE frequency bands supported by SCs. To stimulate the UE TX emission of trace mobile phones, each trace mobile has been programmed to upload a 100 MB filed via FTP protocol to a server repeatedly. This allows us to record the variation of throughput, emitted power and received power density during the path.

These measurements were repeated the first time when SCs were turned on and were operational and the second time when SCs were turned off:

- SC On: This corresponds to the scenario were SCs were operational and the trace mobile was connected to an SC (shown with green path in Figure 28) or to an MC (shown with

red path in Figure 28) when the quality of service (QoS) provided by MC is better than the one provided by SCs.

- SC off: This corresponds to the scenario when SCs are turned off and the trace mobile phones are connected to MCs during the whole path.

3. **Path loss measurements:** Measurements are performed in line of sight (LoS) direction of SC antennas through trace mobile phones. Trace mobile phones were locked on LTE frequency bands and transfer a 100 MB file to a server repeatedly. The variation of RX and TX powers are recorded during the path for different distances from SCs. These results are used to construct propagation models of SCs.

Figure 27, SCs in Annecy under measurement and the location of measurement antennas at fixed positions for stationary measurements

Regarding spatial measurements, the objective was to compare the E-field, RX, TX and throughput values for points were the trace mobile is connected to an SC in SC On scenario to approximately the same points when SCs are off. Thus, in SC On scenario, only points where the trace mobile is connected to an SC are considered. The location of SCs and MCs for the Annecy and Montreuil campaign is respectively presented in Figure 28 and Figure 29.

In Annecy trial, as it will be explained later in Section 3.4.3, it is possible to identify two SC clusters in terms of network architecture. The first one where SCs are deployed far from the MC to provide coverage and the second cluster which is implemented in the vicinity of the MC to increase the network capacity.

It should be noted that site number 7 in Montreuil trial (see Figure 29) is consisted of two sites because of their proximity we have considered them as one site.
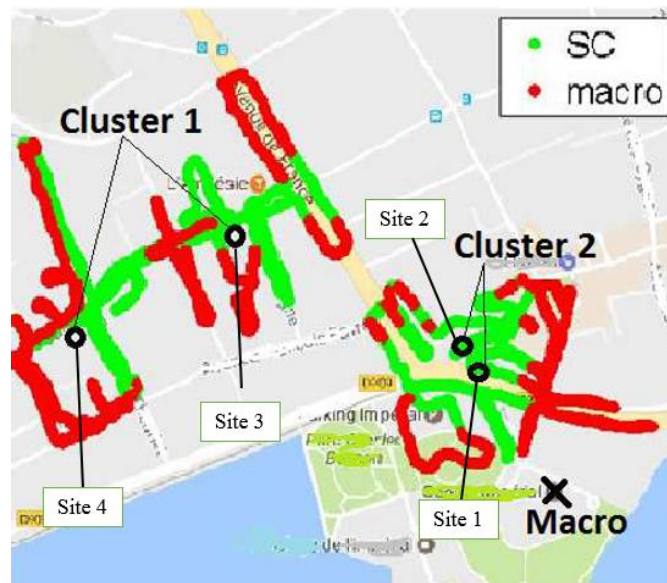
Figure 28, Annecy measurement map. Black circles present the location of SCs, Cross shows the nearest MC. The trace mobile phone is connected to MC (red) and SCs (green) during the path.

Figure 29, Montreuil measurement map, black circles represent SCs and black stars MCs of the same operator, arrows represent the direction of antennas

3.4.2 E-field Stationary and Spatial measurement results

Measurement results show that the measured E-field at a fixed point close to the SCs follow a normal distribution and the average E-field values depend on the position of measurement probe according to SC antenna. Figure 30 illustrates the CDFs of the E-field measured with SRM-3006 for each site, of Annecy trial, normalized to its mean value. Results are presented in Table 7. It should be noted that E-field is the quadratic sum of measured E-field values in 800 MHz, 1800 MHz, and 2600 MHz LTE frequency bands. In the Annecy trial, SCs use only one frequency band (LTE 2600), while in Montreuil campaign SCs use two frequency bands (LTE 1800 and LTE 2600). MCs operate at 800 MHz, 1800 MHz, and 2600 MHz LTE bands in both cities.

Figure 31 shows the CDF of measured stationary E-field for SC On and SC Off scenarios in Montreuil scenario. Since the measurement probe is placed very close to SCs and not necessarily close to the MCs, in SC On scenarios the measured E-field is higher than SC Off scenarios. The results for each scenario are presented in Table 7.

Figure 30, CDFs of normalized measured E-field for static measurements in Annecy, E-field values are the quadratic sum of the measured fields at 800 MHz, 1800 MHz and 2600 MHz LTE bands.
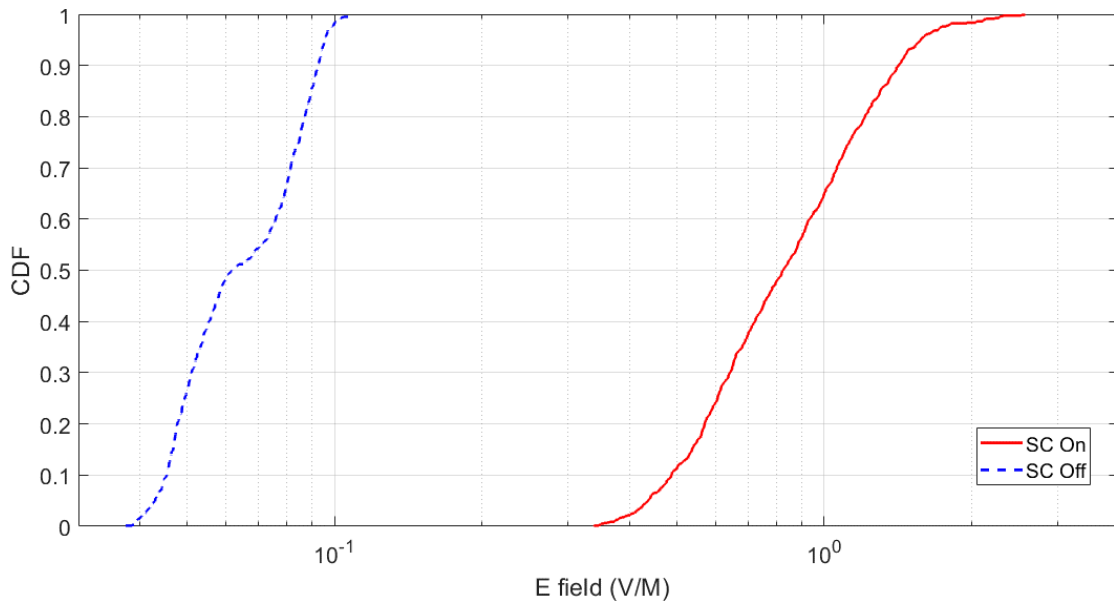
Figure 31, CDF, Montreuil stationary E-field results for SC On and SC Off scenarios at the same locations. E-field values are the quadratic sum of the measured fields at 800 MHz, 1800 MHz, and 2600 MHz LTE bands.

Since in Montreuil, SCs operate on two frequency bands (1800 MHz and 2600 MHz) thus the measured E-field in SC On scenarios is higher in Montreuil (see Figure 32).
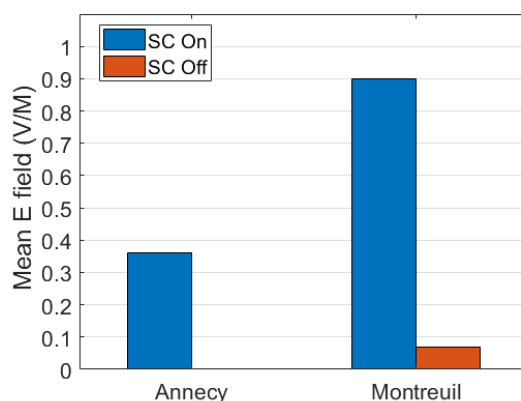
Figure 32, Annecy and Montreuil stationary mean E-field comparison. E-field values are the quadratic sum of the measured fields at 800 MHz, 1800 MHz and 2600 MHz LTE bands.

Table 7, Stationary measurements result for all sites in Annecy and Montreuil campaigns. E-field values are the quadratic sum of the measured fields at 800 MHz, 1800 MHz, and 2600 MHz LTE bands.

Campaign	Site number	Mean *(V/m)*		Median *(V/m)*		Quantile 95 *(V/m)*	
		SC ON	SC OFF	SC ON	SC OFF	SC ON	SC OFF
Annecy	Site 1	0.43	--	0.43	--	0.55	--
	Site 2	0.22	--	0.21	--	0.30	--
	Site 3	0.74	--	0.73	--	1.01	--
	Site 4	0.05	--	0.04	--	0.06	--
	Aggregated	0.36	--	0.32	--	0.86	--
Montreuil	Site 5	0.55	0.05	0.53	0.05	0.75	0.06
	Site 6	0.95	0.08	0.91	0.08	1.54	0.09
	Site 7	1.30	0.04	1.25	0.04	2.0	0.05
	Site 8	0.79	0.08	0.79	0.08	1.10	0.10
	Aggregated	0.90	0.07	0.82	0.06	1.57	0.09

The CDF of measured spatial E-field strength is presented in Figure 33. The measured values for Montreuil trials are slightly higher due to the fact that SCs are operating on two frequency bands. These results are presented in Table 8. Due to the vicinity of Site 1 and Site 2 in Annecy trial one spatial measurement is performed for both sites.
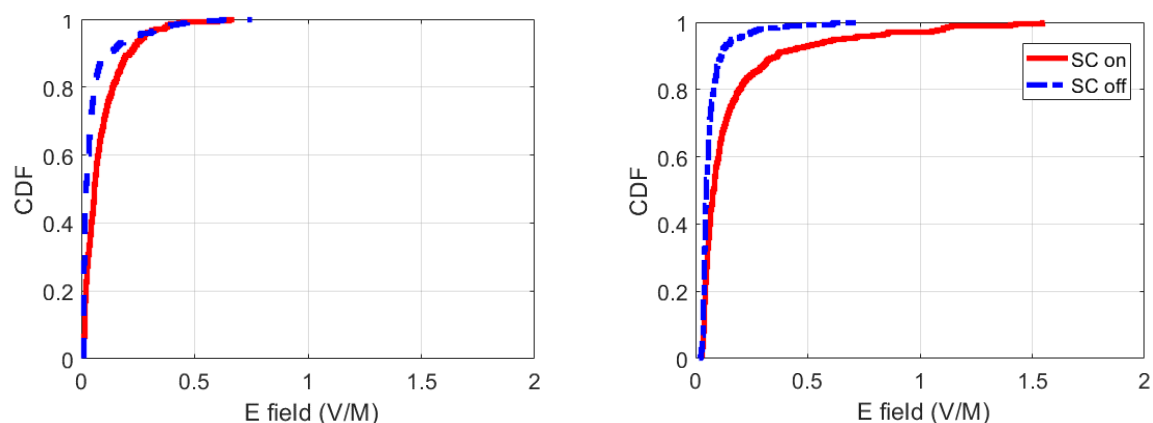
Figure 33, CDF, Spatial measurements, left Annecy and right Montreuil. E-field values are the quadratic sum of the measured fields at 800 MHz, 1800 MHz, and 2600 MHz LTE bands.

It is worth mentioning that in all cases the measured E-field values are very low comparing to ICNIRP levels. For instance, the measured E-field quantile 95 in Montreuil SC On scenario with respect to ICNIRP levels (59V/m for 1800MHz) is about 2%.

Table 8, E-field values are the quadratic sum of the measured fields at 800 MHz, 1800 MHz, and 2600 MHz LTE bands.

Campaign	Site number	Mean *(V/m)*		Median *(V/m)*		Quantile 95 *(V/m)*	
		SC ON	SC OFF	SC ON	SC OFF	SC ON	SC OFF
Annecy	Site 1 & 2	0.13	0.11	0.09	0.05	0.37	0.39
	Site 3	0.06	0.02	0.03	0.01	0.23	0.05
	Site 4	0.05	0.02	0.02	0.01	0.16	0.07
	Aggregated	0.09	0.05	0.06	0.02	0.28	0.22

	Site 5	0.09	0.04	0.06	0.04	0.32	0.05
	Site 6	0.22	0.04	0.10	0.04	0.87	0.06
Montreuil	Site 7	0.17	0.05	0.06	0.04	1.05	0.09
	Site 8	0.14	0.09	0.10	0.07	0.42	0.24
	Aggregated	0.16	0.07	0.08	0.05	0.65	0.17

3.4.3 TX/RX Stationary and Spatial measurement results

Nemo handy was used to measure the UE TX power at a fixed position close to SC. The results are presented in Table 9. Results suggest that the emitted power by UE reduces significantly when SCs are on due to the low path loss. In download scenario, the UE does not emit power most of the time and the TX values are based on the rare occasions when the UE emits.

Table 9, Stationary measurement results for all sites in Annecy and Montreuil campaigns.

Scenario		Parameters	Stationary upload UE TX power (dBm)	Stationary download UE TX power (dBm)
Montreuil*	SC On	Mean	2.6	-4.4
		Median	-7	-18
		Quantile 95	9	1
	SC Off	Mean	21.1	19.5
		Median	21	20
		Quantile 95	21	21
Annecy*	SC On	Mean	2.4	--
		Median	-0.7	--
		Quantile 95	6.8	--
	SC Off	Mean	--	--
		Median	--	--
		Quantile 95	--	--

* **In Montreuil stationary trace mobile measurements are performed for 30 minutes, however, in Annecy for 15 minutes.**

In addition, Montreuil measurement results show that SC deployment can increase the channel capacity thus throughput (see Table 10). This extreme increase in throughput is due to the better channel quality (shorter distance between UE and SC) and to more available resources (lower number users are connected to SC due to its limited coverage).

Table 10, Uplink and downlink measured throughput in the Montreuil campaign for SC On and SC Off scenarios.

Scenario		Parameters	Stationary upload 30 min Throughput (Mbps)	Stationary download 30 min Throughput (Mbps)
Montreuil	SC On	Mean	28	119
		Median	28	131
		Quantile 95	30	203
	SC Off	Mean	7	13
		Median	6	7
		Quantile 95	15	39

Concerning the Annecy campaign, it is possible to identify two different SC clusters in terms of network architecture. Cluster 1 corresponds to two SCs (sites 3 and 4) deployed at MC cell edges to increase the coverage and QoS. Cluster 2 corresponds to SCs (sites 1 and 2) deployed close to the MC to offload MC traffic in high traffic hours.

As it is mentioned before the uplink emitted power highly depends on the channel condition mainly to the measured path loss between UE and BS. Path loss is inversely proportional to the received signal strength by UE i.e. RSRP. Figure 34, illustrates the variation of RSRP for SC On and SC Off scenarios recorded by Nemo and JDSU trace mobile phones. In SC On scenario for both clusters, the average measured RSRP is higher than in SC off scenario. In both scenarios the measured RSRP in cluster 2 is higher.
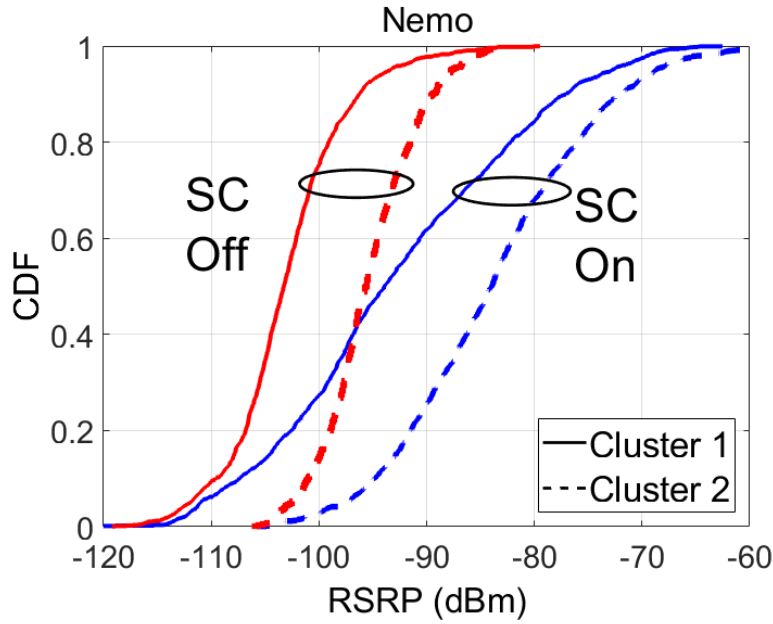
Figure 34, CDF, Measured RSRP values for cluster 1 and 2 in SC On and SC Off scenarios for spatial measurement

As shown in Figure 35 the UE TX power is directly related to the measured path loss between the BS antenna and UE antenna, when UE is connected to an SC, the measured path loss as well as UE TX power decrease. Also, by moving toward the BS or being in the line of sight of the SC antenna, the propagation channel is improved thus a higher RSRP value and a lower UE TX power are observed. The correlation between RSRP and UE TX power is presented in Figure 36.
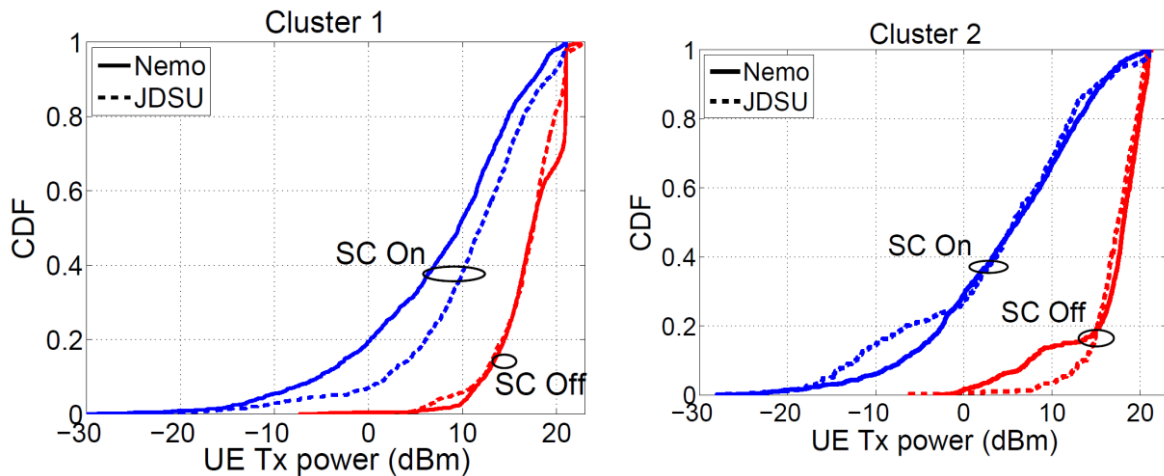
Figure 35, CDF of measured UE TX power in cluster 1 (left) and cluster 2 (right) from Nemo and JDSU for spatial trace mobile measurements
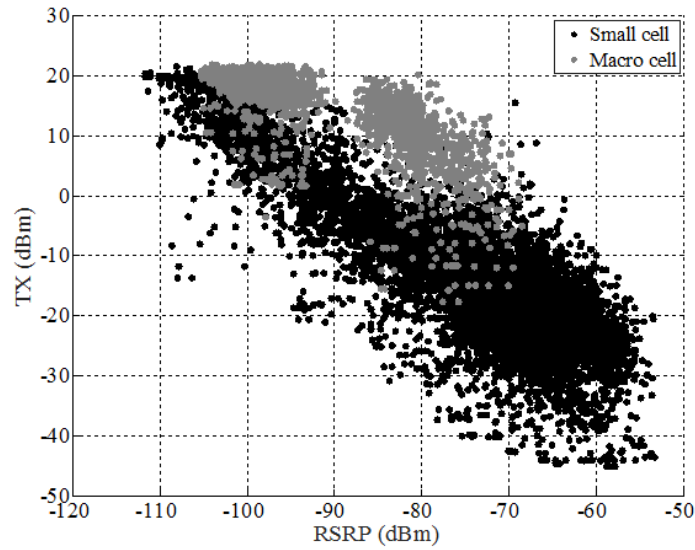
Figure 36, RSRP vs TX power for SC On and SC Off scenarios in Annecy trial for all sites for spatial trace mobile measurements

As shown in Figure 35, Nemo and JDSU trace mobile phones show a consistent behavior for both scenarios. Hence it is reasonable to aggregate all the TX powers from both trace mobile phones and analyze them together. Table 11 summarizes the characteristics of measured TX in both scenarios. The UE TX power is reduced by 5 dB in cluster 1 and by 7 dB in cluster 2 when UE is connected to an SC.

Table 11, Characteristics of the UE TX powers and throughput in Annecy and Montreuil spatial trace mobile measurements for cluster 1 and 2 in SC On and SC Off scenarios

Scenario		Parameters	UE TX power (dBm)	Throughput (Mbps)
Annecy Cluster 1	SC On	Mean	13.7	26
		Median	10.9	28.3
		Quantile 95	19.7	39.2
	SC Off	Mean	18.2	5.9
		Median	17.5	4
		Quantile 95	21	17.6
Annecy Cluster 2	SC On	Mean	11.2	27.7
		Median	6.4	30.1
		Quantile 95	17.6	38.1
	SC Off	Mean	18.3	28.9
		Median	18.2	31

		Quantile 95	21	37.7
		Mean	17.2	22
	SC On	Median	14	24.5
Montreuil		Quantile 95	21	30
		Mean	20.8	8
	SC Off	Median	21	6.8
		Quantile 95	23	19.2

Figure 37, illustrates different statistical percentiles of the ratio between the throughputs measured in SC On and SC off scenarios for different trace mobile and for both clusters. On cluster 1 where SCs are placed at the cell edge of MC, deploying SCs significantly improves the coverage and throughput. Results show that the throughput when the SCs are on increases by a factor of 8 on average, 6 in median and 3 in 95th percentile. Besides, the 5th percentile is improved by a factor of 4 which means that the throughput is much higher even in worst connection conditions.
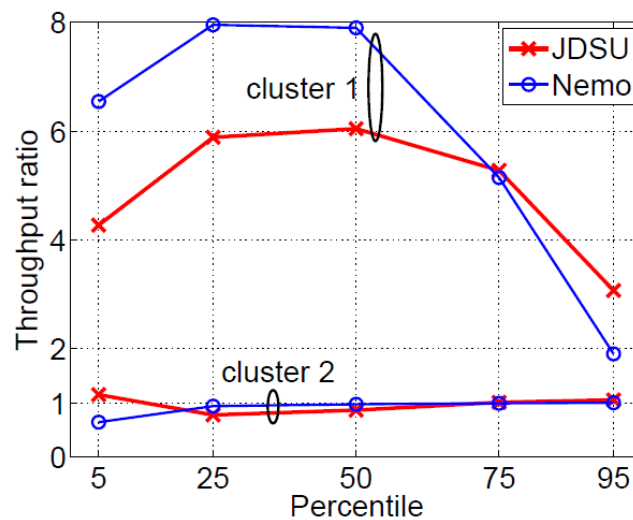
Figure 37, SC On and SC Off throughput ratio for cluster 1 and 2 measured by JDSU and Nemo trace mobiles

Table 12, SC On and SC off Throughput ratio for cluster 1 and cluster 2

Scenario	Parameters	Throughput ratio
Annecy Cluster 1	Mean	4.5
	Median	7
	Quantile 95	2.2
Annecy Cluster 2	Mean	0.09
	Median	0.9
	Quantile 95	1.0

Results suggest that for cluster 1 where the measured area is not well covered by MCs, deploying SCs is advantageous for UEs in terms of throughput and coverage. In the case of cluster 2, however, SC deployment does not provide better throughput since the area is already well covered by the MC and the throughput is already very good on MC. Generally, SCs deployed in a well-covered area are used to offload traffic when there is an important service request and not to improve the coverage and throughput. As it is mentioned earlier, since measurements have been performed out of tourist seasons, no difference in terms of throughput is observed but the emitted power is always lower in SC On scenario (see Table 11).

Regarding the Montreuil trial, SCs were deployed to increase network capacity by offloading nearby MCs traffic. Since the area is crowded during work hours, SC deployment results in higher throughput and lower UE TX power (see Table 11).

3.4.4 Global exposure assessment

In this section, we try to assess the global exposure based on measurements presented in Section 3.4.2. As it is explained in Chapter 2, the global exposure can be expressed as the sum of downlink and uplink exposures.

The DL exposure can be represented as:

$$DL\ Exposure = \frac{t_{DL}}{T} \times \sum_i (SAR_{DL,i} \times S_{DL,i}) \tag{19}$$

Where t_{DL} is the time that the user is exposed to DL exposure, $S_{DL,i}$ represents the received power density from i^{eme} BS and T is the time for which exposure is assessed. $SAR_{DL,i}$ is

whole-body SAR value calculated for an incident emitted reference power of P^{ref} and normalized to this power. As mentioned earlier, the DL exposure is permanent thus in DL Exposure, the exposure time t_{DL} is equal to T.

UL dose is computed from equation (**20**):

$$UL\ Exposure = \frac{t_{UL}}{T} \times SAR_{UL} \times P_{UL} \qquad (20)$$

Where t_{UL} is the time during which the UE has emitted power and P_{UL} is the emitted power by UE (UE TX power) and SAR_{UL} is the whole-body SAR value induced by user's device and normalized to a reference transmitted power of 1W. Considering that in average a user uploads 100 MB of data each day, the emission time is calculated based on the average measured throughput in SC On and SC Off scenarios. SAR_{DL} and SAR_{UL} values are collected from Table 3 for an adult standing mobile data posture. The summary of the scenario configuration is presented in Table 13.

Table 13, Global exposure parameters

Time period	24 hours
Technology	LTE
Cell type	Small cell and Macrocell
User profile	Moderate (100 MB upload per day)
Usage	data
Posture	Adult, Standing

The DL received power density and UE TX power values are the average measured values for two scenarios. We have not considered the effect of traffic on the received power density thus the DL exposure is considered as permanent and constant for the whole day. UL, DL and Global exposure is calculated and are presented in Table 14.

The comparison between scenarios in terms of UL, DL and Global exposure is illustrated in Figure 38.

Table 14, Computed DL dose, UL dose and Global exposure for one day, 100 upload for a user based on measured data

Scenario		DL Exposure (µW/kg)	UL Exposure (µW/kg)	Global Exposure (µW/kg)
Annecy Cluster 1	SC On	0.0363	0.0246	0.0609
	SC Off	0.0052	0.3146	0.3198
Annecy Cluster 2	SC On	0.1885	0.0134	0.2019
	SC Off	0.1559	0.0659	0.2218
Montreuil	SC On	0.2852	0.0669	0.3521
	SC Off	0.0546	0.4225	0.4771

When SCs are off, the global exposure is mainly governed by the UL Exposure. By turning on the SCs, the DL exposures increases however the UL exposure decreases significantly. Consequently the Global exposure is reduced in every scenario. A better channel condition and a higher channel capacity provide a better throughput, which causes less UL exposure time in average.
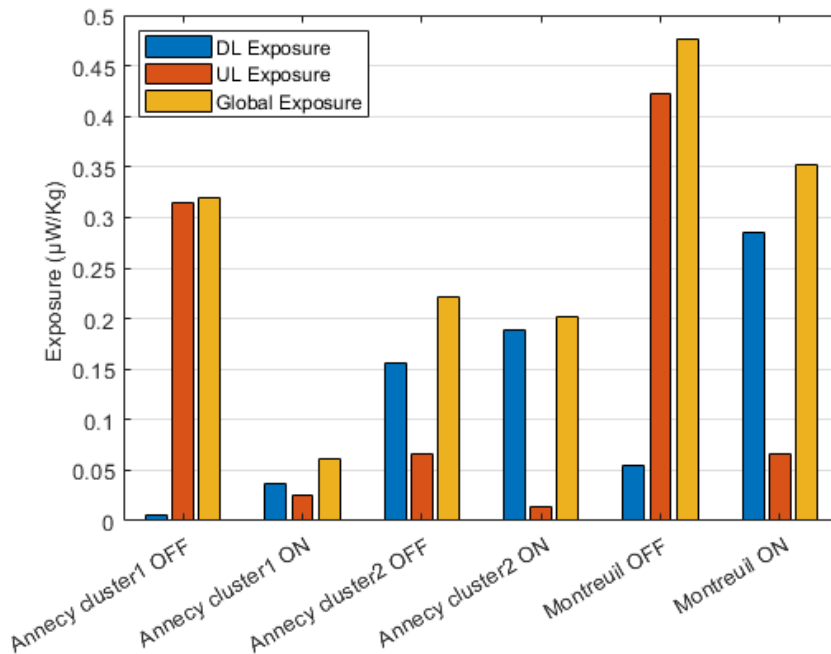
Figure 38, Induced exposure for each scenario, Annecy cluster 1: SC on cell edge of MC, Annecy cluster 2: SC near MC, Montreuil: crowded urban environment

3.5. Path loss measurements and modeling

Due to the difficulties of performing measurements in personal spaces (such as apartments), the indoor exposure evaluation is a complicated task. Thus it is of interest to make exposure models based on outdoor measurements and assess the indoor exposure by extending those models into indoor areas. In this regard, the path loss between UE and BS can be modeled to assess the received power density from BS as well as the UL emitted power by UE through LTE UL power control algorithm.

This section is dedicated to construct a model to estimate both indoor and outdoor exposure induced by outdoor SCs based on outdoor measurements. DL exposure can be assessed by evaluating the received power from the SC and the UL one by estimating the emitted power by UE from the UL power control algorithm presented in equation (23). In this regard, a series of measurements using trace mobile phones has been carried out during the Montreuil experiment (see Section 3.4) to record the characteristics such as throughput, emitted and received power by UE and OLPC parameters in LoS direction of the SC antenna. As a matter of fact, the received power by a user depends on the emitted power by the SC, on the SC antenna gain, on UE antenna gain and also on the path loss between the UE and SC (see Figure 39). The UL exposure depends on the number of uplink allocated resource blocks and also the path loss measured by UE. The DL received power by UE can be computed by the following equation:

$$P_{RX\_UE} = P_{SC} + Gain_{SC}(\theta, \phi) - PL + Gain_{UE}(\theta, \phi) \qquad (21)$$
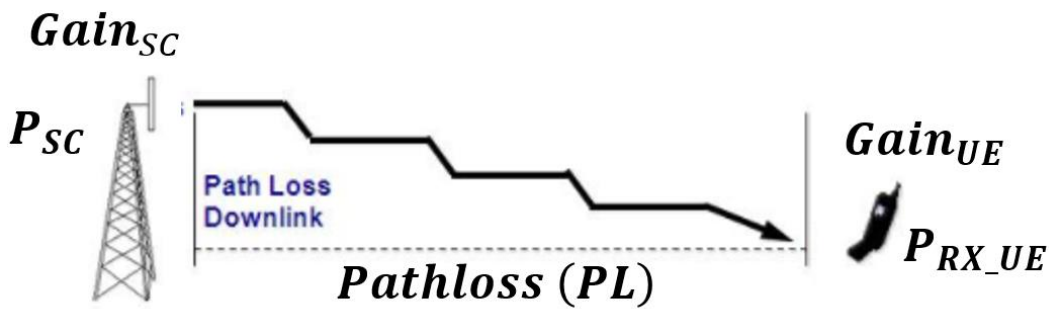
Figure 39, SC-UE downlink link budget

PL denotes the channel path loss, P_{SC} the transmitted power by the SC, $Gain_{UE}$ represents the UE antenna gain, $Gain_{SC}(\theta, \phi)$ is the BS antenna gain when UE is placed at the direction (θ, ϕ)

and P_{RX_UE} is the received power by UE. For the sake of simplicity, we have considered that the UE antenna is omnidirectional ($Gain_{UE}(\theta, \phi)= 0$).

The reference emitted power by SC and the received power by UE are named in LTE protocol respectively as Reference Signal (RS) and RSRP thus, the received power by the UE can be assessed through the following equation:

$$RSRP = RS + Gain_{SC}(\theta, \phi) - PL \tag{22}$$

In LTE technology, the emitted power by UE is determined through an uplink power control algorithm that is a combination of open and closed-loop components (23). The open-loop power control (OLPC) is responsible for a rough setting of uplink transmitted power. It compensates slow changes of path loss to achieve a target power P_0 for one resource block. Then the total number of allocated uplink resources block (M) is added to this power. Once OLPC has determined the appropriate UL power, the closed-loop power control (CLPC) performs fine adjustments to compensate rapid changes in channel condition.

The power control algorithm LTE technology is defined by 3GPP and can be expressed as follow [88]:

$$P_{UE} = \min\{P_{UE}^{max}, \underbrace{P_0 + \alpha.PL + 10\log_{10}(M)}_{Open\ loop\ correction\ factors} + \underbrace{\Delta_{mcs} + f(\Delta_r)}_{Closed\ loop\ correction\ factors}\} \tag{23}$$

Path loss (PL) is compensated by a factor α which can be fixed at one of the [0, 0.4, 0.5, 0.6, 0.7, 0.8, 0.9, 1] values. When α is 1, the measured path loss is fully compensated in uplink transmissions. For $\alpha = 0$, path loss between UE and BTS is ignored in the power control algorithm and the emitted power is constant for all users. For α between 0.4 and 1, path loss compensation would be fractional [89]. CLPC component considers fast variations of propagation channel by use of a corrector $f(\Delta_r)$ and also uplink modulation scheme Δ_{mcs}.

The measurement path consisted of a round trip of about 200 meters (see Figure 40). Trace mobiles were programmed to upload 100 MB files on an FTP server repetitively and RX, UE TX, throughput, UL power control algorithm parameters and GPS coordinates of each measurement point were recorded simultaneously. It is worth mentioning that at the post-processing stage, all the measurements have been merged and processed together. These parameters have been used in the model construction and validation process described in Section 3.5.3.
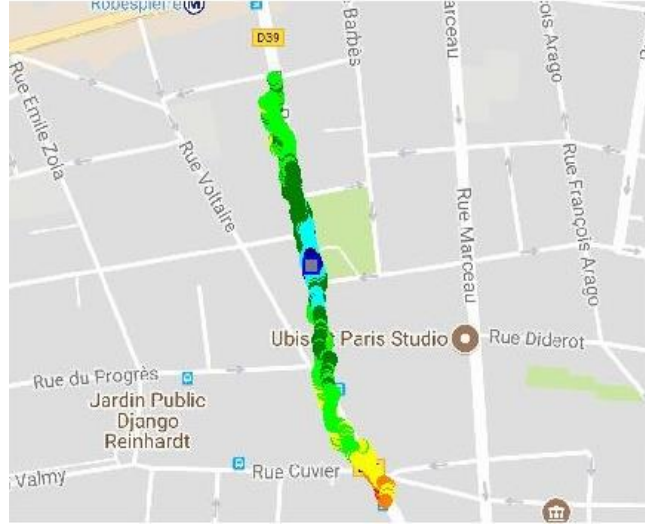
Figure 40, Example of path loss measurement path, SC is represented as the blue square. Colors represent the RSRP values from blue (highest) to orange (lowest) during the path.

3.5.1 Linear regression modelling method

Generally, path loss can be modelled in terms of geographical distance between the transmitter and the receiver. The propagation loss can be modelled as $\frac{1}{d^{\alpha}}$, where d is the geographical distance between receiver and transmitter and $\boldsymbol{\alpha}$ is the path loss exponent (PLE). In this study, path loss model is constructed, based on a widely used propagation model, according to the following equation [90]:

$$PL = A + 10 \cdot \gamma \cdot \log_{10}(\frac{d}{d_0}) \tag{24}$$

$$A = 20 \log_{10}(\frac{4\pi}{\lambda}) \tag{25}$$

Where λ represents the wavelength of the signal, d_0 is the unit of distance (1m) and γ is PLE. On a log-log plot, for the scattered data, a linear curve has been fitted using linear regression method. Figure 41 illustrates the measured path loss and the fitted model in decibels in terms of the distance between SC and UE for 1800 and 2600 MHz frequency bands. Table 2 summarizes the PL models characteristics obtained by the linear regression at both frequencies.
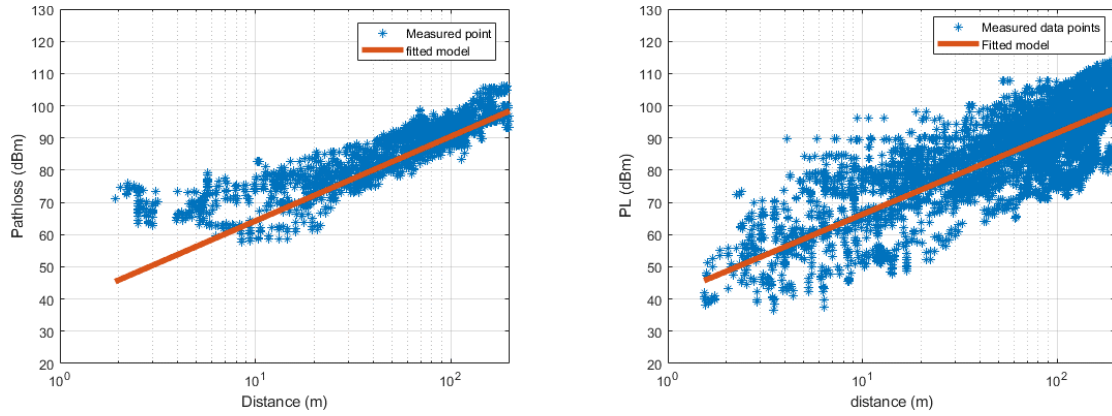
Figure 41, Path loss in terms of distance to the SC for frequency bands 1800 MHz (left) and 2600 MHz (right)

Table 15, Charactersitics of fitted models via linear regression to measured path loss

Frequency (MHz)	γ	A	Mean difference (dB)	Standard deviation (dB)
1800	2.85	37	0.5	5.7
2600	2.52	41	0.1	7.1

The main challenge in path loss modelling is to consider the attenuation and variations in the propagation environment. Since SCs are installed at low heights, environmental variations such as moving cars and pedestrians can significantly affect the propagation channel conditions, even more than for usual MC networks. For instance, a bus could completely block the SCs antenna. Therefore, the environment becomes highly variable especially for the distances close to the antenna. This variability of the environment implies that at the same distance from SC, at different times, different path loss values highly different from each other, are measured. In such an environment, using usual deterministic approaches such as the linear regression method applied to model the path loss introduces important uncertainties in the final results. To take into account these variabilities, PLE has been modeled through a statistical approach as presented in [91].

3.5.2 Statistical modelling of path loss exponent

To assess the PLE value for each measurement point the following equation is used [91]:

$$\gamma = \frac{PL - A}{10 \log_{10}(\frac{d}{d_0})} \tag{26}$$

By having the variation of PLE in terms of distance, it is possible to make a statistical model for PLE in SC environment. This leads to computing the path loss at a specific distance not as one value but as a statistical distribution. Consequently, this model represents all the possible variations in the SC-UE channel in an urban area in LoS direction of an SC antenna.

PLE has been computed for about 20000 measurement points on two sites at 1800 and 2600 MHz. Figure 42 shows that PLE varies highly close to SC while it becomes more stable, for further distances.
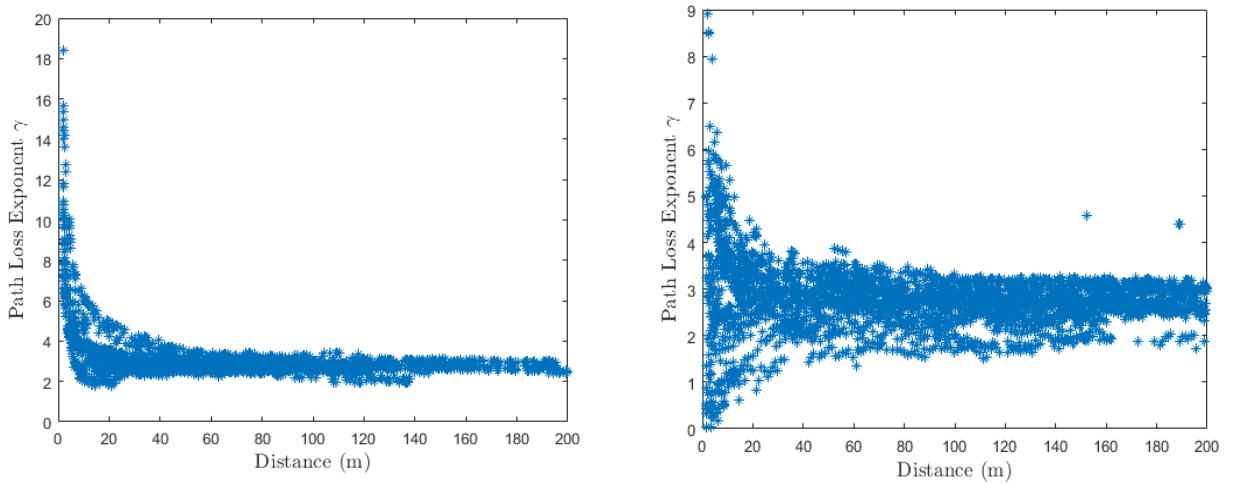
Figure 42, PLE vs distance (m) between UE and SC at 1800MHz (left) and 2600 MHz (right).

Thus, it is possible to classify two different PLE models depending on the distance. According to measurements and using the Kolmogorov Smirnov test, for distances less than 60m from the SC, PLE follows a generalized extreme value (GEV) distribution and for distances larger than 60m, it follows a Beta distribution. These distributions are further used as inputs to assess the emitted and received power by the user. Figure 43 illustrates the distributions of PLE at 1800MHz and 2600MHz for distances lower and higher than 60 m from the SC. The characteristics of these distributions are presented in Table 16.

1m < r < 60m   **60m< r <200m**
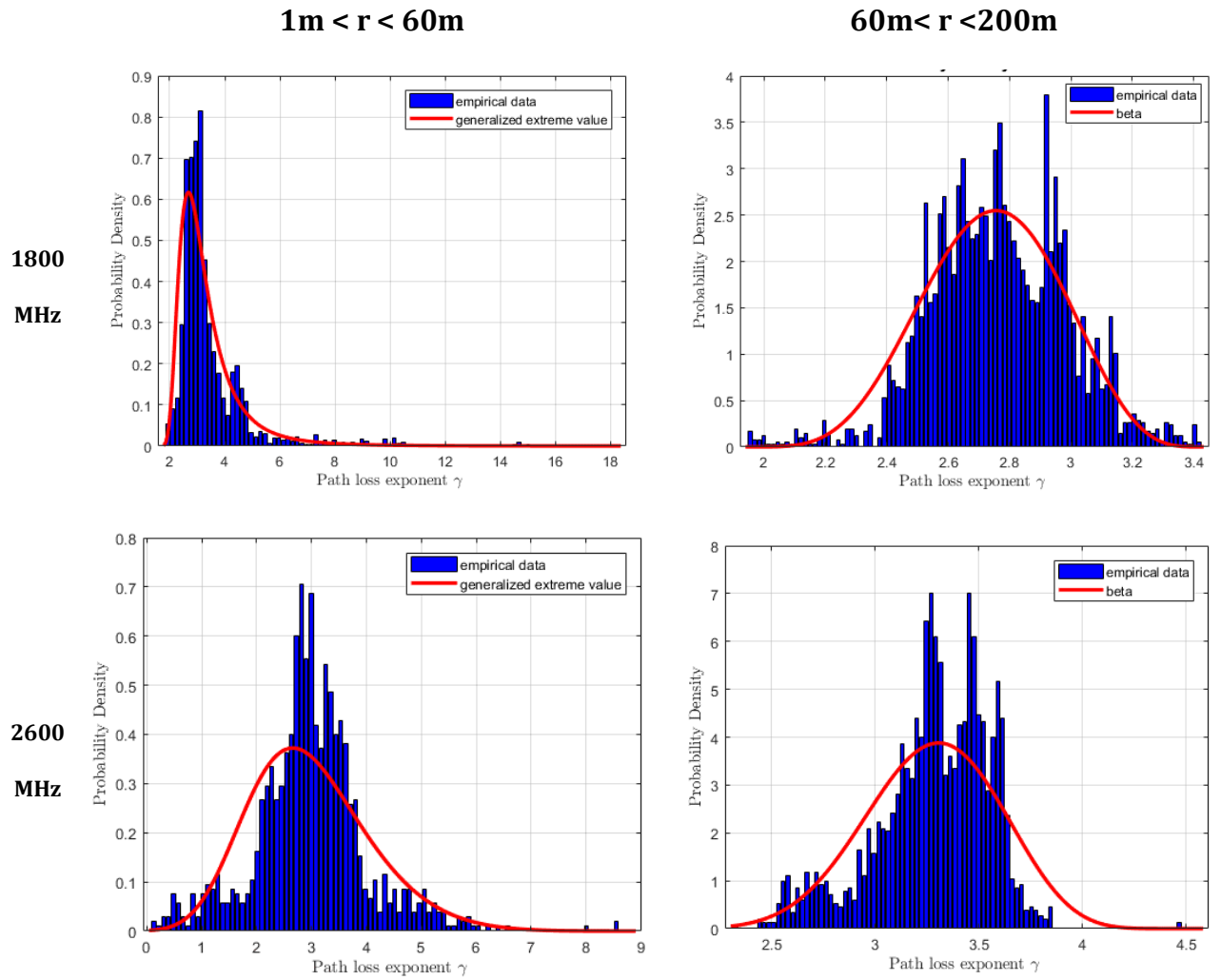
Figure 43, PDF, distribution of measured PLE for 1800 and 2600MHz frequencies and for distances closer than 60m and further than 60m from the SC

Table 16, Characteristics of PLE distributions for 1800MHz and 2600MHz, closer and further than 60m from the SC

Frequency (MHz)	Distance	Distribution	Parameter 1	Parameter 2	Parameter 3	Parameter 4
1800	r < 60m	GEV	k = 0.27	s = 0.61	m = 2.8	-
1800	r > 60m	Beta	α_1=47	α_2=36	a = 0	b = 5
2600	r < 60m	GEV	k = -0.23	s = 0.93	m = 2.6	-
2600	r > 60m	Beta	α_1= 21	α_2=18	a = 0	b = 5

These distributions are going to be used to compute the received power by UE by using equation (**27**) for each measurement point and for uplink emitted power by using (**23**).

3.5.3 Uplink emitted and downlink received powers

The received power by a user can be assessed through the following formula:

$$RSRP = RS + Gain_{smallcell}(\theta, \phi) - PL \qquad (27)$$

For each measurement point, the statistical distribution corresponding to the distance between the point and the SC is used to sample PLE. Then, path loss value is computed for these points by equation (**24**). Finally, the received power by UE at this point has been computed using equation (**27**). This process has been done for all the measurement points.

Figure 44 shows the distribution of computed and measured RSRP and Table 17 gives the main characteristics of measured and computed RSRP.
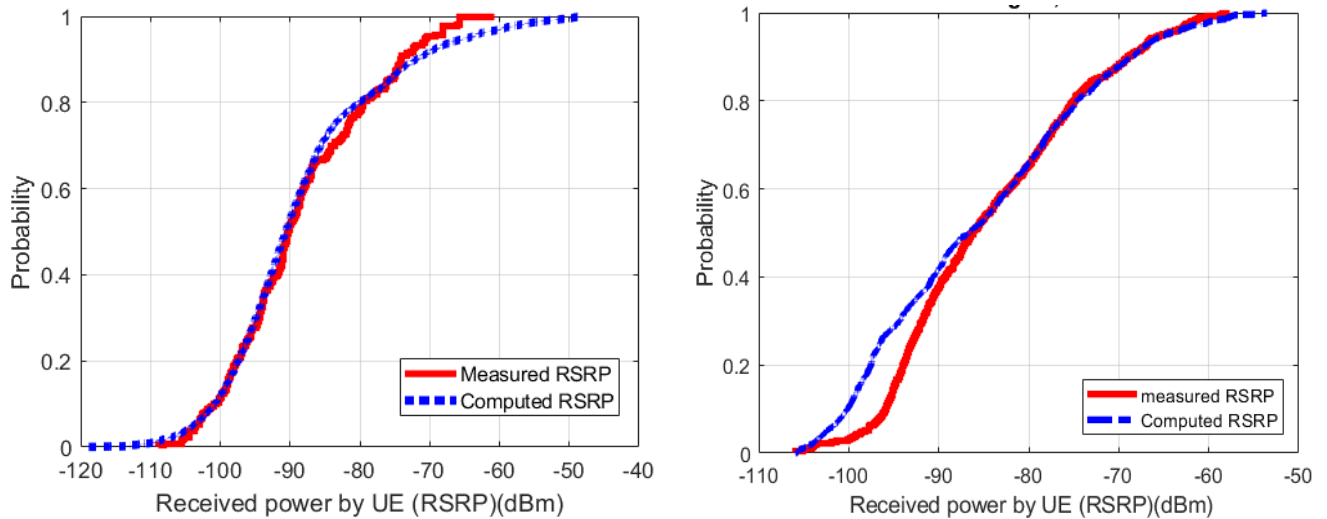
Figure 44, CDF, Comapraison between measured and computed RSRPs for 2600 MHz (left) and 1800 MHZ (right) frequency bands

Table 17, characteristics of the computed and measured RSRP values

Frequency	RSRP	Mean (dBm)	Median (dBm)	Quantile 95% (dBm)
1800	Measured	-84.3	-86.2	-65.1
	Computed	-86.0	-88.3	-65.2
2600	Measured	-88.6	-90.6	-65.9
	Computed	-88.6	-90.1	-70.3

Regarding the uplink UE TX power, since CLPC has a minor effect on emitted power compared to OLPC [89], it has been ignored in this study. As mentioned before, by neglecting close-loop part, the uplink emitted power is assessed using the equation (**28**):

$$P_{UE} = \min\{ P_{UE}^{max}, \ P_0 + \alpha \cdot PL + 10 \log_{10}(M) \} \tag{28}$$

Trace mobile equipment record the number of uplink assigned resources block (M) for each time slot. Measured α shows that this parameter is constant and fixed to 1 at all the time for SCs: the path loss is fully compensated by the uplink power control algorithm. Based on recorded values, Po value has been fixed at -96 dBm. PL has been computed by using statistical models determined in Section 3.5.2. Figure 45, compares the distribution of computed uplink emitted powers and measured uplink emitted powers. Table 18 gives the characteristics of measured and predicted emitted powers.
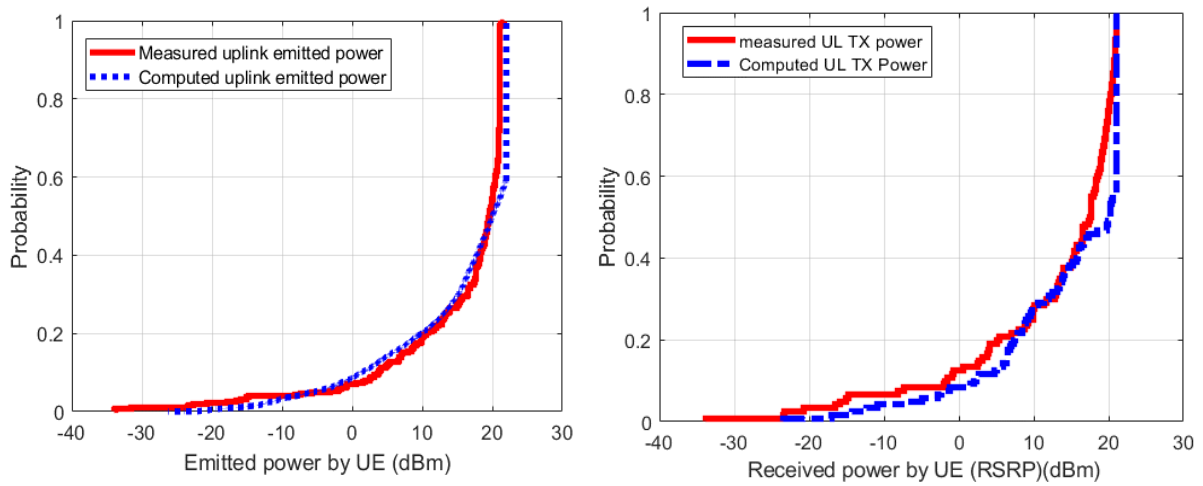
Figure 45, Comparison between measured and computed UE TX power for 2600 MHz (left) and 1800 MHZ (right) frequency bands

Table 18, Characteristics of computed and measured UE TX and RX for 1800 and 2600 MHz

Frequency	UE TX power	Mean (dBm)	Median (dBm)	Quantile 95% (dBm)
	Measured	12.5	17.6	21
1800	Computed	14.3	20	21
	Difference	1.8	2.4	0

	Measured	15.2	19.5	21
2600	Computed	15.8	20.3	22
	Difference	0.6	0.8	1

3.6. Exposure Index assessment in an LTE scenario using proposed models

3.6.1.1. Scenario description

In this section the exposure in a simplistic scenario for a population connected to an LTE SC in indoor and outdoor areas is assessed by using models proposed in Section 3.5.2. The scenario consists of a street of 8 m width and 400 m length. Two series of buildings are considered at each side of the street. The penetration depth is considered to be 6 m in buildings. Each building has 4 floors and the height of each floor is 3 m. The height of the UE from the ground is 1.5 m. Due to the lack of information on the architecture of indoor environment, the penetration loss has been taken into account as a random variable uniformly distributed on the interval [7 dB   13 dB] dB. Figure 46, illustrates the structure of the scenario.
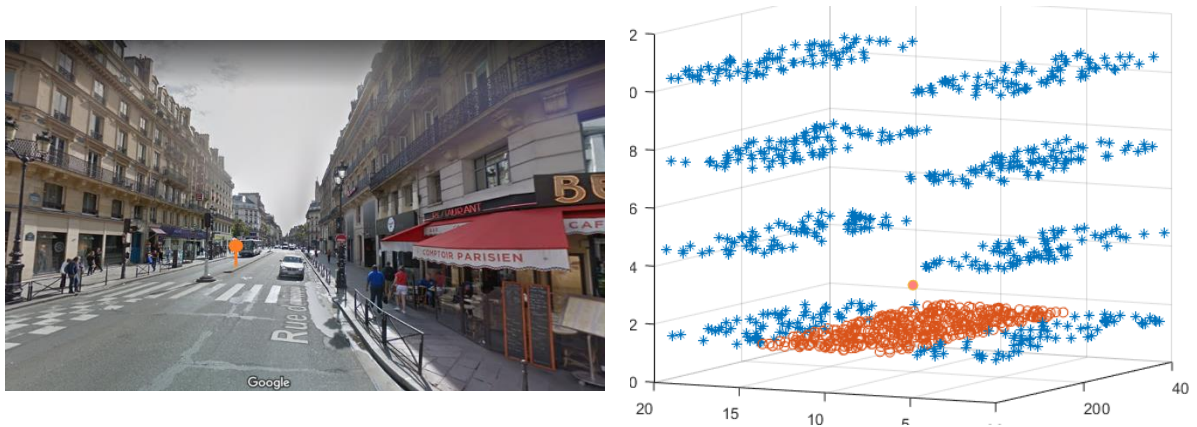
Figure 46, Left: the scenario is inspired from a typical Parisian street. Right: Distribution of observations in indoor (blue stars) and outdoor (orange stars) areas. The SC is placed in the center of the area (red dot).

10^5 different random observations have been sampled in order to cover user's positions. Users are distributed uniformly in indoor and outdoor areas. Since people spend about 70% of their

time in indoor [39], we have considered that 70% of the occurrences happen in the indoor area. The SC is located at the center of the map in the outdoor area and the height of the SC antenna is 3 m. For each observation, we have computed the distance between the user and the SC. Then random sampling of the appropriate distribution of path loss distribution (GEV or Beta according to distance) has been carried out to assess a path loss distribution for each observation.

Having the path loss distribution, we can assess the distribution of received and emitted powers for each observation as described in Section 3.5.2. Simulation configurations are presented in table Table 19. The EI was evaluated over one hour time frame for LTE SC users in a dense urban area. Only adult users and moderate data usage have been taken into account. The scenario includes indoor and outdoor users and it is assumed that on average each user uploads 100 MB of data through SC each day. This means that during one hour time frame, each user uploads on average 4.16 MB. Based on the received power by the user and the Signal to Noise ratio (SNR), each user's throughput been assessed. For the sake of simplicity, the SC antenna is considered as omnidirectional and the emitted reference signal power by SC is fixed as 10 dBm.

Table 19, Scenario network configurations

Environment	Typical European dense city	
	Cell type	Small cell
	Carrier	LTE
	Carrier frequency	1800MHz, 2600MHz
System	Antenna	Omnidirectional with 0dBi gain
	Reference signal	10 dBm
	Bandwidth	20MHz at 1800MHz 15MHz at 2600MHz
	Antenna height	3m
	Max/min transmission	23 dBm/-40dBm
	Antenna	Omnidirectional with 0dBi gain
User equipment	Penetration loss (indoor ↔ outdoor)	10±3 dB
	Upload file volume	4.16 MB per hour
	UE height	1.5m

The uplink emission time (time taking by a user to upload 4.16 MB of data to the network) is the time that takes to upload the file which is inversely linked to the throughput. Thus, it can be assessed by dividing the data volume by the throughput.

Table 20, Exposure configuration

Time period (t)	**1 h**
Rat (r)	LTE
Cell type (c)	Small cell
Environment (e)	Urban city Indoor Outdoor
Population (p)	Adult
User profile (l)	Moderate (100 MB upload per day)
Usage (u)	data
Posture (pos)	Standing

3.6.1.2.Results

Once the average values of emitted and received powers of all the observations are computed, the EI is estimated using normalized whole-body SAR values in Table 3. Table 21 summarizes EI results obtained at 1800 and 2600 MHz.

Table 21, EI for different frequencies

Parameters	Frequencies	
	1800 MHz	2600 MHz
$\overline{P_{TX}}$ **(W)**	6.3×10^{-3}	7.5×10^{-3}
$SAR^{UL}_{p,r,u,pos}$ **(W/kg)**	0.0039	0.0029
$\overline{S_{RX_{inc}}}$ **W/m²**	9.15×10^{-10}	9.36×10^{-10}
$SAR^{DL}_{p,r,pos}$ **(W/kg)**	00.47	00.42
DL Exposure (W/kg)	1.95×10^{-9}	3.71×10^{-9}
UL Exposure (W/kg)	3.13×10^{-8}	2.66×10^{-8}
EI (W/kg)	3.32×10^{-8}	3.03×10^{-8}

Detailed EI values, received, and emitted powers are presented in Table 22. As it was expected the contribution of indoor exposure on EI is higher than the outdoor users and the contribution of the UL exposure is higher than the DL one.

Table 22, computed detailed EI for different frequencies and evironments

Parameters	1800 MHz		2600 MHz	
	Outdoor	Indoor	Outdoor	Indoor
$\overline{P_{TX}}$ (W)	1.56×10^{-3}	1.70×10^{-2}	1.3×10^{-3}	1.16×10^{-2}
$SAR_{p,r,u,pos}^{UL}$ (W/kg)	0.0039	0.0039	0.0029	0.0029
$\overline{S_{RX_{inc}}}$ W/m^2	3.2×10^{-9}	1.1×10^{-11}	2.32×10^{-9}	7.6×10^{-12}
$SAR_{p,r,pos}^{DL}$ (W/kg)	0.0047	0.0047	0.0042	0.0042
DL Exposure (W/kg)	4.15×10^{-9}	3.11×10^{-11}	3.84×10^{-9}	3.01×10^{-11}
UL Exposure (W/kg)	1.35×10^{-8}	5.66×10^{-8}	9.23×10^{-9}	4.63×10^{-8}
EI (W/kg)	1.76×10^{-8}	5.66×10^{-8}	1.30×10^{-8}	4.64×10^{-8}

3.7. Conclusion

In this chapter, the exposure induced by Small cells (SC) and Macrocells (MCs) has been assessed through measurements. Three measurement trials are conducted, the first one, in Basel, Switzerland on LTE MC homogenous networks. The second and third ones respectively in Annecy, France and Montreuil, France on LTE heterogeneous networks consisting of MCs and SCs for two scenarios when SCs are turned off and when SCs are operational. The downlink (DL) received power density, uplink (UL) emitted power by UE, throughput and DL E-field are measured and compared when UE is connected to an MC and when UE is connected to an SC.

Measurement results illustrate that in MC networks, the UL exposure is higher for indoor users comparing to outdoor users. This is due to the higher UE TX power emitted by UEs in indoor areas. According to the UL control power algorithm used by the LTE PUSCH channel, the UL emitted power by UE depends on the measured path loss between UE and BS antenna in order to adapt the UL power to different propagation conditions. Thus, due to the power losses in

walls and furniture in indoor areas, UE is designed to adapt its power to reach the MC, as a consequence UE emits at higher power in indoor areas compared to outdoor areas.

The UE TX power in SC On scenario is always lower than the one in SC Off scenario. This is due to the fact that when UE is connected to an SC, the received power by UE (RSRP) is higher thus the TX power by UE reduces. Also, it is shown that implementing SCs in areas which are poorly covered by MCs, notably improves the UL throughput. It is considered that the usage duration may be inversely proportional to the throughput since, with higher throughput, data is transmitted faster resulting in less usage duration. Since the UL exposure depends on the usage duration, increasing the throughput results in reduced UL exposure, however, in case of areas that are well covered by MCs, implementing SCs may not necessarily increase the throughput. However, it is shown that implementing SCs reduces the UE TX power in all cases. E-field measurement results indicated that the DL E-field is moderately higher when SCs are operational.

Based on measurement results, global exposure is assessed for an adult user uploading 100 MB per day for data usage in standing posture for SC On and SC Off scenarios. As a result, by turning on the SCs, the global exposure reduces in every case. The latter is due to the fact that by connecting to an SC the emitted power and usage duration and as a consequence UL exposure reduces significantly.

Finally, we have modeled the UL and DL exposures in an LTE SC environment, by performing path loss measurements in LoS direction of SC antennas. Initially, through linear regression method, the measured path loss has been modeled, nevertheless, due to the high variation of the received signal because of the low height of SCs antennas, these models have high uncertainties. Therefore, the path loss exponent (PLE) has been statistically modeled for 1800MHz and 2600 MHz frequency bands. It has been observed that the variation of PLE close to the SC antenna is very high, although by going further from the SC antenna, the PLE value becomes less variable. Hence, two different models have been proposed for each frequency band, one for distances closer than 60 m to the SC antenna and the other for distances further than 60 m. These models have been compared to measurements and good accuracy is observed. Using these models, we have computed EI for a simplistic scenario containing one SC for indoor and outdoor users over one hour. According to results, the EI is higher for indoor users since the UE TX power by UEs placed in indoor areas due to worse propagation conditions comparing to outdoor users.

It should be noted that the measurements are performed in urban cities and since propagation condition depends on the type of environment then results may differ in other types of environments such as suburban and rural areas. In addition, these measurements have only considered data usage. Uploading data to an FTP server provides the highest UE TX power values, although since the UE is placed in front of the user, this may not represent the highest possible exposure. For instance, in case of voice usage, since the UE is placed near the user's head the exposure may be higher compared to data usage even if the UE is not emitting at elevated powers. Results are subject to uncertainties regarding closed-loop power control (CLPC) parameters consisting of fast UE TX power adjustments. The uncertainties regarding the propagation environment (rural, sub-urban, urban and dens environments) and CLPC parameters should be investigated in future works..

4. INFLUENCE OF USAGE AND TECHNOLOGY ON HUMAN EXPOSURE

4.1. Introduction

As mentioned in Chapter 2, people now use their mobile phones for a large variety of tasks such as browsing, checking emails, social media, streaming etc., however, voice communication remains as one of the mobile phone usages. Voice over IP (VoIP) applications such as Skype has become very popular since they provide cheap international voice communication and can be used on mobile devices. Since LTE systems only support packet services, the voice service uses Voice over LTE (VoLTE) technology instead of classical circuit switched (CS) voice technology as in GSM and UMTS.

Regarding voice communication, the uplink exposure can be linked to the average power emitted by UE during the call duration. Power emitted by UE can be assessed using trace mobile phones (see Chapter 3) for different scenarios. Contrary to data usage, the usage duration for voice communication does not depend on throughput [68]. In voice call communication the required DL and UL throughput are known and constant. The emitted power during a CS voice call depends on the signal-to-noise ratio (SNR) achieved at the base station (BS). A target SNR is required in order to have an acceptable communication quality, then the emitted power by UE is adapted through power control algorithms to achieve this target SNR. Regarding VoIP calls, the required data throughput is fixed through the application based on the quality of channel. For a better channel quality, a better voice call quality is offered.

In a voice call communication whether CS or VoIP technology, the UE may not emit power continuously. For instance in GSM technology, UE emits power once every eight time slots [53] due to the signal modulation. The latter is important since the human exposure induced by UE depends on both the emitted power by UE and the power emission duration.

In this chapter, the effect of usage and technology on the human exposure in cellular networks is analyzed based on measurements. In this regard, two measurement campaigns are performed: The first trial consists of the characterization of emitted power in different technologies for several types of usages including voice call communications in various locations. The second one is focused on temporal aspect of voice call exposure. These measurements are performed in laboratory through an oscilloscope in order to assess the temporal behavior of emitted power by UE in each voice call technology.

4.2. Circuit switched and packet switched communication

Circuit switching is a link establishment method in telecommunication systems used in GSM and UMTS technologies in order to make calls between two users through the network. GSM uses the time-division multiplex access (TDMA) technique that allows up to eight users to share the same frequency band. Thus, a handset connected to GSM technology emits one eight of the communication time. A burst is the unit of a transmission during a time slot and a GSM time slot duration is 0.577ms. GSM uses a power control technique allowing to minimize the emitted power during a call. Once a call is established the handset starts to reduce the power in steps of 2 dB down to 0 dBm (for GSM 1800 MHz). Discontinuous transmission (DTX) is a technique used in GSM technology to reduce the interference and increase the UEs battery life. DTX algorithm turns on and off the transmitter rapidly during speech pauses. When DTX is active, not all TDMA frames might be transmitted.

The UMTS radio interface is based on Code Division Multiple Access (CDMA) enabling users to communicate using the same frequency band. Users are distinguished by the base station through orthogonal codes. WCDMA or wideband CDMA, is the access method adopted by UMTS. In WCDMA the user signal is spread over a channel width of 5 MHz (instead of 1.25 MHz as in CDMA). Signal spreading is performed by the Direct Sequence Spread Spectrum (DSSS) method where the information signal is multiplied by a binary sequence called spreading code. The data stream which transports audio, is spread to a higher transmission rate. Spreading reduces the necessary output power compared to GSM. In addition, UMTS technology does not employ time slots, instead, it uses a frequency band continuously. UMTS uses a fast power control method which adjusts the mobile's output power every 0.667 ms. In order to prevent interference, each mobile station has to be adjusted to the lowest possible output power.

Packet switching is a technique of transmitting data over a network in forms of packets. In VoIP technique the voice data are compressed and transmitted via data packets over internet rather than the traditional circuit-switched signals. VoIP technique is widely used by mobile phone users through mobile apps such as WhatsApp, Skype etc. The amount of data needed to be transferred in during a call depends on compressing and encryption algorithms (speech or audio codecs) used by the VoIP service provider.

In LTE, based on the required throughput, the network allocates a number of physical resource blocks (PRBs) repetitively in UL and DL directions in order to maintain the call. By nature, a

voice call service must be handled in real-time thus the quality of a voice call is very sensitive to network latency. Therefore, VoIP call quality can be highly affected by channel quality and in poor channel quality situations, call quality drops very fast.

CS voice call capability is not natively implemented in LTE technology, however, to be able to make calls via LTE technology, VoLTE is introduced. VoLTE is a packet switching IP based technique that is largely used by mobile operators all over the world. VoLTE allows high-quality voice calls and simultaneous data and call transfer. Since VoLTE is a native LTE application, it has the luxury to guarantee PRBs allocation to achieve an acceptable QoS. Semi-Persistent-Scheduling (SPS) is a method used in LTE to minimize granting overhead for real-time applications such as voice calls [92]. It takes advantage of the consistent and predictable transmission pattern of VoLTE packets (constant transmission period, predictable number of packets and required number of PRBs, etc.) to make a persistent grant of uplink PRBs rather than scheduling the user in every cycle (see Figure 47). A VoLTE call can be in two different states: the active state where the voice activity detection (VAD) algorithms detect the existence of voice/sound and UE sends data packets in a fast frequency and the idle state during which VAD algorithms do not detect any voice/sound and the UE transmit silence insertion descriptor (a.k.a. comfort noise payload) frames in a lower frequency. For SPS scheduling, the time between two PRB allocations in idle and active state is defined by the network. In active state, the cycle time can be configured as 10ms, 20ms, 32ms, 40ms, 64ms, 80ms, 128ms, 160ms, 320ms, or 640ms and in idle state the cycle time can be 160ms, 320ms or 640ms.
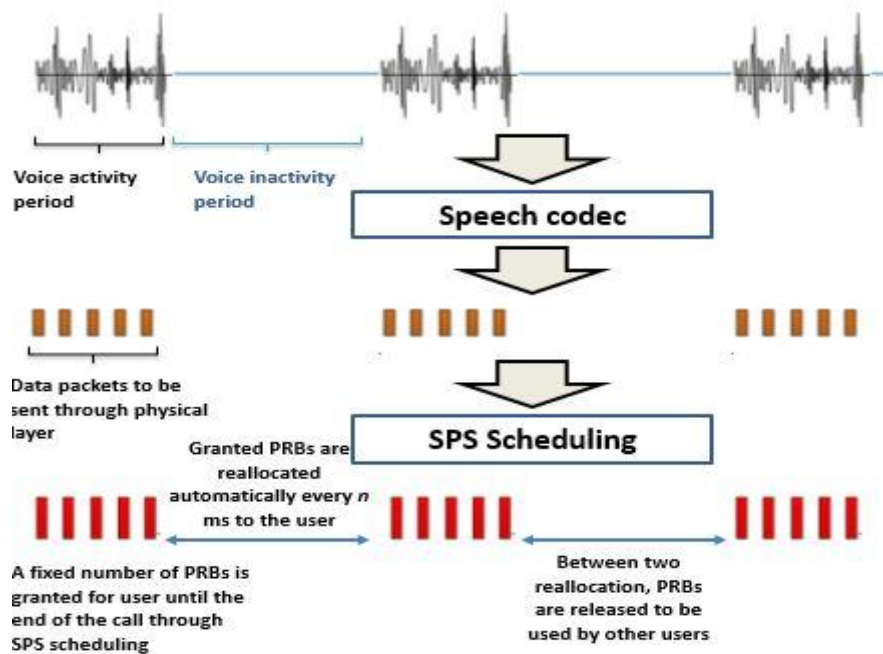
Figure 47, Illustration of PRB allocation for a third-party VoIP application and a native VoIP application (VoLTE) in LTE technology.

It should be noted that due to the critical requirements of delay in VoLTE, the network sets a higher priority to VoLTE users for having access the PRBs. In case of data usage, the network tries to maximize the number PRBs allocated to the user, in order to maximize the throughput and minimize the usage time. In contrast, VoLTE usage time is not linked to the throughput, thus the network tries to allocate the lowest required number of PRBs to VoLTE users in order to maintain the communication while avoiding overloading the network by VoLTE PRBs.

4.3. Assessment and analysis of TX and RX during different types of voice and data communication (Basel measurements)

As already mentioned, the emitted power by UE is determined by power control algorithms implemented in cellular network technologies. For each technology, the uplink emitted power is adjusted to channel condition in order to guarantee the connection to the BS. Thus, the emitted power by UE depends on the path loss between UE and BS, network technology and usage. In order to characterize the effect of these parameters on UE TX power, we have performed measurements in Basel Switzerland (see Section 3.3) on three operators for four different types of usages for GSM, UMTS and LTE technologies. Usages consist of on the one hand data usage by uploading a 100 MB and 10 MB files to an FTP server repeatedly and on other hand voice usage by performing CS, VoIP and VoLTE calls for a fixed duration (see Table 23). Measurements are performed on three operators, but the results are aggregated and analyzed together.

Table 23, Measurements scenarios for each location for Basel campaign

Technology	Usage	Duration
GSM	CS call	3 minutes
UMTS	CS call	3 minutes
	VoIP call (Skype)	2 minutes
	FTP file transfer 100 MB	5 minutes
	FTP file transfer 10 MB	
LTE	VoLTE call	3 minutes
	VoIP call (Skype)	2 minutes
	FTP file transfer 100 MB	5 minutes
	FTP file transfer 10 MB	

Measurements are performed on 14 sites consisting of 12 indoor and 2 outdoor locations. UE TX and RX powers, throughput and power control algorithm parameters are recorded during the measurements by two Nemo Handy trace mobile phones installed on a Sony Xperia and a Samsung Galaxy S8. It should be noted that VoLTE technology was active only by one operator. In order to stimulate the VAD algorithms during voice calls, it is ensured that there is voice/sound to be transmitted by talking to the phone during the experiment. The choice of 100MB and 10MB files was made to assess the throughput and power variation for applications that require respectively high data transfer and low data transfer and compare them to each other from an exposure point of view. Measurements are performed in urban and suburban environments covered by Macrocells. Measurements performed on all sites are aggregated and results are presented in terms of technology and usage. The correlation between the uplink emitted power by UE and the received power density is analyzed.

Regarding LTE technology, the emitted power mainly depends on the measured path loss in the downlink by UE and the number of uplink resource blocks allocated to UE. Therefore, the results of measured UE TX power in this experiment are highly dependent on the scenario. Thus the emitted UL power is on average higher in file transfer scenarios (see Table 24 and Figure 48). For high numbers of allocated PRBs, the UE emits higher than 10 dBm even if the RX value is relatively high. The maximum allowed UE TX power is measured as 23±1 dBm. The measured UE TX powers in 10 MB and 100 MB file transfer scenarios are almost identical which are 20 dBm in average.

Table 24, Characteristics of UE TX power in different usages for LTE technology

Usage	Mean (dBm)	Median (dBm)	Quantile 95%
VoLTE call	18.1	11	24
Skype call	17.3	14.1	23
FTP 10 MB	20	20	23
FTP 100 MB	21	21	23
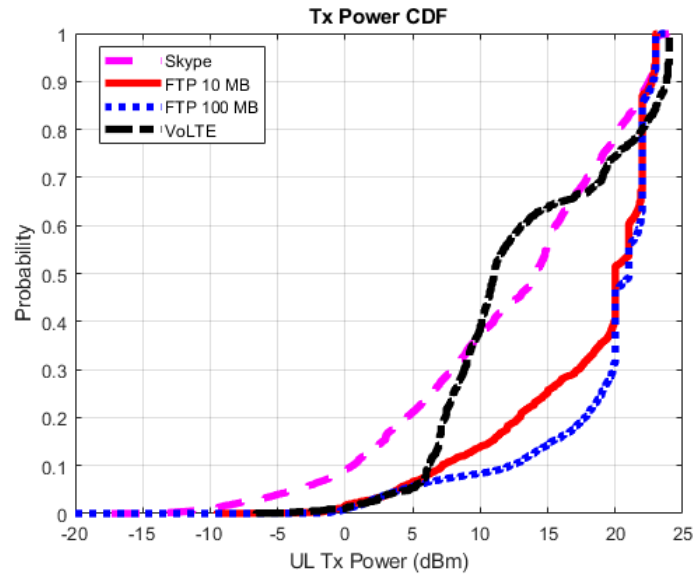
Figure 48, CDF emitted uplink TX power for LTE technology and different usages in Basel campaign

TX vs RX for VoLTE call
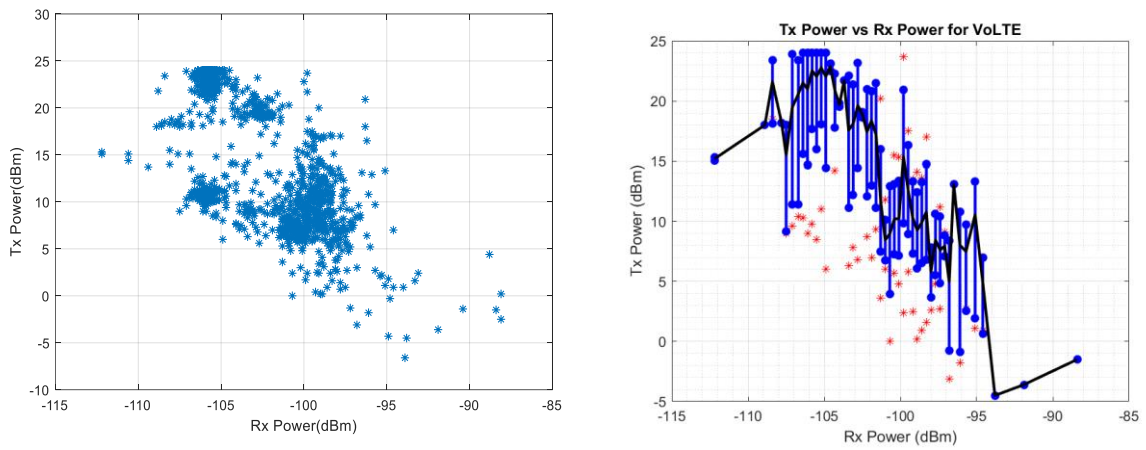
TX vs RX for VoIP (Skype) call
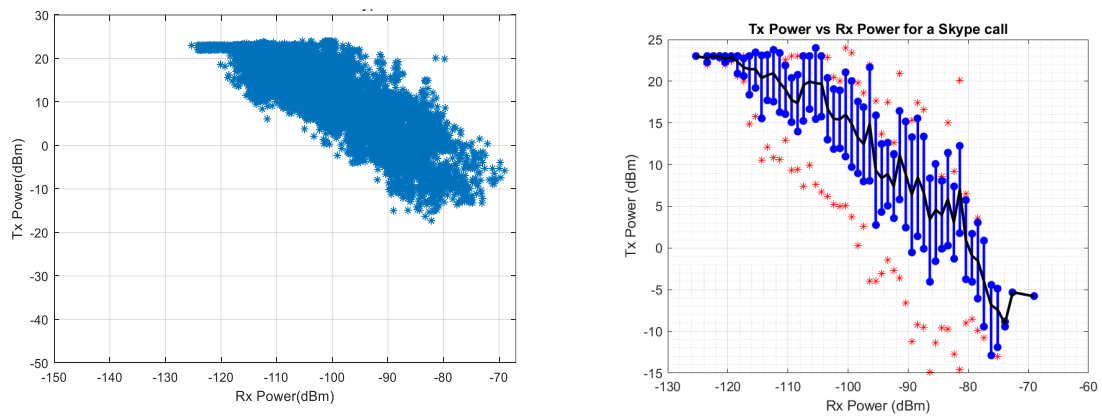
TX vs RX for FTP 10 MB file transfer
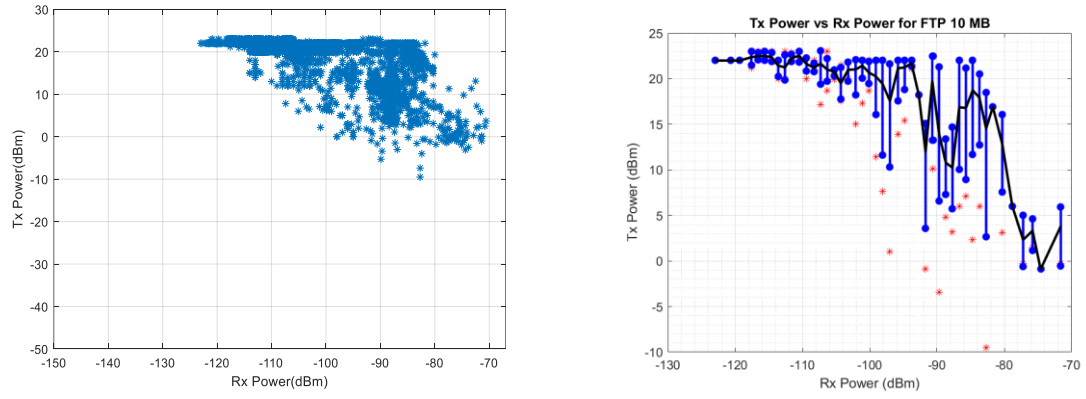
TX vs RX for FTP 100 MB file transfer
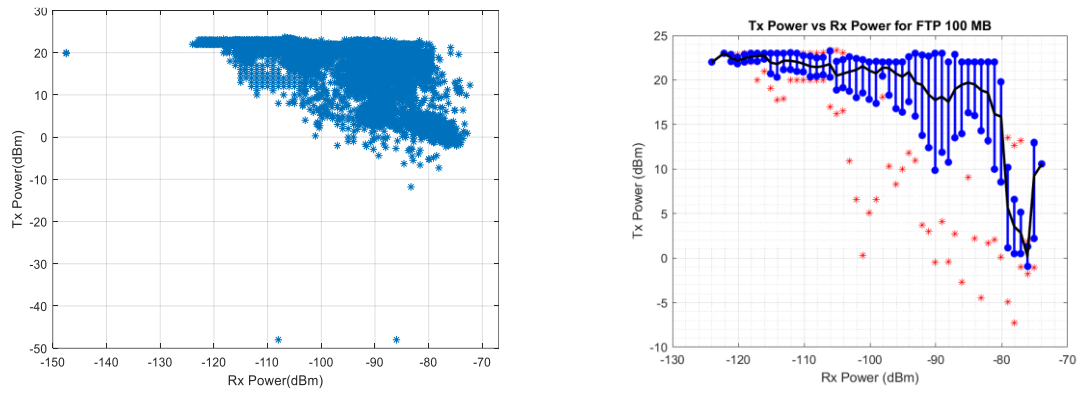
Figure 49, LTE TX power vs RX power for VoLTE, VoIP (skype), 10 MB file transfer, and 100 MB file transfer in Basel campaign. On left figures, blue dots represent measurement points. On right figures, red dots represent the minimum and maximum measured values, blue lines represent the standard deviation and black line represents the mean value.
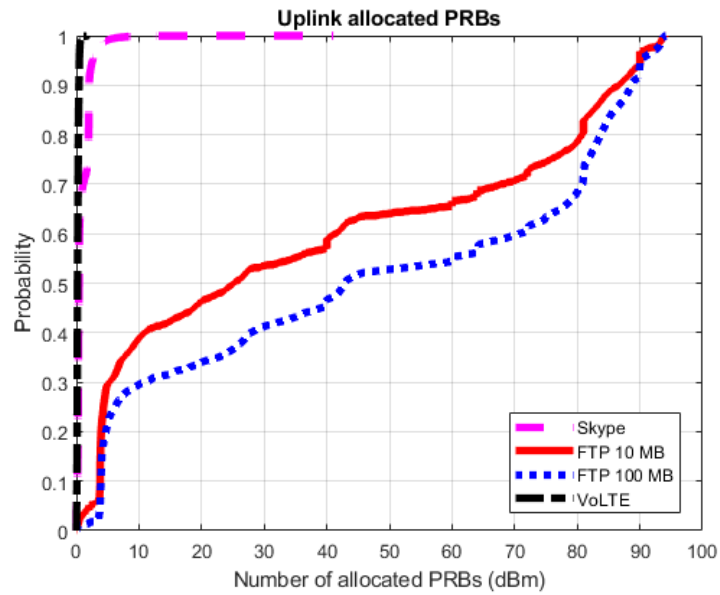
Figure 50, CDF, distribution of allocated UL PRBs for different usages in Basel campaign for LTE technology

Table 25, Characteristics of the allocated UL PRBs to UE for different usages in Basel campaign for LTE technology

LTE, PRBs (total 100)	Mean	Median	Quantile 95%
FTP 100	46	42	90
FTP 10	37	25	90
Skype call	0.9	0.4	2.60
VoLTE call	0.2	0.2	0.49

The characteristics of measured throughput for each usage scenario are presented in Table 26. Results confirm that in voice call scenarios the required throughput is very low comparing to FTP scenarios.

Table 26, Characteristics of LTE UL throughput for different usages in Basel trial

LTE, throughput	Mean (Mbps)	Median (Mbps)	Quantile 95% (Mbps)
FTP 100	14	8	46
FTP 10	11	2	44
Skype call	0.3	0.2	1
VoLTE call	0.06	0.1	0.2

Results and figure for UMTS and GSM technologies are presented in Appendices (Sections 6.1 and 6.2). GSM power control mechanism is not as efficient as the ones in UMTS and LTE. As a consequence, the relation between TX and RX powers is not obvious especially for GSM900 (see Figure 55). The UE tends to emit at higher power levels in GSM comparing to UMTS and LTE. The maximum allowed power in GSM 900 is 33 dBm and in GSM 1800 is 30 dBm.

4.4. Analysis of temporal power emission variation for voice communication technologies and applications

In order to characterize the power emission time during a voice call, a series of measurements have been performed in an indoor urban office environment at 1800 MHz frequency band for LTE and 900 MHz band for UMTS and GSM technologies. A Nemo trace mobile phone (see Section 3.2) is used in order to record the uplink emitted power and to lock on the communication frequency band and technology during trials. The trace mobile phone was connected to a French commercial cellular network operator and is placed in cheek position between a SAM head full of absorbent liquid and an absorbent dummy hand (see Figure 51). An antenna has been mounted in order to measure the emitted power and power emission time. Tektronix TDS6124C Digital Storage Oscilloscope is used to monitor and store the emitted power variation by mobile phone during a call. The distance between the receiver antenna and the trace mobile is 2 cm. The sampling rate of the oscilloscope is fixed to 20000 Samples/s.
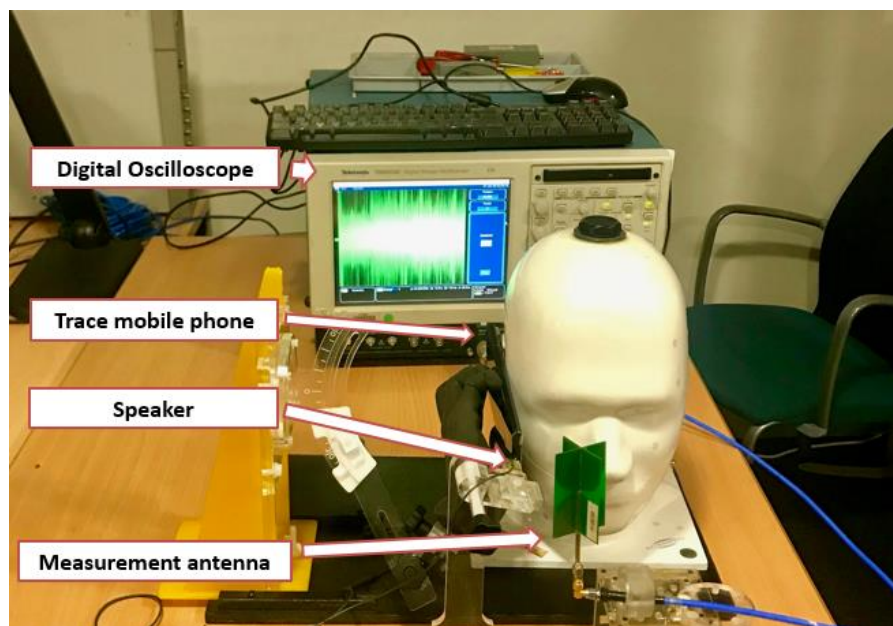
Figure 51, Temporal UE TX power measurement configuration

A 6 minutes voice speech file has been prepared which is a collection of multiple pieces of randomly chosen French audiobooks. The conversation rate of the audio file is 64%. During the measurement, the speech file has been played through a speaker, placed near the trace mobile microphone. The entire system has been caged by wave absorbents during the measurements in order to minimize the environmental noise. The lowest measurable value by oscilloscope is -16dBm. By measuring the environmental noise level, it is possible to define a threshold to eliminate the noise from the measurement results. Thus, the values below the

threshold will be considered as noise and the values above the threshold as the emitted power by UE. Therefore, the temporal occupation rate can be computed as the ratio of the measured signal duration above the threshold to the total measurement duration.

4.5. Temporal occupation rate results

The temporal variation of UE TX power is presented in Figure 52 for different technologies and usages. Temporal occupation rate values are presented in Table 27. In GSM technology the UE emits power one-eighth of the time that is 577µs every 4.61ms when VAD detects the user's voice. When VAD algorithm does not detect any voice, instead of voice frames, silence insertion descriptor frames are sent every now and then. Therefore, in theory, the UL temporal occupation rate is 12.5%. The measured temporal occupation rate over 6 minutes in speech is measured as 12.6% and in silence as 4.7%. The average length of bursts in speech mode is 0.53 ms is both cases.

In UMTS technology two completely different temporal power emission behaviors in CS and VoIP protocols are observed. In case of CS protocol, the UE is emitting almost continuously, however, in case of UMTS VoIP the UE emits in form of non-periodic bursts with variable durations. In addition, WCDMA air interface uses the spread spectrum modulation technique to spread the data bandwidth to the channel bandwidth which results in an increased variation of the signal in time domain. Thus, the detection of signal from noise needs advanced demodulation processing and applying the threshold noise elimination method introduces uncertainties to the results.

**Table 27, UE TX temporal occupation rate over 6 minutes for GSM, UMTS and LTE technologies for Speech and Silence scenarios**

Technology	Voice communication protocol	Scenario	Temporal occupation rate
GSM	CS	Speech	12.6%
		Silence	4.7%
UMTS (WCDMA)	CS	Speech	60.9%
		Silence	54.8%
	VoIP	Speech	27.9%
		Silence	9.9%

LTE	VoLTE	Speech	3.1%
		Silence	0.6%
	VoIP	Speech	18.4%
		Silence	9.8%

Regarding LTE technology, it is observed that power emission bursts are repeated every 20ms which means that the SPS scheduling interval is fixed to 20ms. Regarding Silence scenario, SPS interval is fixed to 160ms and each burst duration is slightly less than 1ms in both cases. The temporal occupation rate of VoLTE in speech mode is 3.1% and in silence mode is 0.6%. The temporal occupation rate in VoIP communication is measured as 18.4% which is due to the PRB allocation every 3 or 5ms. In Silence scenario the number of bursts are less than in Speech scenario with a temporal occupation rate of 9.8%. It should be noted that the average burst duration is about 1ms in both scenarios.

GSM CS Silence (500 ms)
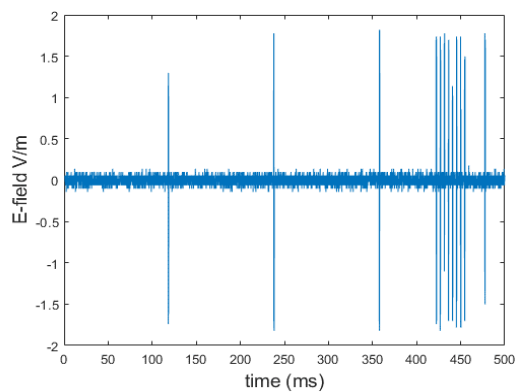
GSM CS Speech (50 ms)
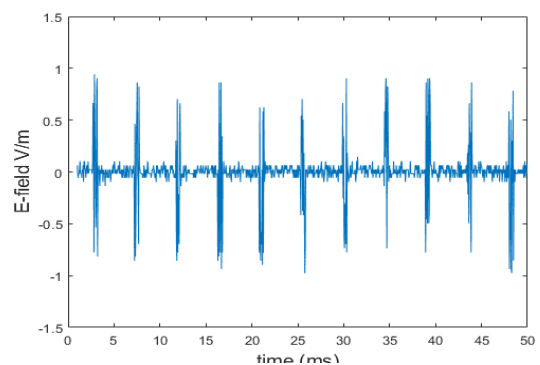
UMTS CS Silence (50 ms)
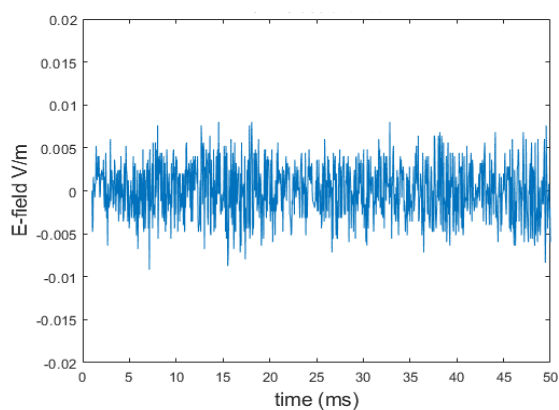
UMTS SC Speech (50 ms)
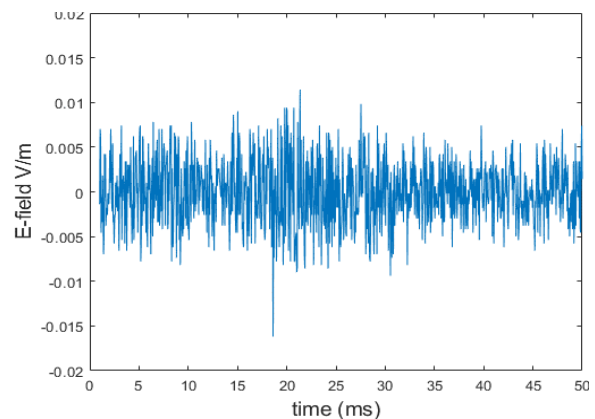
UMTS VoIP (Skype) Silence (50 ms)   UMTS VoIP (Skype) Speech (50 ms)
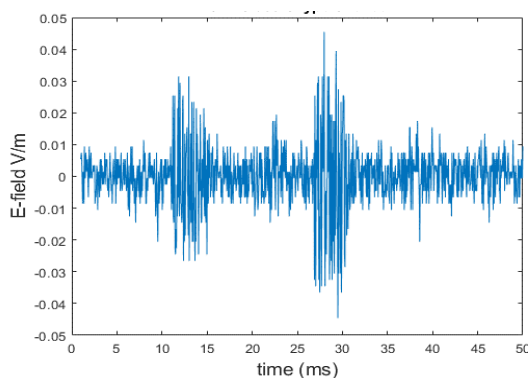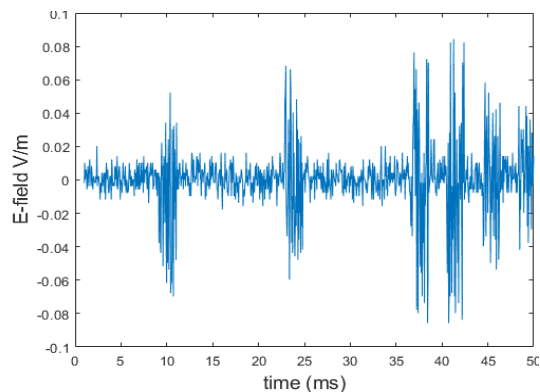
LTE VoLTE Silence (500 ms)   LTE VoLTE Speech (50 ms)
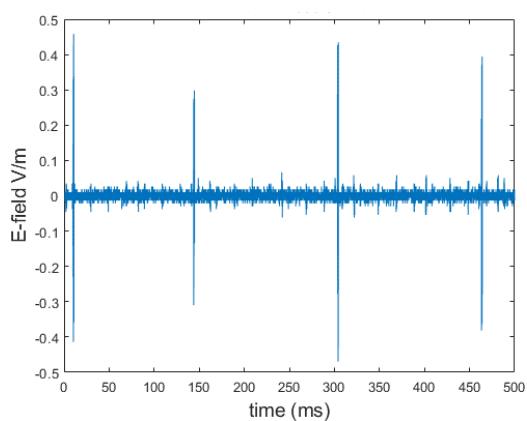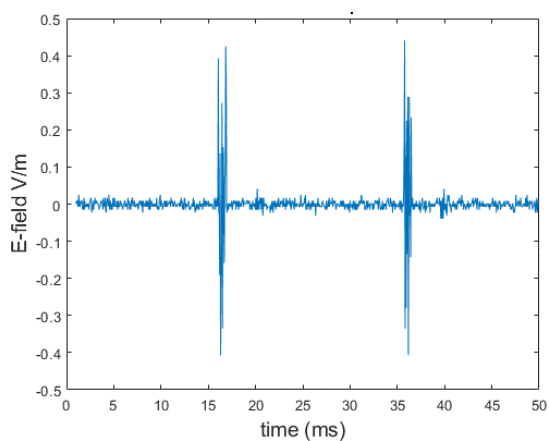
LTE VoIP (Skype) Silence (500 ms)   LTE VoIP (Skype) Speech (50 ms)
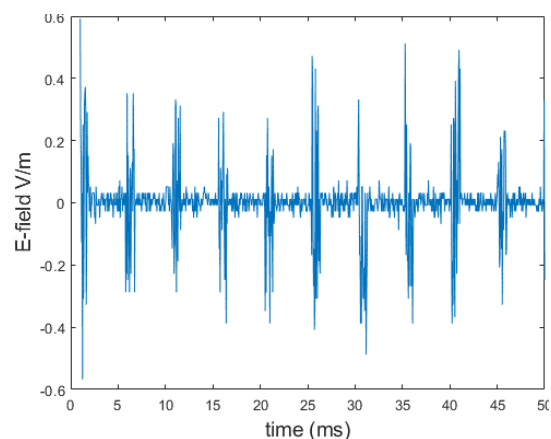
Figure 52, temporal variation of emitted power by UE for different technologies

It should be mentioned that these temporal occupation rate values cannot be applied to trace mobile phone measurement results. Trace mobile phones report the UE emitted power only

114

when they emit power. Also, the number of reported values per second differs from one trace mobile phone to another. For instance, Nemo reports maximum two UE TX power values per second. Besides, it is not completely clear that the reported value is either the sum of the emitted power or the average power during this period. Thus, it is not possible to apply temporal occupation rates to the trace mobile measurement results with no further information about the reported UE TX power.

4.6. Conclusion

The UL emitted power and the emission time duration by a mobile phone is highly dependent on the usage and the network technology. Mobile phones are used on the one hand, for a large variety of data u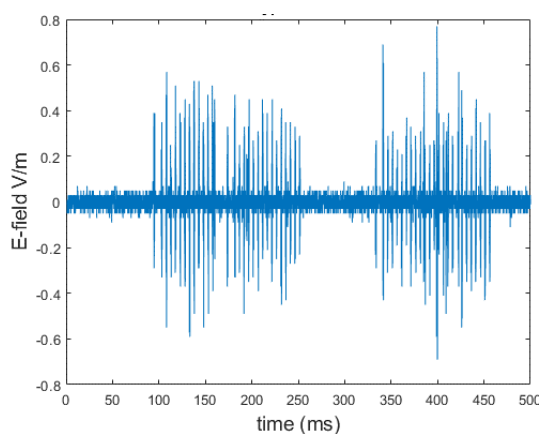sages that require different amount of data and throughput and on the other hand to make phone calls. The power control algorithms used in cellular networks are different from one technology to another in terms of efficiency.

In this chapter we tried to assess the UE TX power by mobile phone in different technologies and usages. Usages consist of CS and VoIP voice calls and FTP file uploading. Results of measurements performed in Basel, Switzerland illustrates that the emitted power by UE in FTP file transfer scenarios is higher in both UMTS and LTE technologies comparing to the voice call ones. In other words, the UE TX power depends not only on the path loss between UE and BS but also to the usage. Results show the same UE TX power for FTP 10 MB and 100 MB file transfers, however, about 10 times lower emission duration time is reported in 10 MB cases. Therefore, in FTP file transfer scenarios high UE TX power values are measured even with a good channel condition. It should be noted that in FTP file transfer the throughput is variable, however, in voice call scenarios the throughput is generally very low. As a consequence, the UE TX power during a voice call highly depends on the path loss between UE and BS.

In LTE technology, the lowest UE TX power is measured during a VoLTE call due to the SPS scheduling and optimized LTE native algorithms. In GSM technology, the UL power control algorithm used in GSM has the lowest efficiency due to the very slow power adaptation procedure.

Voice call communication requires a continuous and generally low throughput in order to maintain the communication during the call. On the contrary, in data usage the UE requires a higher data and throughput to perform the task as fast as possible. Therefore, it is expected that during a voice call even if the user is using the UE for a relatively long time, the exposure time

duration should be lower since the usage does not require high amount of data. In this regard, measurements are performed by using a digital oscilloscope to assess the temporal occupation rate for different types of voice communication in different technologies. Results show that the exposure duration during a voice call is highly variable. For instance, in VoLTE technology the UE emits for only 5.7% of the time while in UMTS CS call the UE transmits 60.9% of the time. These results should be taken into account for actual exposure assessment.

5. CONCLUSION

The main objective of this thesis was to assess the influence of new network architectures and usages on the actual human exposure induced by cellular networks. In this respect, several measurement campaigns and analyses were carried out in various cities and environments. The second chapter of this thesis is dedicated to introducing the state of the art on the electromagnetic radiofrequency exposure subject. It has been shown that the network architecture and usage can highly influence the population exposure and there is a lack of information on these subjects.

In this regard, the third chapter is dedicated to the analysis of the exposure in LTE Small cell heterogeneous networks. Two measurement campaigns were conducted to compare the induced global exposure in a heterogeneous network by measuring downlink E-field, throughput, downlink received power, and uplink emitted power by the user equipment.

Small cells are generally implemented for two purposes: on the one hand to bring coverage for users located at Macrocells cell-edge area and on the other hand to provide additional channel capacity in crowded areas near Macrocells. Results suggest that in both scenarios, deploying Small cells improves the propagation condition therefore, due to the LTE uplink power control algorithms, the user equipment TX power reduces significantly. However, in the first scenario, the uplink throughput was considerably increased which can imply the reduction of exposure duration time for data usage. In both cases, the global exposure reduced after deploying the Small cells.

Measurements were performed in outdoor environment on one point or while walking on predefined paths. Therefore, in order to be able to evaluate the exposure of indoor users based on outdoor measurements, statistical models were proposed for the uplink and downlink exposures in an LTE Small cell environment through the results of Small cell path loss measurements. It is observed that due to the high variability of the received signal, simple regression modeling methods do not provide a good estimation and they introduce high uncertainties to the output results. Thus, the path loss exponent is statistically modeled. It is shown that the path loss exponent is highly variable close to the Small cell while it becomes more stable in further distances. Therefore, two statistical models based on the distance to the Small cell antenna were built for 1800 MHz and 2600 MHz frequencies. The accuracy of these models has been examined using the measurement results and good accuracy is observed. Finally, using these models, Exposure Index is assessed in a simplistic scenario including one Small cell antenna for indoor and outdoor users in a typical French city model. Exposure Index

is a global exposure metric taking into account a series of influencing parameters such as technologies, cell types, user profiles, user postures, etc. for downlink and uplink exposure and provides the global exposure of a population in a given geographical area (see Section 2.6.2.). According to results, the EI is higher for indoor users since the TX power by user equipment placed in indoor areas is higher due to worse propagation conditions comparing to outdoor ones.

The last part of the thesis was devoted to assessing the exposure for new types of usages through measurements. The first measurement trial was conducted in different locations in indoor and outdoor, urban, suburban and rural areas considering several types of usages (voice call: circuit switch calls, VoIP and VoLTE calls, data usage: uploading 10 MB and 100 MB files). Results suggest that the highest UE TX powers are observed in file transfer scenarios. Also, the amount of emitted power is nearly equal for 100 MB and 10 MB file transfer, however, the exposure duration in 100 MB case is higher. Furthermore, in addition to the channel condition, the UE TX power is highly dependent on usage. Results show high UE TX powers in file transfer scenarios even with a good channel condition. Since in voice usage, whether VoIP or CS call, the amount of data volume to be transferred is very low, the UE TX power depends mainly on the channel condition. The last section of the thesis investigated the UE TX power emission duration for different types of voice communications. It is observed that the emission time during a call is highly dependent on the technology. For instance, in VoLTE technology, UE TX bursts follow a repetitive pattern at a constant rate and the temporal occupation rate is measured to be lower than 5%. However, in case of CS UMTS voice call, the temporal occupation rate is measured to be more than 50%. These values can be helpful to assess the actual UL exposure which takes into account the exposure time and exposure intensity at the same time.

5G technology aims to answer to the increasing traffic and capacity demand in the near future. In this respect, a wide range of new spectrums will be used by cellular communication networks and current networks will be massively densified by indoor and outdoor Small cells and Picocells. It is expected that in future networks a large number of Small cells, equipped with massive MIMO antennas and operating at millimeter-wave frequencies will be deployed to offload the traffic from LTE and 5G base stations.

These new techniques will have an important impact on propagation conditions, therefore on the EMF exposure. Millimeter wave propagation consists of sever path loss, high penetration loss, and narrow beamwidth. Thus, results and analyses performed in LTE frequency bands

cannot be directly applied for these frequencies. However, by improving the network coverage through Small cell densification, the uplink exposure hence the global exposure will be significantly reduced. Also, millimeter-wave spectrums bring access to larger frequency bands and as a result a higher network capacity and throughput. Since the uplink exposure duration for data usage is related to the throughput, using millimeter-wave spectrums may decrease the uplink exposure duration and the global exposure. Regarding the downlink exposure, because the path loss is extremely high in these frequencies, densifying the network may have a small impact on the downlink exposure though it should be investigated through measurements.

Besides, through 5G technology, new types of cellular network usages such as connected cars, internet of things, and new gaming features will be introduced and will be used by users. The impact of these new usages on exposure should be investigated in terms of the absorbed power and the exposure duration. We have seen that for instance in voice usage, even if the user is using the UE for a relatively long period of time, the real power emission duration can be highly variable in terms of technology. In any case, the actual exposure assessment of the population induced by future cellular networks will become a more complex task, and new methods should be developed to deal with these complexities. The work presented in this thesis can be considered as an initiative to assess the actual population exposure in future networks.

6. APPENDICES

6.1. Basel measurement UMTS TX/RX results

In UMTS technology the emitted uplink power is highly dependent on the channel condition [54] and is determined by measuring the received signal code power (RSCP) in open-loop and SINR in a closed-loop manner. The emitted power reduces when there is a better reception and vice versa (see Figure 54). The emitted power is higher for data transmission and the distribution of measured TX power values for 10 MB and 100 MB file transfer are almost identical (see Figure 53). The characteristics of measured throughput for different usages is presented in Table 29.
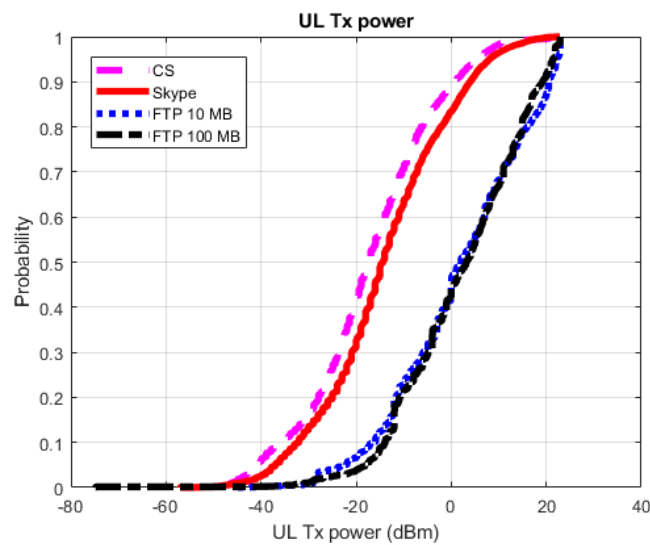
Figure 53, CDF, Distribution of UE TX powers for different usages in Basel trial for UMTS technology

TX vs RX for CS call
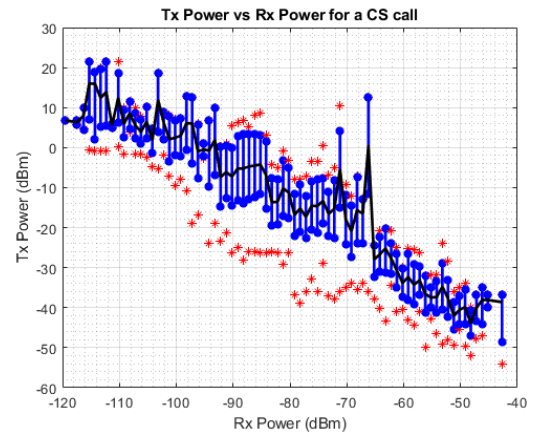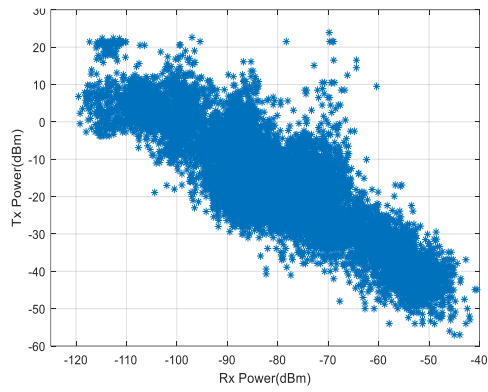
TX vs RX for VoIP (Skype) call
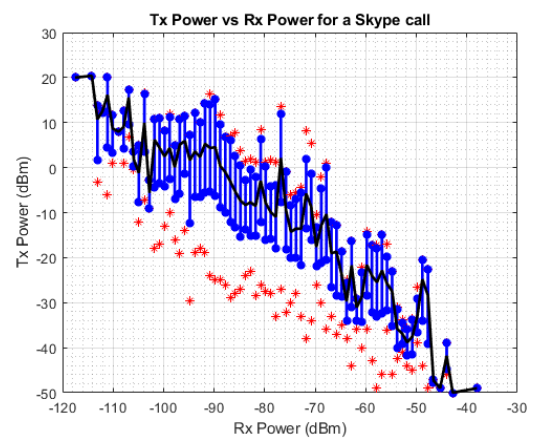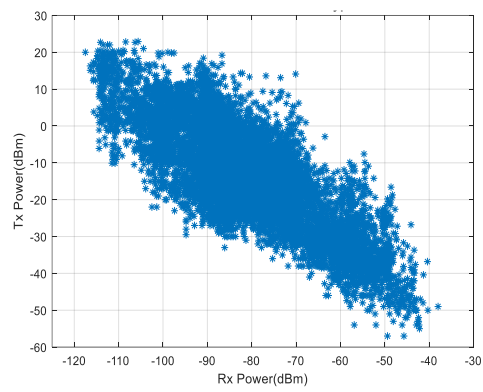
TX vs RX for FTP 10 MB file transfer
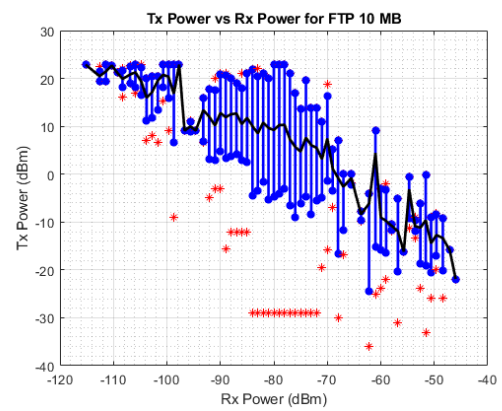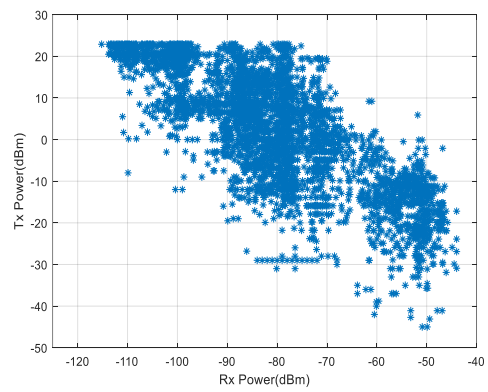
TX vs RX for FTP 100 MB file transfer
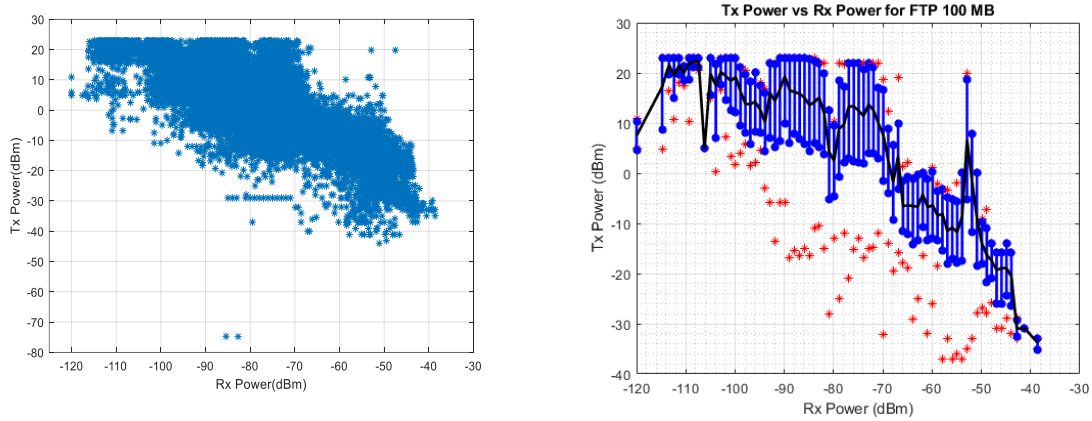
Figure 54, UMTS TX vs RX power for CS, VoIP (skype), 10 MB file transfer and 100 MB file transfer. Blue dots on left figures represent measurement points. on the right figures, red dots represent the minimum and maximum measured values, blue lines the standard deviation and black line represent the mean.

Table 28, characteristics of UE TX power for different usages in Basel trial for UMTS technology

Usage	Mean (dBm)	Median (dBm)	Quantile 95% (dBm)
CS call	1.1	-17	5.3
Skype call	2.4	-14.4	8
FTP 10 MB	14.5	2.1	22.4
FTP 100 MB	13.4	3.1	21.4

Table 29, Characteristics of UL throughput for different usages in Basel trial for UMTS technology

Usage	Mean (Mbps)	Median (Mbps)	Quantile 95% (Mbps)
Skype	0.06	0.1	0.2
FTP 10MB	1.5	1.7	3.3
FTP 100MB	1.8	1.7	4

6.2. Basel measurement GSM TX/RX results

In GSM technology the correlation between TX and RX values is less clear. The UL power control mechanism in CS GSM is managed through BS by adjusting the UE TX power according to the received signal level at the BS. This adjustment is performed approximately 2 times per second. Power variations due to handover are not taken into account since measurements are static.

TX vs RX for GSM 900 CS call
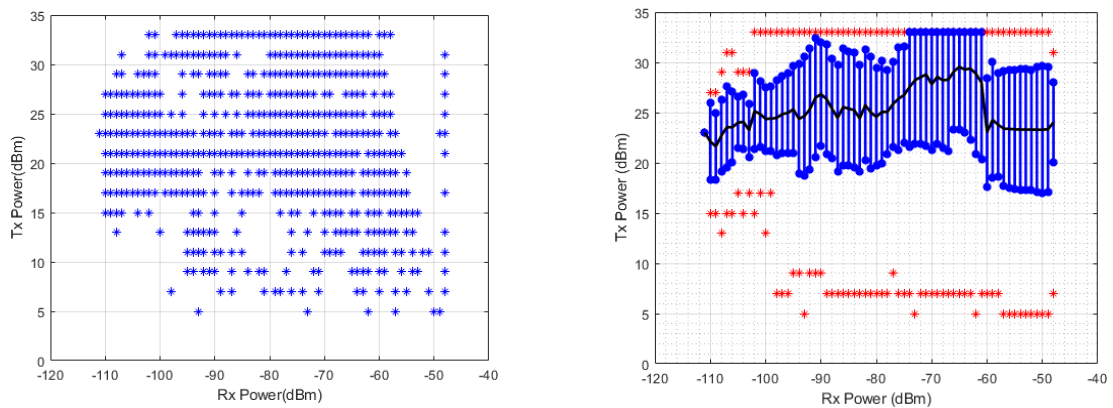
TX vs RX for GSM 1800 CS call
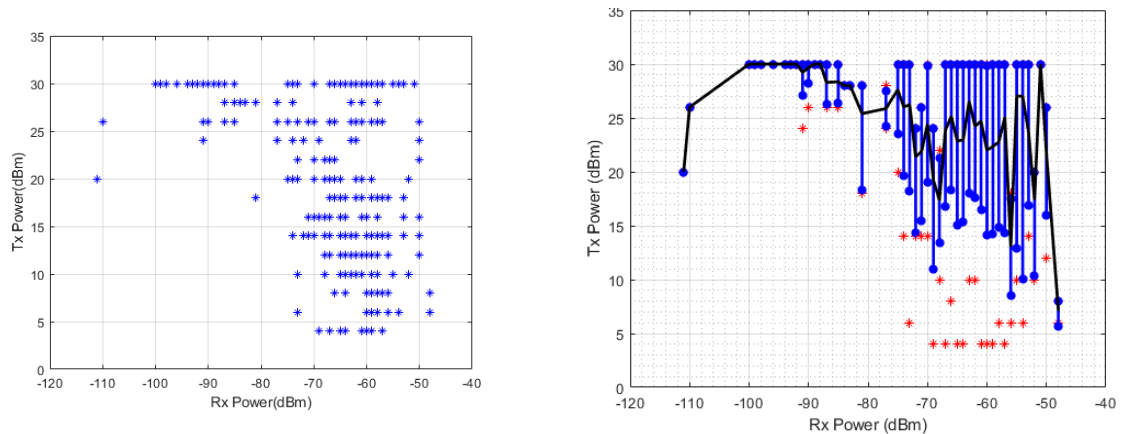
Figure 55, GSM TX vs RX power for CS. Blue dots on the left figures represent measurement points. on the right figures, red dots represent the minimum and maximum measured values, blue lines the standard deviation, and black lines represent the mean value.

Table 30, Characteristics of UE TX power during GSM CS call

Technology	Usage	Mean (dBm)	Median (dBm)	Quantile 95% (dBm)
GSM 900	CS call	26.5	23	33
GSM 1800	CS call	25.42	20	30

7. BIBLIOGRAPHY

[1]   Cisco, "Cisco Annual Internet Report (2018–2023)," 2018. [Online]. Available: https://www.cisco.com/c/en/us/solutions/collateral/executive-perspectives/annual-internet-report/white-paper-c11-741490.html.

[2]   "ICNIRP statement on the 'guidelines for limiting exposure to time-varying electric, magnetic, and electromagnetic fields (up to 300 ghz).'" icnirp, 2009, [Online]. Available:https://www.icnirp.org/cms/upload/publications/ICNIRPStatementEMF.pdf.

[3]   "ICNIRP." https://www.icnirp.org/ (accessed Feb. 20, 2020).

[4]   A. Gati, E. Conil, M.-F. Wong, and J. Wiart, "Duality Between Uplink Local and Downlink Whole-Body Exposures in Operating Networks," *IEEE Transactions on Electromagnetic Compatibility*, vol. 52, no. 4, pp. 829–836, Nov. 2010, doi: 10.1109/TEMC.2010.2066978.

[5]   O. Lauer, P. Frei, M.-C. Gosselin, W. Joseph, M. Röösli, and J. Fröhlich, "Combining near- and far-field exposure for an organ-specific and whole-body RF-EMF proxy for epidemiological research: A reference case," *Bioelectromagnetics*, vol. 34, no. 5, pp. 366–374, 2013, doi: 10.1002/bem.21782.

[6]   N. Varsier *et al.*, "A novel method to assess human population exposure induced by a wireless cellular network," *Bioelectromagnetics*, vol. 36, no. 6, pp. 451–463, Sep. 2015, doi: 10.1002/bem.21928.

[7]   "International Committee on Electromagnetic Safety," *ICES*. https://www.ices-emfsafety.org/ (accessed Mar. 04, 2020).

[8]   "Council recomendation of 12 July 1999 on the limitation of exposure of the general public to electromagnetic fields (0 Hz to 300 GHz), (1999/519/EC)." Jul. 30, 1999.

[9]   International Commission on Non-Ionizing Radiation Protection, "ICNIRP guidelines for limiting exposure to time-varying electric, magnetic and electromagnetic fields (up to 300 ghz)." 1998.

[10]   International Commission on Non-Ionizing Radiation Protection, "ICNIRP guidelines for limiting exposure to time-varying electric, magnetic and electromagnetic fields (100 khz to 300 ghz)." mar. 2020.

[11]   S. Hagness and A. Taflove, *Computational electrodynamics: The finite-difference time-domain method.* Norwood, MA: Artech House, 2000.

[12]   P. Bernardi, M. Cavagnaro, and S. Pisa, "Evaluation of the SAR distribution in the human head for cellular phones used in a partially closed environment," *IEEE Transactions on Electromagnetic Compatibility*, vol. 38, no. 3, pp. 357–366, Aug. 1996, doi: 10.1109/15.536066.

[13]   P. Bernardi, M. Cavagnaro, S. Pisa, and E. Piuzzi, "SAR distribution and temperature increase in an anatomical model of the human eye exposed to the field radiated by the user antenna in a wireless LAN," *IEEE Transactions on Microwave Theory and Techniques*, vol. 46, no. 12, pp. 2074–2082, Dec. 1998, doi: 10.1109/22.739285.

[14]   M. Hagmann and O. Gandhi, "Numerical calculation of electromagnetic energy deposition in models of man with grounding and reflector effects," *Radio Science - RADIO SCI*, vol. 14, pp. 23–29, Nov. 1979, doi: 10.1029/RS014i06Sp00023.

[15]   O. P. Gandhi, G. Lazzi, A. Tinniswood, and Q. S. Yu, "Comparison of numerical and experimental methods for determination of SAR and radiation patterns of handheld wireless telephones," *Bioelectromagnetics*, vol. Suppl 4, pp. 93–101, 1999, doi: 10.1002/(sici)1521-186x(1999)20:4+<93::aid-bem11>3.0.co;2-8.

[16]   A. Christ *et al.*, "The Virtual Family--development of surface-based anatomical models of two adults and two children for dosimetric simulations," *Phys Med Biol*, vol. 55, no. 2, pp. N23-38, Jan. 2010, doi: 10.1088/0031-9155/55/2/N01.

[17] N. Varsier *et al.*, "Influence of pregnancy stage and fetus position on the whole-body and local exposure of the fetus to RF-EMF," *Phys Med Biol*, vol. 59, no. 17, pp. 4913–4926, Sep. 2014, doi: 10.1088/0031-9155/59/17/4913.

[18] S. Gabriel, R. W. Lau, and C. Gabriel, "The dielectric properties of biological tissues: II. Measurements in the frequency range 10 Hz to 20 GHz," *Phys. Med. Biol.*, vol. 41, no. 11, pp. 2251–2269, Nov. 1996, doi: 10.1088/0031-9155/41/11/002.

[19] D. E. Merewether, R. Fisher, and F. W. Smith, "On Implementing a Numeric Huygen's Source Scheme in a Finite Difference Program to Illuminate Scattering Bodies," *IEEE Transactions on Nuclear Science*, vol. 27, no. 6, pp. 1829–1833, Dec. 1980, doi: 10.1109/TNS.1980.4331114.

[20] R. Holland and J. W. Williams, "Total-Field versus Scattered-Field Finite-Difference Codes: A Comparative Assessment," *IEEE Transactions on Nuclear Science*, vol. 30, no. 6, pp. 4583–4588, Dec. 1983, doi: 10.1109/TNS.1983.4333175.

[21] IT'IS Foundation., "The Virtual Population." [Online]. Available:https://itis.swiss/assets/Downloads/VirtualPopulation/1302-virtual-population.pdf.

[22] E. Conil, A. Hadjem, F. Lacroux, M. F. Wong, and J. Wiart, "Variability analysis of SAR from 20 MHz to 2.4 GHz for different adult and child models using finite-difference time-domain," *Phys Med Biol*, vol. 53, no. 6, pp. 1511–1525, Mar. 2008, doi: 10.1088/0031-9155/53/6/001.

[23] T. Wu *et al.*, "Chinese adult anatomical models and the application in evaluation of RF exposures," *Phys Med Biol*, vol. 56, no. 7, pp. 2075–2089, Apr. 2011, doi: 10.1088/0031-9155/56/7/011.

[24] M.-C. Gosselin *et al.*, "Estimation Formulas for the Specific Absorption Rate in Humans Exposed to Base-Station Antennas," *IEEE Transactions on Electromagnetic Compatibility*, vol. 53, no. 4, pp. 909–922, Nov. 2011, doi: 10.1109/TEMC.2011.2139216.

[25] A. Hirata, Y. Nagaya, F. Osamu, T. Nagaoka, and S. Watanabe, "Correlation Between Absorption Cross Section and Body Surface Area of Human for Far-Field Exposure at GHz Bands," in *2007 IEEE International Symposium on Electromagnetic Compatibility*, Jul. 2007, pp. 1–4, doi: 10.1109/ISEMC.2007.143.

[26] E. Conil, A. Hadjem, A. Gati, M.-F. Wong, and J. Wiart, "Influence of Plane-Wave Incidence Angle on Whole Body and Local Exposure at 2100 MHz," *IEEE Transactions on Electromagnetic Compatibility*, vol. 53, no. 1, pp. 48–52, Feb. 2011, doi: 10.1109/TEMC.2010.2061849.

[27] T. Kientega *et al.*, "A surrogate model to assess the whole body SAR induced by multiple plane waves at 2.4 GHz," *Ann. Telecommun.*, vol. 66, no. 7, pp. 419–428, Aug. 2011, doi: 10.1007/s12243-011-0261-z.

[28] R. P. Findlay and P. J. Dimbylow, "Effects of posture on FDTD calculations of specific absorption rate in a voxel model of the human body," *Phys Med Biol*, vol. 50, no. 16, pp. 3825–3835, Aug. 2005, doi: 10.1088/0031-9155/50/16/011.

[29] Z. Altman *et al.*, "Efficient models for base station antennas for human exposure assessment," *IEEE Transactions on Electromagnetic Compatibility*, vol. 44, no. 4, pp. 588–592, Nov. 2002, doi: 10.1109/TEMC.2002.801776.

[30] A. Faraone, Roger Yew-Siow Tay, K. H. Joyner, and Q. Balzano, "Estimation of the average power density in the vicinity of cellular base-station collinear array antennas," *IEEE Transactions on Vehicular Technology*, vol. 49, no. 3, pp. 984–996, May 2000, doi: 10.1109/25.845115.

[31] J. Wiart, "Propagation des ondes radioelectriques en milieu urbain dans un contexte microcellulaire. analyse par la gtd et validation experimentale," École nationale supérieure des télécommunications, 1995.

[32] J.-P. Rossi, J. Wiart, and F. Eynard, "In situ measurement of reflection and diffraction coefficients of UHF radio waves on buildings using a ring array," *Radio Science*, vol. 35, no. 2, pp. 361–369, 2000, doi: 10.1029/1998RS002146.

[33] D. Tse and P. Viswanath, *Fundamentals of Wireless Communication*. Cambridge University Press, 2005.

[34] CENELEC, "CENELEC - EN 50492, Basic standard for the in-situ measurement of electromagnetic field strength related to human exposure in the vicinity of base stations." 2008.

[35] "IEC 62232:2017 , Determination of RF field strength and SAR in the vicinity of radiocommunication base stations for the purpose of evaluating human exposure." 2017.

[36] E. Larcheveque, C. Dale, Man-Fai Wong, and J. Wiart, "Analysis of electric field averaging for in situ radiofrequency exposure assessment," *IEEE Transactions on Vehicular Technology*, vol. 54, no. 4, pp. 1245–1250, Jul. 2005, doi: 10.1109/TVT.2005.851334.

[37] "Cartoradio - ANFR." https://www.cartoradio.fr/index.html#/ (accessed Feb. 21, 2020).

[38] E. Chiaramello *et al.*, "Radio Frequency Electromagnetic Fields Exposure Assessment in Indoor Environments: A Review," *International Journal of Environmental Research and Public Health*, vol. 16, no. 6, p. 955, Jan. 2019, doi: 10.3390/ijerph16060955.

[39] "How is the time of women and men distributed in Europe? - Issue number 4/2006." https://ec.europa.eu/eurostat/web/products-statistics-in-focus/-/KS-NK-06-004 (accessed Mar. 13, 2020).

[40] U. Knafl, H. Lehmann, and M. Riederer, "Electromagnetic field measurements using personal exposimeters," *Bioelectromagnetics*, vol. 29, no. 2, pp. 160–162, 2008, doi: 10.1002/bem.20373.

[41] "EME Spy Evolution | MVG." https://www.mvg-world.com/en/products/rf-safety/public-rf-safety/eme-spy-evolution (accessed May 04, 2020).

[42] Y. Pinto and J. Wiart, "Surrogate model based on polynomial chaos of indoor exposure induced from a WLAN source," in *2017 XXXIInd General Assembly and Scientific Symposium of the International Union of Radio Science (URSI GASS)*, Aug. 2017, pp. 1–3, doi: 10.23919/URSIGASS.2017.8105170.

[43] Joe Wiart, *Radio-Frequency Human Exposure Assessment: From Deterministic to Stochastic Methods | Wiley*. Wiley.

[44] "Starlab | MVG." https://www.mvg-world.com/en/products/antenna-measurement/multi-probe-systems/starlab (accessed Apr. 03, 2020).

[45] "IEC/IEEE 62704-1:2017 Determining the peak spatial-average specific absorption rate (SAR) in the human body from wireless communications devices, 30 MHz to 6 GHz - Part 1: General requirements for using the finite difference time-domain (FDTD) method for SAR calculations." 2017.

[46] Y. Pinto *et al.*, "Numerical mobile phone models validated by SAR measurements," in *Proceedings of the 5th European Conference on Antennas and Propagation (EUCAP)*, Apr. 2011, pp. 2585–2588.

[47] INTERPHONE Study Group, "Brain tumour risk in relation to mobile telephone use: results of the INTERPHONE international case-control study," *Int J Epidemiol*, vol. 39, no. 3, pp. 675–694, Jun. 2010, doi: 10.1093/ije/dyq079.

[48] M. B. Toledano *et al.*, "An international prospective cohort study of mobile phone users and health (COSMOS): Factors affecting validity of self-reported mobile phone use," *Int J Hyg Environ Health*, vol. 221, no. 1, pp. 1–8, 2018, doi: 10.1016/j.ijheh.2017.09.008.

[49] W. Kainz *et al.*, "Dosimetric comparison of the specific anthropomorphic mannequin (SAM) to 14 anatomical head models using a novel definition for the mobile phone positioning," *Phys Med Biol*, vol. 50, no. 14, pp. 3423–3445, Jul. 2005, doi: 10.1088/0031-9155/50/14/016.

[50] N. Kuster, J. Schuderer, A. Christ, P. Futter, and S. Ebert, "Guidance for exposure design of human studies addressing health risk evaluations of mobile phones," *Bioelectromagnetics*, vol. 25, no. 7, pp. 524–529, 2004, doi: 10.1002/bem.20034.

[51] A. Ghanmi, "Analyse de l'exposition aux ondes électromagnétiques des enfants dans le cadre des nouveaux usages et nouveaux réseaux," 2013.

[52] A. Krayni, A. Hadjem, A. Sibille, C. Roblin, and J. Wiart, "A Novel Methodology to Evaluate Uplink Exposure by Personal Devices in Wireless Networks," *IEEE Transactions on Electromagnetic Compatibility*, vol. 58, no. 3, pp. 896–906, Jun. 2016, doi: 10.1109/TEMC.2016.2524543.

[53] J. Wiart, C. Dale, A. V. Bosisio, and A. Le Cornec, "Analysis of the influence of the power control and discontinuous transmission on RF exposure with GSM mobile phones," *IEEE Transactions on Electromagnetic Compatibility*, vol. 42, no. 4, pp. 376–385, Nov. 2000, doi: 10.1109/15.902307.

[54] A. Gati, A. Hadjem, W. Man-Fai, and J. Wiart, "Exposure Induced by WCDMA Mobiles Phones in Operating Networks," *IEEE TRANSACTIONS ON WIRELESS COMMUNICATIONS*, vol. 8, no. 12, p. 5723, Dec. 2009.

[55] K. Pokovic, T. Schmid, J. Frohlich, and N. Kuster, "Novel probes and evaluation procedures to assess field magnitude and polarization," *IEEE Transactions on Electromagnetic Compatibility*, vol. 42, no. 2, pp. 240–244, May 2000, doi: 10.1109/15.852419.

[56] C. Grangeat, C. Person, D. Picard, and J. Wiart, "Mesure du Débit d'Absorption Spécifique (das) des téléphones mobiles — contribution du projetcomobio à la normalisation internationale," *Ann. Télécommun.*, vol. 58, no. 5, pp. 740–765, May 2003, doi: 10.1007/BF03001528.

[57] C. Gabriel, S. Gabriel, and E. Corthout, "The dielectric properties of biological tissues: I. Literature survey," *Phys. Med. Biol.*, vol. 41, no. 11, pp. 2231–2249, Nov. 1996, doi: 10.1088/0031-9155/41/11/001.

[58] S. Gabriel, R. W. Lau, and C. Gabriel, "The dielectric properties of biological tissues: III. Parametric models for the dielectric spectrum of tissues," *Phys. Med. Biol.*, vol. 41, no. 11, pp. 2271–2293, Nov. 1996, doi: 10.1088/0031-9155/41/11/003.

[59] "IEC 62209-2:2010/AMD1:2019, Human exposure to radio frequency fields from hand-held and body-mounted wireless communication devices - Human models, instrumentation, and procedures - Part 2: Procedure to determine the specific absorption rate (SAR) for wireless communication devices used in close proximity to the human body (frequency range of 30 MHz to 6 GHz)." 2019, Accessed: Mar. 19, 2020. [Online]. Available: https://webstore.iec.ch/publication/61098.

[60] "ART-Fi SAR Measurement," *ART-Fi*. https://www.art-fi.eu/ (accessed Mar. 13, 2020).

[61] Z. Liu, D. Allal, M. Cox, and J. Wiart, "Discrepancies of Measured SAR between Traditional and Fast Measuring Systems," *International Journal of Environmental Research and Public Health*, vol. 17, no. 6, p. 2111, Jan. 2020, doi: 10.3390/ijerph17062111.

[62] International Electrotechnical Commission, Ed., "IEC 62209-3 ED. 1.0 B:2019, Measurement procedure for the assessment of specific absorption rate of human exposure to radio frequency fields from hand-held and body-mounted wireless communication devices - Part 3: Vector measurement-based systems (Frequency range of 600 MHz to 6 GHz)." Sep. 24, 2019.

[63] S. Aerts, J. Wiart, L. Martens, and W. Joseph, "Assessment of long-term spatio-temporal radiofrequency electromagnetic field exposure," *Environmental Research*, vol. 161, pp. 136–143, Feb. 2018, doi: 10.1016/j.envres.2017.11.003.

[64] J. F. B. Bolte and T. Eikelboom, "Personal radiofrequency electromagnetic field measurements in the Netherlands: Exposure level and variability for everyday activities, times of day and types of area," *Environment International*, vol. 48, pp. 133–142, Nov. 2012, doi: 10.1016/j.envint.2012.07.006.

[65] M. Vrijheid *et al.*, "Determinants of mobile phone output power in a multinational study: implications for exposure assessment," *Occup Environ Med*, vol. 66, no. 10, pp. 664–671, Oct. 2009, doi: 10.1136/oem.2008.043380.

[66] M. A. Kelsh *et al.*, "Measured radiofrequency exposure during various mobile-phone use scenarios," *J Expo Sci Environ Epidemiol*, vol. 21, no. 4, pp. 343–354, Aug. 2011, doi: 10.1038/jes.2010.12.

[67] "Lexnet." http://www.lexnet.fr/ (accessed May 04, 2020).

[68] Y. Huang *et al.*, "Comparison of average global exposure of population induced by a macro 3G network in different geographical areas in France and Serbia," *Bioelectromagnetics*, vol. 37, no. 6, pp. 382–390, Sep. 2016, doi: 10.1002/bem.21990.

[69] "LTE; Evolved Universal Terrestrial Radio Access (E-UTRA); Physical layer; Measurements,(3GPP TS 36.214 version 4.2.0 Release 14)." ETSI.

[70] D. Plets *et al.*, "Joint minimization of uplink and downlink whole-body exposure dose in indoor wireless networks," *Biomed Res Int*, vol. 2015, p. 943415, 2015, doi: 10.1155/2015/943415.

[71] S. Aerts, D. Plets, L. Verloock, L. Martens, and W. Joseph, "Assessment and comparison of total RF-EMF exposure in femtocell and macrocell base station scenarios," *Radiat Prot Dosimetry*, vol. 162, no. 3, pp. 236–243, Dec. 2014, doi: 10.1093/rpd/nct272.

[72] S. Aerts, D. Plets, A. Thielens, L. Martens, and W. Joseph, "Impact of a small cell on the RF-EMF exposure in a train," *Int J Environ Res Public Health*, vol. 12, no. 3, pp. 2639–2652, Feb. 2015, doi: 10.3390/ijerph120302639.

[73] J. Stephan, M. Brau, Y. Corre, and Y. Lostanlen, "Joint analysis of small-cell network performance and urban Electromagnetic Field exposure," in *The 8th European Conference on Antennas and Propagation (EuCAP 2014)*, Apr. 2014, pp. 2623–2627, doi: 10.1109/EuCAP.2014.6902360.

[74] T. Mazloum, S. Aerts, W. Joseph, and J. Wiart, "RF-EMF exposure induced by mobile phones operating in LTE small cells in two different urban cities," *Ann. Telecommun.*, vol. 74, no. 1, pp. 35–42, Feb. 2019, doi: 10.1007/s12243-018-0680-1.

[75] T. Mazloum, B. Fetouri, N. Elia, E. Conil, C. Grangeat, and J. Wiart, "Assessment of RF human exposure to LTE small-and macro-cells: UL case," in *2017 11th European Conference on Antennas and Propagation (EUCAP)*, Mar. 2017, pp. 1592–1593, doi: 10.23919/EuCAP.2017.7928743.

[76] J. Baumann, F. M. Landstorfer, L. Geisbusch, and R. Georg, "Evaluation of radiation exposure by UMTS mobile phones," *Electronics Letters*, vol. 42, no. 4, pp. 225–226, Feb. 2006, doi: 10.1049/el:20064180.

[77] D. Jovanovic, S. Bragard, D. Picard, and S. Chauvin, "Mobile telephones: a comparison of radiated power between 3G VoIP calls and 3G VoCS calls," *Journal of Exposure*

Science and Environmental Epidemiology, vol. 25, no. 1, pp. 80–83, Jan. 2015, doi: 10.1038/jes.2014.74.

[78] A. Sarbu, S. Miclaus, P. Bechet, and C. Munteanu, "Assessment of mobile phone user exposure to UMTS and LTE signals: comparative near-field radiated power levels for various data and voice application services," *Journal of Electromagnetic Waves and Applications*, vol. 30, pp. 1–15, May 2016, doi: 10.1080/09205071.2016.1167634.

[79] Anonymous, "Small cells, big network." https://www.jcdecaux.com/blog/small-cells-big-network (accessed Apr. 03, 2020).

[80] A. Boursianis, P. Vanias, and T. Samaras, "Measurements for assessing the exposure from 3G femtocells," *Radiat Prot Dosimetry*, vol. 150, no. 2, pp. 158–167, Jun. 2012, doi: 10.1093/rpd/ncr398.

[81] C. ALIAGA, "Comment se répartit le temps des Européennes et des Européens?" Apr. 2006,[Online].Available: https://ec.europa.eu/eurostat/documents/3433488/5438917/KS-NK-06-004-FR.PDF/e7aef033-8e5d-4254-9ed9-43720f09f5e4.

[82] "Enquête emploi du temps 2009-2010." Institut National de la Statistique et des Études Économiques Première n° 1377.

[83] "Narda STS." https://www.narda-sts.com/en/ (accessed Feb. 08, 2020).

[84] "Viavi." https://www.viavisolutions.com/en-us (accessed Oct. 08, 2019).

[85] "AZQ Android-LTE/WCDMA/GSM DriveTest Tool on Android. https://sites.google.com/azenqos.com/home (accessed Oct. 08, 2019).

[86] "Nemo Handy Handheld Measurement Solution | Keysight (formerly Agilent's Electronic Measurement)." https://www.keysight.com/en/pd-2767485/nemo-handy?cc=FR&lc=fre (accessed Mar. 08, 2019).

[87] Conil E and Agnani JB, "RF Exposure Assessments in Proximity of Small Cells," presented at the 2018 2nd URSI Atlantic Radio Science Meeting (AT-RASC), Meloneras. IEEE, 2018: 1-3, 2018, doi: 10.23919/URSI-AT-RASC.2018.8471480.

[88] LTE; Evolved Universal Terrestrial Radio Access (E-UTRA); Physical layer procedures (3GPP TS 36.213 version 13.0.0 Release 13), Accessed: Oct. 07, 2019. [Online]. Available: https://www.etsi.org/deliver/etsi_ts/136200_136299/136213/13.00.00_60/ts_136213v13 0000p.pdf.

[89] "Performance of Uplink Fractional Power Control in UTRAN LTE - IEEE Conference Publication." https://ieeexplore.ieee.org/document/4526110 (accessed Oct. 08, 2019).

[90] J. D. Parsons and J. G. Gardiner, *Mobile Communication Systems*. Springer, Boston, MA.

[91] Y. Huang and J. Wiart, "Simplified Assessment Method for Population RF Exposure Induced by a 4G Network," *IEEE Journal of Electromagnetics, RF and Microwaves in Medicine and Biology*, vol. 1, no. 1, pp. 34–40, Jun. 2017, doi: 10.1109/JERM.2017.2751751.

[92] X. Lv, X. Gu, X. Deng, L. Zhang, and W. Li, "Resource Allocation Algorithm for VoLTE with Semi-Persistent Scheduling," in *2015 IEEE 81st Vehicular Technology Conference (VTC Spring)*, Glasgow, United Kingdom, May 2015, pp. 1–5, doi: 10.1109/VTCSpring.2015.7146053.

8. PUBLICATIONS

8.1. Journal

Statistical Model of the human RF Exposure in Small cell Environment,

Amirreza Chobineh, Yuanyuan Huang, Taghrid Mazloum, Emmanuelle Conil, Joe Wiart

Annals of telecommunication, 74(6):1-10, December 2018

Abstract:

Small cells are one of the solutions to face the imperative demand on increasing mobile data traffic. They are low-powered base stations installed close to the users to offer better network services and to deal with increased data traffic. In this paper, the global exposure induced in such networks as a whole from user equipment and base stations has been investigated. As the small cell is close to the user, the propagation channel becomes highly variable and strongly susceptible by environmental factors such as the road traffic. An innovative statistical path loss model is constructed based on measurements on two French commercial LTE small cells, operating at LTE 1800 MHz and 2600 MHz. This statistical path loss model is then used to assess global exposure of the adult proportion of a population in a scenario composed of a street lined with buildings and indoor and outdoor data users.

8.2. Conferences

Use of a Statistical Measurement Based Propagation Model for Small Cells to Evaluate Global Exposure

Amirreza Chobineh, Yuanyuan Huang, Taghrid Mazloum, Emmanuelle Conil, Joe Wiart

2nd URSI Atlantic Radio Science Meeting (AT-RASC), 2018

Assessment Of Temporal Uplink Emitted Power Variation For VoLTE Calls

Amirreza Chobineh, Emmanuelle Conil, Joe Wiart,

URSI Atlantic Radio Science Meeting (AT-RASC), 2020

Small cell EMF exposure assessment using propagation model based on measurement and statistical method

Amirreza Chobineh, Yuanyuan Huang, Taghrid Mazloum, Emmanuelle Conil & Joe Wiart1

Titre : **Influence des nouvelles architectures et des nouveaux usages sur l'exposition humaine aux radiofréquences dans les réseaux cellulaires**

Mots clés : **Réseaux de communication, électromagnétisme, traitement des données, LTE, statistique, exposition,**

Résumé : Dans les années à venir, le trafic de données dans les réseaux cellulaires connaîtra une forte croissance en raison de l'augmentation d'utilisation des téléphones mobiles et de la mise en œuvre de la technologie des objets connectés. Par conséquent, les opérateurs de réseaux mobiles visent à augmenter la capacité de leurs réseaux avec une latence plus faible et à supporter des milliers de connexions simultanément. L'un des principaux efforts est de densifier les réseaux Macrocells actuels par les Small cells afin d'offrir plus de couverture et de débit aux utilisateurs. Les antennes Small cells émettent de faibles puissances et sont souvent déployées à de faibles hauteurs. En conséquence, ils sont plus proches des utilisateurs, peuvent être déployés massivement mais génèrent également des inquiétudes chez les riverains.

Les téléphones portables sont utilisés pour une grande variété d'utilisations qui nécessitent différentes quantités de données et de débit.

Les applications de voix sur IP telles que Skype sont devenues très populaires car elles fournissent une communication vocale internationale peu onéreuse et peuvent être utilisées sur les appareils mobiles. Étant donné que les systèmes LTE ne prennent en charge que les services par paquets, le service vocal utilise la technologie voix sur LTE au lieu de la technologie « circuits » classique comme avec le GSM et UMTS.

L'objectif principal de cette thèse est d'évaluer l'influence des nouvelles architectures des réseaux et usages sur l'exposition actuel du publique induite par les réseaux cellulaires. À cet égard, plusieurs campagnes de mesures ont été menées dans différentes villes et environnements.

En ce qui concerne l'exposition aux champs électromagnétiques dans les réseaux hétérogènes, les résultats suggèrent qu'en déployant les Small cells, la puissance émise par le téléphone mobile, en raison de la proximité de l'antenne et par conséquent l'exposition global diminue. De plus, pour évaluer l'exposition EMF des utilisateurs indoor induite par les Small cells, deux modèles statistiques sont proposés pour les expositions montante et descendante induite dans un réseau hétérogène LTE.

La dernière partie de cette thèse est consacrée à l'évaluation de l'exposition aux nouveaux types d'usages. Les résultats suggèrent que la puissance émise et la durée d'émission par un téléphone mobile dépendent fortement de l'usage et de la technologie du réseau. Les communications voix nécessitent un débit continu et généralement faible afin de maintenir la communication pendant l'appel.

Title: Influence of new network architectures and usages on RF human exposure in cellular networks

Keywords : Communication networks, electromagnetism, data processing, LTE, statistics, exposure,

Abstract: In coming years, there will be a sharp growth in wireless data traffic due to the increasing usage of mobile phones and implementation of IoT technology. Therefore, mobile network operators aim to increase the capacity of their networks, to provide higher data traffic with lower latency, and to support thousands of connections. One of the primary efforts toward these goals is to densify today's cellular Macrocell networks using Small cells to bring more coverage and higher network capacity. Small cell antennas emit lower power than Macrocells and are often deployed at lower heights. As a consequence, they are closer to the user and can be implemented massively. The latter can result in an important raise in public concerns. Mobile phones are used on the one hand, for a large variety of data usages that require different amounts of data and throughput and on the other hand for making phone calls. Voice over IP applications such as Skype has become very popular since they provide cheap international voice communication and can be used on mobile devices. Since LTE systems only support packet services, the voice service uses Voice over LTE technology instead of classical circuit-switched voice technology as in GSM and UMTS.

The main objective of this thesis is to characterize and analyse the influence of new network architectures and usages on the actual human exposure induced by cellular networks. In this respect, several measurement campaigns were carried out in various cities and environments.

The last part of the thesis is devoted to the assessment of the exposure for new types of usages through measurements. Results suggest that the amount of uplink emitted power and the emission time duration by a mobile phone is highly dependent on the usage and network technology. Voice call communications require a continuous and generally low throughput in order to maintain the communication during the call. On the contrary, in data usage, the mobile phone requires higher data and throughput to perform the task as fast as possible. Therefore, during a voice call even if the user is using the mobile phone for a relatively long time, the exposure time duration should be lower since the usage does not require high amounts of data. The temporal occupation rate for several types of voice calls for different technologies is assessed through measurements.